GEORG-AUGUST-UNIVERSITÄT
GÖTTINGEN

Functions of the Cold Shock Proteins in *Bacillus Subtilis*

Dissertation

for the award of the degree

“Doctor rerum naturalium”

by the Georg-August-University Göttingen

within the doctoral program “Microbiology and Biochemistry”

of the Graduate School for Neurosciences, Biophysics, and Molecular Biosciences (GGNB)

submitted by

Patrick Faßhauer

from Witzenhausen

Göttingen, 2021

Thesis committee

Prof. Dr. Jörg Stülke (Supervisor and 1st Reviewer)

Institute for Microbiology and Genetics, Department of General Microbiology, Georg-August-University Göttingen

Dr. Oliver Valerius (2nd Reviewer)

Institute for Microbiology and Genetics, Department of Yeast and Proteomics, Georg-August-University Göttingen

Prof. Dr. Fabian M. Commichau

Institute for Biotechnology, Department for Synthetic Microbiology, BTU Cottbus -Senftenberg

Additional members of the examination board

Prof. Dr. Rolf Daniel

Institute for Microbiology and Genetics, Department of Genomic and Applied Microbiology, Georg-August-University Göttingen

Prof. Dr. Stefanie Pöggeler

Institute for Microbiology and Genetics, Department of Genetics of Eukaryotic Microorganisms, Georg-August-University Göttingen

PD Dr. Till Ischebeck

Albrecht-von-Haller-Institute for Plant Sciences, Department of Plant Biochemistry, Georg-August-University Göttingen

Date of oral examination: July 1st, 2021

Affidavit

I hereby declare that this doctoral thesis named “Functions of the Cold Shock Proteins in *Bacillus Subtilis*” has been written independently and with no other sources and aids than quoted.

Patrick Faßhauer

The ability to observe without evaluating is the highest form of intelligence. – Jiddu Krishnamurti

Acknowledgements

Zunächst möchte ich mich bei Prof. Jörg Stülke für seine positive und hilfsbereite Art bedanken. Dein Vertrauen und deine Unterstützung haben mir ermöglicht neugierig zu bleiben und vieles zu lernen.

Ich danke Dr. Oliver Valerius für die Begleitung und das Mitdenken im gesamten Projekt. Ebenso möchte ich mich bei Prof. Fabian Commichau für das offene Ohr und all seine Ideen bedanken. Ich danke Prof. Rolf Daniel, Prof. Stefanie Pöggeler und Dr. Till Ischebeck für die Teilnahme an meiner Prüfungskommission.

Außerdem geht mein Dank an Dr. Anja Pöhlein und das gesamte G2L Team für die Hilfe und Geduld mit all den Genom- und RNA-Sequenzierungen. Vielen Dank auch an Dr. Ulrike Mäder und Dr. Tobias Busche für die Aufbereitung und Verarbeitung der Transkriptomdaten. Ebenso danke ich Dr. Stephan Michalik und Dr. Alexander Reder für das gemeinsame Wasser schöpfen im Mini*Bacillus* Projekt, ich freue mich auf die Veröffentlichungen.

Besonderer Dank geht an Julia Busse für die tatkräftige Unterstützung im Labor, ohne deine Hilfe hätte ich das alles nicht geschafft. Ebenso danke ich meinen Bachelor- und Masterstudenten Leon Driehaus-Ortiz, Laura Helms und Georg Aschenbrandt für ihre Mitarbeit. Ebenso danke ich Sabine Lentes, Christina Herzberg und Silvia Carillo-Castellón für ihre praktische und emotionale Unterstützung in all den Jahren.

Des Weiteren danke ich Dr. Martin Benda für all die Diskussionen und die Möglichkeit am RNase Y Paper mitzuwirken, es war immer sehr angenehm mit dir das Büro zu teilen. Vielen Dank auch meinen weiteren Laborkollegen Janek Meißner und Dennis Wicke, mit euch kann man immer lachen! Ebenso danke ich allen weiteren Kollegen die mich in den verschiedenen Laboren begleitet haben und die immer gerne mitgedacht und für eine geniale Arbeitsatmosphäre gesorgt haben.

Ganz besonderer Dank geht an meinen Leidens- und Freudensgenossen Björn Richts. Es lebe das Prinzip! Selbstverständlich danke ich auch all meinen Freunden die mich all die Zeit begleitet und geerdet haben. Ihr habt all die Zeit zu etwas besonderem gemacht und inspiriert mich bis heute.

Danke an meine Eltern Iren und Uwe Faßhauer, ohne eure Unterstützung und euren Glauben an mich wäre nichts davon möglich gewesen. Ebenso danke an meine Großeltern Helga und Dieter Faßhauer, sowie danke lieber großer Rest der Familie, für all den Zuspruch und Zusammenhalt.

Aus tiefstem Herzen danke Ieva Grigonyte, dank dir war der Weg nur halb so weit!

Table of contents

List of abbreviations

% (v/v)	% (volume/volume)
% (w/v)	% (weight/volume)
A	Alanine
Amp	ampicillin
AP	alkaline phosphatase
APS	ammonium persulfate
B.	*Bacillus*
bp	base pair
CAA	casamino acid
cat	chloramphenicol resistance gene
CAT	co-antiterminator domain
CCR	combined-chain reaction
CSD	Cold shock domain
chrom. DNA	chromosomal DNA
dH_2O	deionized water
DMSO	dimethyl sulfoxide
DNA	deoxyribonucleic acid
DNAse	deoxyribonuclease
d/NTPs	des-/oxyribose nucleoside triphosphates
DTT	dithiothreitol
E.	*Escherichia*
e.g.	*exempli gratia* - latin for example
EDTA	ethylenediaminetetraacetic acid
EMSA	electrophoretic mobility shift assay
et al.	*et alii* – latin for and others
fwd	forward
Glc	glucose
IPTG	isopropyl β-D-1-thiogalactopyranoside
Kan	Kanamycin
kb	kilo base pair
KH	K homology domain
LB	lysogeny broth (medium)
LFH	long flanking homology
L.	*Listeria*
mRNA	messenger RNA
NPKM	normalized reads for nucleotide activities per kilobase of exon model per million mapped reads

OB-fold	oligonucleotide/oligosaccharide (OB) fold
OD_x	optical density, λ = x nm
ORF	open reading frame
P	phosphoryl group
P	Proline
PAGE	polyacrylamide gel electrophoresis
PBS	phosphate buffered saline
PCI	phenol:chloroform:isoamylalcohol
PCR	polymerase chain reaction
pH	power of hydrogen
psi	pound-force per square inch
P_{xxx}	promoter from gene xxx
qRT-PCR	quantitative reverse transcription PCR
RBS	ribosomal binding site
rev	reverse
RNA	ribonucleic acid
RNase	ribonuclease
RNAseq	RNA sequencing
rpm	rounds per minute
RRM	RNA recognition motif
rRNA	ribosomal ribonucleic acid
RT	room temperature
S	Serine
SD	Shine-Dalgarno
SDS	sodium dodecyl sulfate
sRNA	small regulatory RNA
Tet	tetracycline resistance cassette
tRNA	transfer-RNA
U	units
UTR	untranslated region
WGS	Whole genome sequence
ZAP	Zellaufschluss-Puffer

1. Summary

RNA binding proteins are fundamental to the proper functioning of all cells. They are structural components in larger complexes such as ribosomes or regulate cellular processes that involve RNA such as transcription, translation, or the modification, processing, and decay of RNA. Some RNA binding proteins contain the cold shock domain which is highly conserved from bacteria to mammals. Bacterial cold shock proteins consist of a single cold shock domain that binds RNA and single stranded DNA. They have been extensively studied in various species and some act as RNA chaperones that destabilize secondary RNA structures to regulate transcriptional termination, RNA stability and processing, as well as translation. In the Gram-positive model organism *Bacillus subtilis,* the function(s) and targets of cold shock proteins have not been elucidated so far. This work identified the regulon of the cold shock proteins in *B. subtilis* and uncovered their involvement in many biological processes. The *B. subtilis* genome encodes the three cold shock protein paralogs CspB*,* CspC*,* and CspD. While *csp* single-mutants did not exhibit any obvious phenotype and a triple knockout was not possible, the *cspB cspD* double-knockout led to the loss of genetic competence, impairment of biofilm formation, aberrant gene expression, and a strong impairment of growth. This suggests CspC cannot fully replace the function of CspB and CspD. The *cspB cspD* double mutant formed suppressor mutants, which often harbored a point mutation that leads to upregulation of CspC. The overexpression of CspC in these suppressor mutants improved growth and genetic stability but did not restore genetic competence. This suggests CspC is functionally different from CspB and CspD. CspC was the only paralog that was induced at 15°C further highlighting the functional specialization. Comparison of the amino acid residue at position 58 which is important for functional specificity in *Staphylococcus aureus,* revealed that CspC harbors an alanine residue while CspB and CspD carry a proline residue at this position. Therefore, a CspC(A58P) variant was expressed in the *cspB cspD* double mutant background which improved genetic stability, growth, and also restored genetic competence. Hence, a single amino acid is responsible for the functional specificity of the cold shock proteins. Analysis of the *cspB cspD* double mutant transcriptome uncovered up- or downregulation for as many as 21% of genes suggesting numerous potential targets of CspB and CspD. One of these targets is the *cspC* 5'-UTR at which CspB and CspD but not CspC negatively regulated expression. Other targets were identified by analysis of read-through transcription at intergenic regions in the *cspB cspD* double mutant. An increased transcriptional read-through was found at the *manR* and *liaH* terminators. Conversely, transcriptional read-through was decreased at the terminator/ antiterminator switches between the *pyrR-pyrP* and *pyrP-pyrB* genes. These results demonstrate that the *B. subtilis* cold shock proteins have different biological functions and influence gene expression globally at least by regulation of transcription. This study may serve as a starting point for future research on cold shock protein function in *B. subtilis.* It presents methods and interesting targets to further explore the function of cold shock proteins.

2. Introduction

2.1 RNA binding proteins

All living organisms store their genetic information in the DNA molecule. The genetic information is expressed *via* transcription of the DNA into messenger RNA which is finally translated into proteins that comprise one of the major building blocks of cells. They provide structure, catalyze metabolic reactions, transport metabolites, perceive stimuli and allow the ubiquitously essential processes of DNA replication, transcription, translation and gene regulation. Some proteins interact with RNA and are hence called RNA binding proteins. Probably the oldest and most prominent example for RNA binding proteins are ribosomal proteins which are believed to have emerged in a time before the last universal common ancestor and mark the transition from a hypothetical RNA world to a ribonucleoprotein world (Fox, 2010; Cech, 2012). Aside from giving large complexes like ribosomes a structural basis, RNA binding proteins affect all processes that involve RNA such as transcription, the modification, processing and stability of RNAs and finally the process of translation. Bacterial RNA binding proteins act globally or on specific sequences by utilizing one or multiple RNA binding domains (see Figure 1). There are the Csr/Rsm domain, the cold shock domain (CSD), the Sm and Sm-like domains, the FinO-like domain, the co-antiterminator (CAT) domain, the RNA recognition motif (RRM), the K homology domain (KH), the S1 domain, and several more (Manival *et al.*, 1997; reviewed by Holmqvist & Vogel, 2018). An example for globally acting RNA binding proteins are the so-called RNA chaperones.

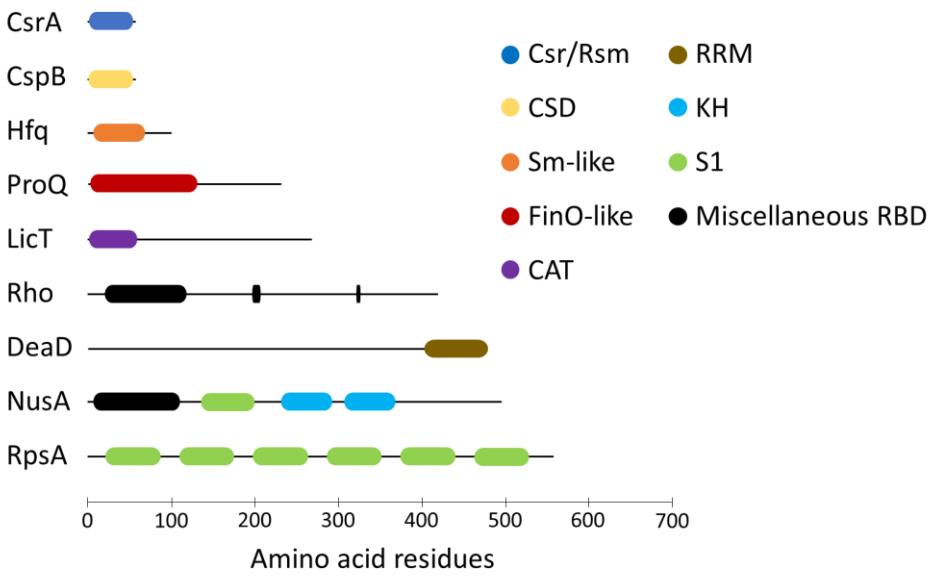

Figure 1: Bacterial RNA binding proteins and the corresponding RNA binding domains. CsrA**:** carbon storage regulator A, CspB: cold shock protein B, Hfq: RNA chaperone/host factor for bacteriophage Q, ProQ: RNA chaperone, LicT: transcriptional antiterminator of the BglG family, Rho: transcription terminator factor, DeaD: DEAD-box RNA helicase, NusA: transcription termination/antitermination protein, RpsA: ribosomal subunit protein S1 (partially adapted from Holmqvist & Vogel, 2018)**.**

By definition, an RNA chaperone is a protein that binds an RNA transiently and facilitates the proper folding of the molecule into its functional three-dimensional structure (reviewed by Semrad, 2011). While the primary structure of an RNA is defined by the sequence itself, the secondary structure is formed *via* base-pairings within the molecule. This allows for a multifold of different conformations. Because RNA duplexes have a high thermodynamic stability this can cause RNAs to be kinetically trapped in a non-functional conformation (reviewed by Herschlag, 1995). This problem is aggravated by forces that determine the tertiary structure of an RNA molecule. These are non-standard base pairings, interactions with phosphoryl or with 2'-hydroxyl groups and also interactions with metal ions (Herschlag, 1995). By binding of an RNA chaperone certain interactions are disrupted which allows the structural rearrangement from an unfolded or misfolded form into the functional one (see Figure 2). RNA chaperones do only bind transiently and do not require external energy such as from ATP binding or hydrolysis (Herschlag, 1995). Some authors specify that not all RNA binding proteins that alter the structure of RNAs are RNA chaperones. For example, proteins that expedite the base pairing of complementary RNAs are dubbed RNA annealers (Rajkowitsch *et al.*, 2007). Other proteins that utilize energy from ATP hydrolysis to unwind RNA duplexes are named RNA helicases. The so-called specific RNA binding proteins recognize distinct sequence motifs and maintain a continuous bond with their RNA target to stabilize the functional structure (Rajkowitsch *et al.*, 2007). However, the term RNA chaperone is usually used very broadly for RNA binding proteins that alter RNA structure and will hereafter be used that way. Examples of important bacterial RNA binding proteins and their functions in the cell are described in the following paragraphs.

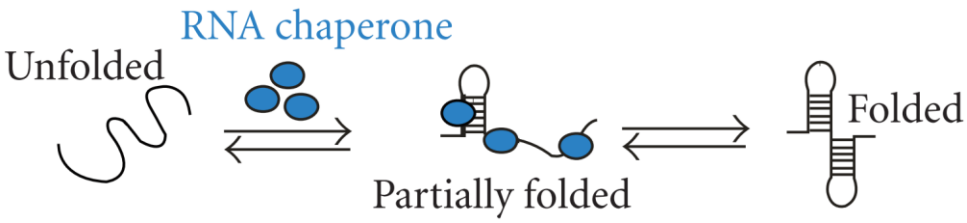

Figure 2: Schematic folding of an RNA molecule by RNA chaperones. Proteins with RNA chaperone activity (blue) prevent misfolding into the non-functional structure and favor folding into the functional structure (Semrad, 2011).

RNA binding proteins in regulation of transcription

RNA is synthesized in the process of transcription which therefore is the first stage that is influenced by RNA binding proteins. The transcriptional elongation factor NusA is a well-studied example. It contains multiple different RNA binding domains (see Figure 1), is essential in *Escherichia coli* as well as in *B. subtilis* and is important for the termination of transcription in both organisms (Belogurov & Artsimovitch, 2015; Koo *et al.*, 2017; Goodall *et al.*, 2018). During termination the newly

transcribed RNA is released from the RNA polymerase either by intrinsic/ Rho-independent termination or by Rho-dependent termination (Ray-Soni *et al.*, 2016).

Intrinsic termination stops transcription *via* secondary RNA structures that lead to dissociation of the RNA from the RNA polymerase. An intrinsic termination signal is comprised of GC-rich inverted repeats that form a hairpin structure which is followed by a poly-uridine stretch at the 3'-end (Adhya & Gottesman, 1978). It can be found at the end of an operon and also upstream, between, or within genes (Peters *et al.*, 2011). The hairpin structure misaligns the RNA 3'-end from the active center. Transcription of the poly-uridine stretch further leads to a weak RNA-DNA duplex which together with the misalignment leads to dissociation of the transcription complex and thus, termination (Farnham & Platt, 1981; Wilson & von Hippel, 1995; summarized in Krebs *et al.*, 2014). The hairpin structure is stabilized by the RNA binding protein NusA. This drastically increases the hairpin induced pausing and thereby termination of transcription, especially at weak intrinsic terminator sequences (Wilson & von Hippel, 1995;. Mondal *et al.*, 2016; reviewed by Zhang & Landick, 2016). In fact, 25% of all terminators in the *B. subtilis* genome are dependent on NusA (Mondal *et al.*, 2016). Examples for genes in *B. subtilis* where NusA is known to enhance transcriptional pausing are at the leader of the *trp* operon transcript and at the FMN riboswitch preceding the *ribDEAHT* operon (Wickiser *et al.*, 2005; Yakhnin & Babitzke, 2002; Yakhnin & Babitzke, 2010). While NusA affects termination globally, other RNA binding proteins like the *trp* RNA binding attenuation protein (TRAP) possess sequence specificity. The 5'-leader region of the *B. subtilis trp* operon contains a weak intrinsic termination signal which by default forms an antitermination structure (Shimotsu *et al.*, 1986). TRAP senses the cellular tryptophan level by binding it at excessive concentrations. Thereby activated, TRAP binds to a specific sequence in the *trp* leader resulting in remodeling of its secondary structure: The antiterminator is resolved and a terminator hairpin is formed, which together with NusA-stimulated pausing leads to termination of transcription (Shimotsu *et al.*, 1986; Babitzke *et al.*, 1994; Yakhnin & Babitzke, 2010; McAdams & Gollnick, 2014).

Rho-dependent termination is performed by the RNA binding protein Rho which is comprised of a homohexameric ring with two RNA binding sites in each monomer (Skordalakes & Berger, 2003). It recognizes the pyrimidine-rich Rho utilization site in the RNA and ATP-dependently translocates to the 3'-end until it reaches the RNA-DNA duplex region which is then unwound by the helicase activity finally resulting in termination (reviewed by Mitra *et al.*, 2017). While Rho is essential and important for termination of over 25% of the operons in *E. coli*, it is not essential in *B. subtilis* and likely plays a less important role (Quirk *et al.*, 1993; de Hoon *et al.*, 2005; Cardinale *et al.*, 2008). Nonetheless, it is of some importance in *B. subtilis* as its loss leads to an increased formation of antisense transcripts often at suboptimal intrinsic terminators (Nicolas *et al.*, 2012). Interestingly, also the deletion of NusA leads to an increase of antisense transcription (Mondal *et al.*, 2016) and it has been discussed to act as Rho antagonist due to competition for overlapping binding sites (Qayyum *et al.*, 2016). Apart from

inhibiting antisense transcription, the termination activity of Rho also influences the quantity of many sense transcripts and is key for central processes in *B. subtilis* such as cell motility, biofilm formation and sporulation (Bidnenko *et al.*, 2017). An RNA binding protein that modulates Rho dependent termination of transcription is the carbon storage regulator A (CsrA). It contains the Csr/Rsm (Rsm=regulator of secondary metabolism from *Pseudomonas fluorescens*) RNA binding domain (see Figure 1), has a size of ~7 kDa and is highly conserved throughout the bacterial phylum as it is encoded by almost 75% of all species (Papenfort & Vogel, 2010; Zere *et al.*, 2015). It is well-studied in *E. coli* and is known to expose Rho utilization sites to induce premature transcription termination by Rho (Figueroa-Bossi *et al.*, 2014). In *B. subtilis*, CsrA is only known to be involved translational control of a specific mRNA (see below).

Other RNA binding proteins have the opposite effect and prevent termination by inhibition of hairpin formation or remodeling of terminators into non-terminating structures. The *hut* operon regulating protein HutP from *B. subtilis* is a transcriptional antiterminator that is important for histidine utilization (Wray & Fisher, 1994). At high cellular levels, L-histidine it is bound by HutP which induces a conformational change in the protein (Kumarevel *et al.*, 2005). HutP then binds the intrinsic terminator upstream of the *hut* operon directly preventing hairpin formation which results in transcriptional readthrough and hence, transcription of the *hut* genes (Oda *et al.*, 2000; Oda *et al.*, 2004; Gopinath *et al.*, 2008). Another antiterminator, is the *B. subtilis* protein LicT from the BglG family which contains the CAT RNA-binding domain (see Figure 1). It controls expression of the *bglPH* operon which is important for β-glucoside utilization. When the preferred carbon source glucose is present and β-glucosides are absent, transcription of the *bglPH* operon is constitutively initiated but stopped by a terminator upstream of the coding sequence (Le Coq *et al.*, 1995; Schnetz *et al.*, 1996). Instead of inhibiting the formation of the terminator, binding of LicT to the so-called RNA antiterminator sequence remodels the secondary structure in a way that mutually excludes the presence of the terminating hairpin (Hübner *et al.*, 2011). The paralogous proteins GlcT, SacT, and SacY in *B. subtilis* function similarly (Aymerich & Steinmetz, 1992; Stülke *et al.*, 1997). This mechanism occurs similarly for the the *bgl* systems in other low-GC Gram-positive as well as Gram-negative bacteria (reviewed by Amster-Choder, 2005). There are many more examples for antiterminator proteins in *B. subtilis* alone. For example the protein GlpP which controls transcription of the *glpFK* and *glpTQ* operons for glycerol-3-phosphate utilization (Glatz *et al.*, 1996) and also the already described TRAP protein acting at the *trp* operon (Shimotsu *et al.*, 1986). While the described antiterminators inhibit transcription at specific loci, other RNA binding proteins act globally. For example, the cold shock proteins are believed to be major global transcription antiterminators as they were shown to affect several genes preceded by intrinsic terminators in *E. coli* (see section 2.3) (Bae *et al.*, 2000). However, RNA binding proteins do not only affect RNA turnover by influencing transcription but also modulate the stability of transcripts.

RNA binding proteins in RNA turnover and processing

The constant synthesis and degradation of RNA is highly regulated. By this, cells are able to quickly react to environmental changes as the half-life of a specific mRNA determines the amount of protein synthesized from it. The stability of an RNA is mainly dependent on how efficiently it is degraded. In bacteria, degradation is carried out by RNases in two sequential steps. It is initiated by internal cutting of the RNA by the endonucleases RNase E in *E. coli* and the structurally distinct RNase Y in *B. subtilis* (reviewed by Mohanty & Kushner, 2016; Durand & Condon, 2018). Both RNases have low sequence specificity and cleave single-stranded RNA regions that are AU-rich (Shahbabian *et al.*, 2009). RNase Y is the major regulator of RNA metabolism in *B. subtilis* and has a large impact on gene expression. Its depletion affects about 25% of the transcriptome (Lehnik-Habrink *et al.*, 2011). Similar to RNase E in *E. coli*, RNase Y is believed to form a multienzyme complex called RNA degradosome in *B. subtilis*. Several studies suggest interactions with glycolytic enzymes like phosphofructokinase and enolase, furthermore with RNases such as PNPase, RNases J1 and J2, as well as DEAD-box helicase CshA (Commichau *et al.*, 2009; Lehnik-Habrink *et al.*, 2010; Newman *et al.*, 2012). RNase Y is not only important for the endonucleolytic initiation of RNA decay but is also involved in the processing of mRNAs. A well-studied example is the transcript of the glycolytic *gapA* operon. The 5' region encodes the repressor of the operon CggR which is expressed much weaker than the glycolytic enzymes encoded downstream from *cggR* (Meinken *et al.*, 2003). This is because RNase Y cleaves behind the promoter-proximal *cggR* open reading frame. Two fragments are generated: A *cggR* fragment which is susceptible to degradation by exoribonucleases and a more stable fragment encoding the glycolytic enzymes (Commichau *et al.*, 2009; Lehnik-Habrink *et al.*, 2012). Another important endoribonuclease is the double-strand-specific RNase III which is essential in *B. subtilis* (Commichau & Stülke, 2012). It is involved in the degradation of toxic prophage mRNA-mRNA hybrids (Durand *et al.*, 2012). Moreover, it is important for processing of ribosomal RNA and small cytoplasmic RNA (Herskovitz & Bechhofer, 2000).

Initiation of RNA decay by endoribonucleolytic cleavage leads to a fragment with an unprotected 3'-end. This fragment is then exoribonucleolytically degraded 3' to 5' by RNases like PNPase, RNase R, or RNase PH in *B. subtilis* (Wang & Bechhofer, 1996; Wen *et al.*, 2005; Oussenko *et al.*, 2005; Bechhofer & Deutscher, 2019). The original transcripts that were not cleaved internally are more stable. This is because their 3'-end is protected by the stem-loop structure of an intrinsic terminator (Durand & Condon, 2018). Consecutive rounds of endoribonucleolytic cleavage result in more fragments susceptible to exoribonucleases leaving only oligonucleotides. These are finally digested to mononucleotides by oligoribonucleases such as NrnA, NrnB, or YhaM in *B. subtilis* (Ghosh & Deutscher, 1999; Mechold *et al.*, 2007; Fang *et al.*, 2009; Bechhofer & Deutscher, 2019). The remaining 3'-ends that are protected by stem-loops, or transcripts whose 5'-end was

dephosphorylated, are degraded 5' to 3' by RNase J1 in *B. subtilis* (Mathy *et al.*, 2007*;* Condon, 2010; Bechhofer & Deutscher, 2019). Among other domains, many of the presented RNases are constituted of several RNA binding domains presented in Figure 1. For example RNase II from *E. coli* and RNase R from *B. subtilis* each contain two cold shock domains and one S1 domain, the K-homology domain can be found in RNase Y as well as in PNPase, whereas the double-strand RNA binding domain is found in RNase III (Hui *et al.*, 2014).

In general, RNA binding proteins modulate the stability of transcripts by either stimulation or inhibition of RNase activity. They can activate RNases by recruiting them to their designated target or inactivate an RNase *via* direct competition for the cleavage site (reviewed by Mohanty & Kushner, 2016; Holmqvist & Vogel, 2018).

A well-studied example for an RNA binding protein that stimulates RNA degradation *via* recruitment of a ribonuclease is the RapZ protein from *E. coli*. This RNase adapter protein was shown to specifically bind the *glmZ* sRNA. This sRNA induces the translation of the glucosamine-6-phosphate synthase which is essential in the biogenesis of peptidoglycan. RapZ also interacts with the catalytic domain of RNase E. Thereby RapZ presents the sRNA to the RNase and is targeting it for decay (Göpel *et al.*, 2013; Gonzalez *et al.*, 2017). The corresponding protein in *B. subtilis* is YvcJ but its mechanism of action there is unknown (Zhu & Stülke, 2018). In contrast to RapZ*,* YvcJ does not interfere with glucosamine-6-phosphate production and is instead involved in the control of competence genes (Luciano *et al.*, 2009). CsrD from *E. coli* is another example for a protein that exposes a transcript to RNase E. By counteracting the interaction of the *csrB* and *csrA* transcripts it exposes a cleavage site in the *csrB* transcript leading to its degradation by RNase E (Vakulskas *et al.*, 2016). Another important class of RNA binding proteins that stimulate RNA decay are the DEAD-box helicases that are ubiquitously found in the RNA degradosomes of bacteria, as well as in archaea and eukaryotes (Zhu & Stülke, 2018). This family of helicases binds RNA *via* the RNA recognition motif as shown for *B. subtilis* DeaD (see Figure 1) (Hardin *et al.*, 2010). DEAD-box helicases use the energy from ATP hydrolysis to unwind self-annealed RNA duplexes (Redder *et al.*, 2015). This allows the efficient attack by RNases that act on single stranded RNA. In addition to the promotion of RNA degradation, the action of RNA helicases is important for a multifold of processes such as transcription, ribosome biogenesis, translation initiation and termination (Redder *et al.*, 2015). *B. subtilis* encodes the four DEAD-box helicases CshA, CshB, DeaD and YfmL. CshA is the major RNA helicase which was shown to affect RNA degradation, ribosome biogenesis and together with the other helicases is important for adaptation to cold temperatures (Lehnik-Habrink *et al.*, 2013).

RNA binding proteins negatively modulate RNA stability *via* direct competition with RNases for the cleavage site. An example for this mechanism is the CsrA protein from *E. coli* which binds the RNase E cleavage sites of the *csrB* (Vakulskas *et al.*, 2016) and *flhDC* transcripts (Yakhnin *et al.*, 2013).

By that, CsrA protects the mRNAs from endonucleolytic cleavage by RNase E. An effect of *B. subtilis* CsrA on RNA stability remains to be found. Another interesting example is the *B. subtilis* aconitase CitB. CitB is a so-called moonlighting protein which in addition to its metabolic enzyme activity binds and stabilizes the *citZ* mRNA (Alén & Sonenshein, 1999; Pechter *et al.*, 2013). The ProQ protein from *E. coli* also stabilizes RNAs. Its RNA binding domain belongs to the FinO-like family (see Figure 1) (Gonzalez *et al.*, 2017). ProQ binds the 3' ends of several mRNAs and protects them from exoribonucleolytic degradation (Holmqvist *et al.*, 2018). Other major RNA binding proteins that were shown to sequester RNase cleavage sites are Hfq and some cold shock proteins (see sections 2.2 and 2.3 respectively). Beside these specific mechanisms that modulate RNA decay, altered transcript stabilities can also be a consequence of changed translation rates.

RNA binding proteins in translation

Translation relies upon a variety of RNA binding proteins and in fact most of them are involved in the synthesis of proteins. Firstly, there are the ribosomal proteins that also form the largest group of RNA binding proteins with 57 that were identified in bacteria of which 34 are conserved in all domains of life (Fox, 2010; Holmqvist & Vogel, 2018). They affect translation by providing the structural basis and mechanistic necessities. There are many proteins influencing translation more indirectly such as aminoacyl-tRNA synthetases, enzymes that modify tRNAs as well as rRNAs, or the signal recognition particle which guides translating ribosomes to the membrane. However, RNA binding proteins also directly affect the rate of translation. They usually achieve this by interfering with the initiation of translation meaning the association of the ribosomal binding site with the 30S ribosomal subunit. RNA binding proteins can alter the secondary structure of mRNAs to change accessibility of the ribosomal binding site or directly compete with the 30S subunit for binding of the mRNA (reviewed by Holmqvist & Vogel, 2018). Another mechanism by which RNA binding proteins influence the rate of translation is the recruitment of sRNAs to sequester or present the ribosomal binding site as it was shown for the Hfq protein (see section 2.2).

A well-studied studied example for a ribosomal protein that induces a structural change in mRNAs is the protein S1. Its RNA binding domain is the S1 domain which belongs to the oligonucleotide/oligosaccharide binding family that is forming a five stranded antiparallel β-barrel which specifically binds single stranded nucleic acids (Subramanian, 1983; Bycroft *et al.*, 1997; Salah *et al.*, 2009). It is present in a variety of RNA binding proteins and is conserved from bacteria to humans (Bycroft *et al.*, 1997). During evolution, some S1 domains have lost their nucleic acid binding capabilities and became responsible for making protein-protein contacts. This happened for some S1 domains in the *E. coli* S1 protein where the domain was originally identified (Guerrier-Takada *et al.*, 1983; Subramanian, 1983). The ribosomal S1 protein is situated in the 30S ribosomal subunit and is

the largest ribosomal protein. It is responsible for recognition and binding of mRNAs with a 5'-leader during translation initiation (reviewed by Hajnsdorf & Boni, 2012). It primarily promotes the synthesis of proteins by unfolding mRNAs to allow binding of the 30S subunit and correct positioning of the start codon (Duval *et al.*, 2013). S1 is essential in Gram-negative bacteria such as proteobacteria and cyanobacteria but is absent in Gram-positive bacteria with low GC content like *B. subtilis* (Salah *et al.*, 2009). The YpfD protein likely represents the S1 protein in *B. subtilis* as it shares high similarity and cross-links with ribosomal proteins (Sorokin *et al.*, 1995; De Jong *et al.*, 2017). However, it only contains four instead of six S1 domains, is not essential for *via*bility and its function has not been elucidated (Sorokin *et al.*, 1995; Akanuma *et al.*, 2012). Other examples for *E. coli* RNA binding proteins containing the S1 domain are the already described ribonucleases RNase E, RNase II, PNPase and RNase G (Schubert *et al.*, 2004), the general transcription factor NusA (Bycroft *et al.*, 1997). In *B. subtilis,* homologs exist for the proteins PNPase (Condon & Putzer, 2002), NusA (Worbs *et al.*, 2001), PNPase and NusA are built of one S1 domain and additionally contain one or two K homology domains respectively (see Figure 1) (Bycroft *et al.*, 1997; Worbs *et al.*, 2001).

An RNA binding protein that directly competes with the 30S ribosomal subunit for the mRNA is the CsrA protein which is a perfect example for the functional versatility of RNA binding proteins. While it affects the regulatory mechanisms of transcription and RNA decay as described above its canonical pathway is the inhibition of translation (Holmqvist *et al.*, 2016). It was originally discovered in *E. coli,* where it is of high importance for glycogen biosynthesis and carbon storage (Romeo *et al.*, 1993). It forms a homodimer that binds two single-stranded GGA triplets in the 5'-leader of the glycogen biosynthesis gene *glgC.* This prevents the initiation of translation because binding of the 30S ribosomal subunit to the ribosomal binding site is spatially blocked (Liu & Romeo, 1997; Baker *et al.*, 2002). Csr/Rsm proteins are global regulators in many Gram-negative bacteria such as *E. coli*, *P. fluorescens*, *Salmonella typhimurium*, or *Legionella pneumophila*. There they bind to the 5'-untranslated regions (5'-UTRs) of hundreds of mRNAs to inhibit translation (Schubert *et al.*, 2004; Dubey *et al.*, 2005; Holmqvist *et al.*, 2016; Potts *et al.*, 2017; Sahr *et al.*, 2017). In Gram-positive bacteria CsrA was first characterized in *B. subtilis* where it binds the 5'-UTR of the *hag* mRNA which encodes the flagellin protein. Binding leads to inhibition of translation initiation by blockage of the ribosomal binding site (Yakhnin *et al.*, 2007). In *E. coli,* repression by CsrA is relieved when the sRNAs *csrB* or *csrC* bind the protein (Weilbacher *et al.*, 2003). In *B. subtilis,* CsrA is sequestered by the FliW protein (Mukherjee *et al.*, 2011). Moreover, a new function was recently shown for CsrA in *B. subtilis* which has so far only been attributed to Hfq or ProQ in Gram-negative bacteria. Müller *et al.* (2019) demonstrated that CsrA promotes the interaction between the regulatory sRNA SR1 and the *ahrC* mRNA. Thereby CsrA indirectly inhibits translation initiation. This is because SR1 binding induces a structural change in the secondary structure of the *ahrC* mRNA which affects the accessibility of the

ribosomal binding site (Heidrich *et al.*, 2007).

The ProQ protein and its related proteins that contain the FinO-like domain offer more examples for RNA binding proteins that not only function in RNA stabilization as described above, but also act as RNA chaperones that likely influence translation. This class of proteins was originally identified in *E. coli* where the FinO protein is encoded on F plasmids. There, it acts as an RNA chaperone and facilitates duplexing of complementary RNAs that would otherwise not associate due to their internal hairpins (Glover *et al.*, 2015). This stabilizes the mRNA which then promotes the process of plasmid conjugation (Glover *et al.*, 2015). ProQ operates on a larger scale than FinO and interacts with over hundred RNAs in *Salmonella enterica* and *E. coli* (Smirnov *et al.*, 2016; Holmqvist *et al.*, 2018). It also has RNA chaperone and RNA annealer properties. This is because ProQ facilitates RNA strand exchange as well as RNA duplexing which is thought to regulate the ProP protein amounts on the level of translation (Chaulk *et al.*, 2011). However, homologs for ProQ in *B. subtilis* do not exist. Whether there is a protein that may have a similar function is not known and was only proposed for CsrA (Müller *et al.*, 2019). Another RNA binding protein that acts as an RNA chaperone and influences translation as well as RNA stability is the Hfq protein.

2.2 Hfq

The essential host factor for bacteriophage Q RNA replication (Hfq) was discovered over 50 years ago in *E. coli* and has since been extensively studied (Franze De Fernandez *et al.*, 1968). Homologs exist throughout all domains of life and include the Sm and Lsm proteins that are found in almost all eukaryotes and archaea (Mura *et al.*, 2013). The Sm and Lsm proteins which contain the Sm and Sm-like domains respectively, function as RNA chaperones. In eukaryotes, they are involved in the post-transcriptional regulation of mRNA splicing, nuclear RNA processing, RNA degradation and in translation (reviewed by Wilusz & Wilusz, 2005). In general, Hfq facilitates the duplexing of short and imperfect base-pairings between an mRNA and a *trans* encoded sRNA (reviewed by Vogel & Luisi, 2011). There are up to 100 regulatory sRNAs that recognize as much as 25% of all mRNAs in *E. coli* and *S. enterica via* the Hfq protein (Tree *et al.*, 2014; Holmqvist *et al.*, 2016; Waters *et al.*, 2017). This activity makes Hfq the major RNA chaperone in Gram-negative bacteria and puts it at the center of a global post-transcriptional network.

Hfq is built from monomers that each contain two Sm-like motifs and form a homohexameric ring-like structure (Zhang *et al.*, 2002). This structure is known to bind RNAs at its proximal and distal sites (Rajkowitsch & Schroeder, 2007; Fender *et al.*, 2010). Hfq homologs also exists in Gram-positive bacteria and the structural resemblance to their Gram-negative counterparts is apparent. The crystal structure of the *B. subtilis* Hfq protein in complex with a synthetic RNA aptamer bound to the distal site is solved (see Figure 3 A). Nevertheless, most of the research on Hfq was performed in *E. coli* or

close relatives and the following mechanistic model cannot simply be translated to *B. subtilis*. In addition to binding of RNAs by the proximal and distal sites, RNAs can be bound by the lateral site and the C-terminal tails which can vary strongly from homolog to homolog (reviewed by Sobrero & Valverde, 2012). The different binding sites also have varying sequence preferences that promote recruitment of distinctive RNAs on the same protein (Mikulecky *et al.*, 2004). While the distal site preferentially binds A-rich sequences of mRNA 5'-UTRs (Mikulecky *et al.*, 2004; Link *et al.*, 2009), the proximal site favors binding of U-rich sRNA 3'-ends (Sauer & Weichenrieder, 2011; Dimastrogiovanni *et al.*, 2014). The binding of both RNAs to the same protein as well as additional contacts with the lateral site altogether promote base pairing of the two RNAs (Panja *et al.*, 2013; Peng *et al.*, 2014; reviewed by Updegrove *et al.*, 2016). The C-terminal tails are hypothesized to displace bound RNAs from the Hfq protein (Santiago-Frangos *et al.*, 2016). Depending on the structural information encoded in the bound RNA molecules, the RNA annealing activity of Hfq has different effects. It is generally known to either promote or inhibit the processes of RNA degradation as well as translation.

Hfq promotes RNA decay by actively recruiting nucleases to the mRNA target (see Figure 3 B i.). For example, the regulatory sRNAs *sgrS* and *ryhB* from *E. coli* seem to present their target mRNAs to RNase E by at least transiently forming an sRNA-Hfq-mRNA complex (Morita *et al.,* 2005). Conversely, Hfq also stabilizes RNAs (see Figure 3 B ii.). The RNase E cleavage sites of some *E. coli* sRNAs overlap with the Hfq binding site (Moll *et al.*, 2003). Occupation of these sites by Hfq spatially blocks RNase E and keeps it from degrading the sRNA. This mechanism also affects the processing of sRNAs, whereby suppression of certain cleavage sites guides RNase E to the designated processing site (Chao *et al.*, 2017). Actually, the protection of sRNAs by Hfq seems to be a common mechanism in Gram-negative bacteria (Holmqvist & Vogel, 2018). The protection of mRNAs against RNase E cleavage on the other hand, is dependent on regulatory sRNAs. Either, the sRNAs directly sequester the cleavage site or they activate translation so efficiently that the increased ribosomal density blocks the access of RNase E to the mRNA (Papenfort *et al.*, 2013; Papenfort & Vanderpool, 2015).

Another role of Hfq in Gram-negative bacteria lies in the regulation of translation. As most RNA binding proteins, Hfq acts at the level of translation initiation but uniquely utilizes its RNA annealing activity. A commonly accepted mechanism for activation of translation was found for several sRNAs in *E. coli* (see Figure 3 B iii.) (Vogel & Luisi, 2011). There, translation of an mRNA is inhibited by an internal secondary structure that blocks the ribosomal binding site. Hfq facilitates duplexing of the mRNA with an sRNA which dissolves the original inhibitory structure and liberates the ribosomal binding site to allow translation initiation (Fröhlich & Vogel, 2009; reviewed by Papenfort & Vanderpool, 2015). The other way around, Hfq blocks translation by forming an mRNA-sRNA duplex that sequesters the

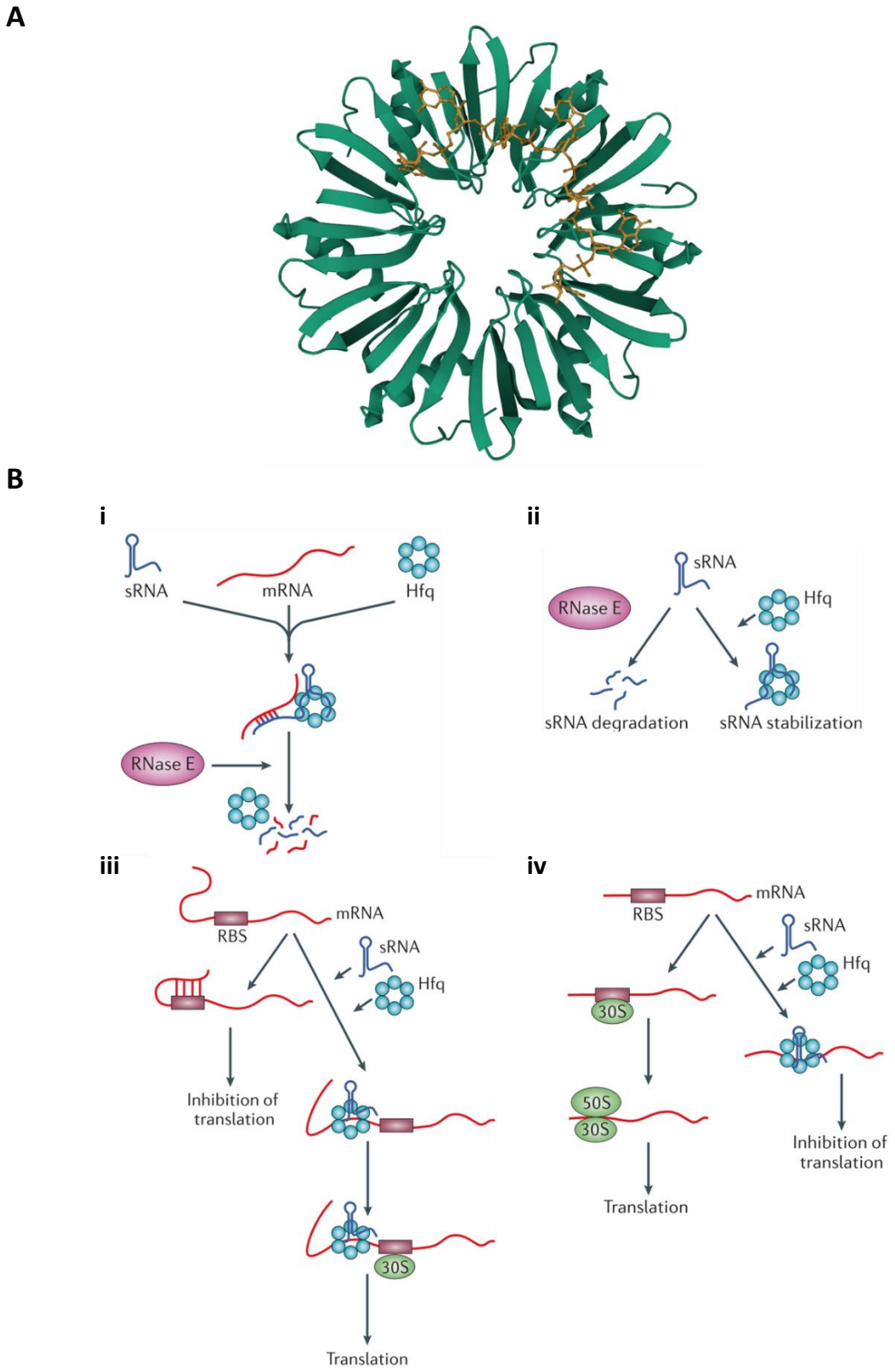

Figure 3: Structure and functions of the Hfq protein. (**A**) Crystal structure of the *B. subtilis* Hfq protein (green) in complex with an $(AG)_3A$ RNA aptamer (brown). Each subunit characteristically consists of an N-terminal α-helix followed by five antiparallel β-strands and ends with an unstructured C-terminus (Someya *et al.*, 2012). (**B**) Schematic examples how Hfq influences RNA decay and translation in *E. coli.* (**i**) Hfq promotes duplexing and degradation of sRNA and target mRNA. (**ii**) Hfq protects sRNAs from cleavage by RNase E. (**iii**) Hfq activates translation by duplexing sRNA with mRNA to resolve an internal hairpin that blocks the RBS. (**iv**) Hfq and/or sRNA sequester the ribosomal binding site (RBS) and block translation (adapted from Vogel & Luisi, 2011).

ribosomal binding site (see Figure 3 B iv.) (Vogel & Luisi, 2011). In addition to that, Hfq is also able to inhibit translation in the absence of sRNAs (Kavita *et al.*, 2018).

Even though the first solved Hfq structure was from *Staphylococcus aureus* (Schumacher *et al.*, 2002), most of the research on Hfq was performed in Gram-negative bacteria and the role of Hfq in Gram-positive bacteria remains elusive. An implication in sRNA-mediated gene regulation was so far only found in Listeria monocytogenes. There, Hfq facilitates binding of an sRNA to its target which influences translation and degradation of the mRNA (Nielsen *et al.*, 2009). However, studies in S. aureus and *B. subtilis* were not able to find a role for Hfq in promoting sRNA stability or sRNA-mRNA annealing (Bohn *et al.*, 2007; Heidrich *et al.*, 2007). It was hypothesized that the requirement of Hfq decreases with lower GC content as there are less stable RNA conformations that would need an RNA chaperone to loosen the interaction (Jousselin *et al.*, 2009). In *B. subtilis*, already the absence of Hfq has little or no influence on post-transcriptional gene regulation in hundreds of tested conditions (Rochat *et al.*, 2015). Moreover, of over 100 known or predicted sRNAs only six showed an altered abundance in a *B. subtilis* hfq deletion mutant (Hämmerle *et al.*, 2014). In addition to that, Hfq from *B. subtilis* and *S. aureus* show no detectable RNA annealing activity (Zheng et al., 2015). These findings could imply that Hfq may serve different functions. For example, the cyanobacterium *Synechocystis* harbors an Hfq protein with divergent RNA binding sites and was shown to be involved in motility by directly binding a subunit of the type IV pili (Schuergers *et al.*, 2014). Also a study in *B. subtilis* suggests a role in motility as Hfq enhances expression of flagellum and chemotaxis genes (Jagtap *et al.*, 2016). Taken together, Hfq does only play a subsidiary role in the RNA metabolism of *B. subtilis.* Therefore, it was proposed that other proteins could fulfill an Hfq-like role in *B. subtilis* such as the RNA chaperone CsrA (Müller *et al.*, 2019).

The major topic of this thesis however, revolves around another class of proteins which also were proposed to act as RNA chaperones. They were reported to interfere with all three processes of transcription, RNA decay, as well as translation: the cold shock proteins.

2.3 Cold shock proteins

Low temperature is an environmental stress factor that almost all species have to face. The bacterial cold shock response affects the growth rate, membrane structure and function, along with altered rates of DNA, RNA and protein synthesis (Weber & Marahiel, 2003). While many proteins expressed under optimal conditions are repressed at cold shock conditions, a subset of proteins exhibits increased expression (Graumann & Marahiel, 1996). The cold shock proteins belong to this group of cold-induced proteins. They comprise a widespread family that is present throughout the bacterial kingdom including psychrotrophic, mesophilic and thermophilic bacteria with only a few exceptions like *Helicobacter pylori* or *Mycoplasma genitalium* (Jones *et al.*, 1987; Graumann *et al.*,

1996; Mayr *et al.*, 1996; Graumann & Marahiel, 1996; Berger *et al.*, 1997; Mega *et al.*, 2010; Bisht *et al.*, 2014).

Structure and properties of cold shock proteins

Cold shock proteins are ~7.4 kDa small, globular and mostly acidic proteins that are comprised of a single RNA binding domain dubbed cold shock domain (see Figure 1) (Perl *et al.*, 1998; Graumann & Marahiel, 1998). It belongs to the oligonucleotide/oligosaccharide (OB) fold protein superfamily and is made up of about 67-73 amino acid residues that form a five-stranded antiparallel β-barrel (reviewed by Budkina *et al.*, 2020). The first crystal structure was solved for *B. subtilis* CspB, CspA from *E. coli,* and CspB from *B. subtilis caldolyticus* and *Thermotoga maritima* (see Figure 4) (Schnuchel *et al.*, 1993; Schindelin *et al.*, 1994; Mueller *et al.*, 2000; Kremer *et al.*, 2001). While the amino acid sequences of cold shock proteins from different species are significantly diverse, the eminent structural similarity is apparent (Budkina *et al.*, 2020). The structure of cold shock proteins is very similar to the S1 domain (Bycroft *et al.*, 1997). Interestingly, the S1 domain of PNPase can suppress the cold sensitivity phenotype of an *E. coli csp* quadruple mutant (Xia *et al.*, 2001). Likewise, the translation initiation factor IF-1 from *E. coli* adopts a very similar structure and suppresses the growth defect of a *cspB cspC* double mutant in *B. subtilis* (Weber *et al.*, 2001). These and more proteins belong to the OB fold superfamily and their structural similarities along with the functional redundancies may hint at a common origin from an ancient RNA binding protein (Holmqvist & Vogel, 2018; Amir *et al.*, 2019). While the OB fold superfamily comprises a large variety of proteins, the cold shock domain itself is also a part of other bacterial proteins such as the PNPase, RNase II, and RNase R (Hui *et al.*, 2014). Cold shock domains are conserved in all three kingdoms of life (Landsman, 1992; Schindelin *et al.*, 1993; Ermolenko & Makhatadze, 2002; Amir *et al.*, 2019; Heinemann & Roske, 2021). The majority of the cold shock domains is found in single-domain bacterial cold shock proteins whereas the eukaryotic analogues are often more complex (Heinemann & Roske, 2021). For example, the human CSDE1 protein contains five cold shock domains and the cold shock proteins of plants or the animal Y-box proteins contain additional structural domains of variable composition (Chaikam & Karlson, 2010; Heinemann & Roske, 2021). All cold-shock domains contain two RNA binding motifs dubbed RNP-1 and RNP-2 which belong to the most highly conserved residues (Landsman, 1992; Burd & Dreyfuss, 1994; Ermolenko & Makhatadze, 2002; Horn *et al.*, 2007; Heinemann & Roske, 2021).

As the RNA binding motifs suggest, cold shock domain containing proteins can bind RNA as well as single stranded DNA. Early on, it was shown for *B. subtilis* CspB, CspC and CspD to bind single stranded DNA and RNA *in vitro* (Graumann *et al.*, 1997). CspB preferentially binds thymidine-rich DNA sequences and a heptameric consensus sequence (5'-GTCTTTG/C) was identified (Lopez *et al.*, 2001; Morgan *et al.*, 2007). Accordingly, a crystal structure of CspB in complex with hexathymidine was

solved and revealed the principles of oligonucleotide binding by cold shock domains (Bienert *et al.*, 2004; Max *et al.*, 2006). The bases of DNA and RNA oligonucleotides are bound across a positively charged groove in which aromatic amino acids stack with the bases which further form hydrogen bond with the amino acid backbone and sidechains (see Figure 4) (Max *et al.*, 2006; Zeeb *et al.*, 2006; Sachs *et al.*, 2012). As a result of this geometry, binding of DNA and RNA by cold shock proteins presumably has little sequence specificity (Heinemann & Roske, 2021). This is in agreement with the global role of cold shock proteins in the physiology of bacterial cells.

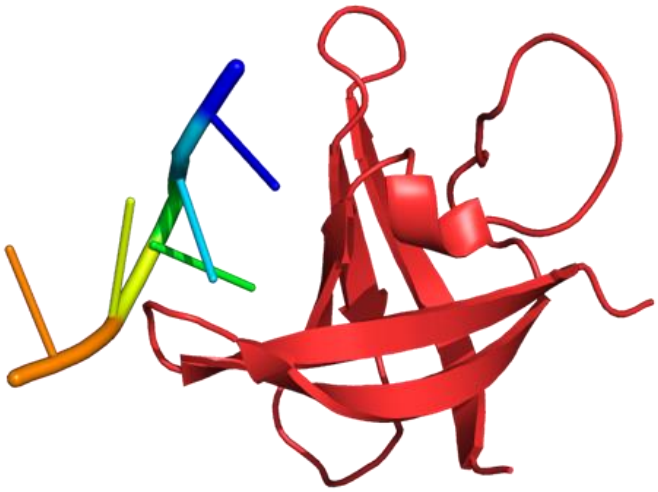

Figure 4: Structure of the *B. subtilis* cold shock protein CspB. Crystal structure of the *B. subtilis* CspB protein in complex with hexathymidine. A single strand oligonucleotide is bound in a positively charged groove. The binding bases face the protein while the backbone is oriented towards the solvent. PDB entry 2es2 (Max *et al.*, 2006).

Role of cold shock proteins at low temperatures

The identified cellular functions of bacterial cold shock proteins stem from their nucleic acid binding capabilities. Several cold shock proteins utilize nucleic acid binding to act as RNA chaperones that destabilize RNA secondary structures. This was shown for the *E. coli* CspA and CspE proteins that unwind different RNA secondary structures (Jiang *et al.*, 1997; Bae *et al.*, 2000; Phadtare *et al.*, 2002; Phadtare & Severinov, 2005; Rennella *et al.*, 2017). *E. coli* CspA can make up 13% of the total cellular protein synthesis at cold shock conditions (Goldstein *et al.*, 1990). Thus, it seems likely that it is involved in the adaptation to cold. Indeed, an *E. coli* quadruple mutant (Δ*cspA,* Δ*cspB,* Δ*cspG,* Δ*cspE*) exhibits a cold sensitive phenotype which can be suppressed by overexpression of any cold shock protein except for CspD (Xia *et al.*, 2001). RNAs form various secondary structures which can impede accessibility of the ribosomal binding site or interfere with ribosome movement (Budkina *et al.*, 2020). The formation of structured RNAs increases with low temperature and hence reduces translation efficiency (Ermolenko & Makhatadze, 2002). A commonly accepted hypothesis is that cold shock proteins act as RNA chaperones to unwind these structures and allow translation at low temperatures

(Jiang *et al.*, 1997; Ermolenko & Makhatadze, 2002; Barria *et al.*, 2013; Budkina *et al.*, 2020). In fact, an *E. coli cspA* mutant exhibits up to 40% loss of translation efficiency at cold shock conditions and additional deletion of *csp* genes almost diminishes translational activity (Zhang *et al.*, 2018). Following this, the authors proposed a cold stress response mechanism: At cold shock, RNAs are forming more secondary structures which globally decreases translation efficiency. Cold shock further induces a different structure in the *cspA* mRNA which stabilizes the transcript and reveals the ribosomal binding site (Fang *et al.*, 1997; Giuliodori *et al.*, 2010). Then, the increased CspA levels reduce the secondary structures in mRNAs globally and enable translation to continue at a higher rate (Zhang *et al.*, 2018). A cold sensitive phenotype was also found for the *B. subtilis cshB cspD* double mutant (Hunger *et al.*, 2006). Due to that, the authors proposed that the helicase and cold shock protein together reduce structured RNAs to maintain translation at cold. Interestingly, unique cold shock proteins may also contain an intrinsic structural temperature sensor. This was shown for a cold shock protein from the hyperthermophilic bacterium *Thermotoga maritima* which undergoes a conformational change to increase affinity for thymidine and uridine heptamers at a reduction of temperature (von König *et al.*, 2020).

Other physiological roles cold shock proteins

Of the nine *csp* genes encoded by *E. coli* (*cspA-I*) only four (*cspA, cspB, cspG, cspI*) are induced upon cold shock (Yamanaka *et al.*, 1998; Wang *et al.*, 1999). In comparison, *B. subtilis* encodes only three *csp* genes (*cspB, cspC, cspD*) which have been reported to exhibit at least transiently increased expression after cold shock (Willimsky *et al.*, 1992; Graumann *et al.*, 1997). However, they are all also highly expressed during optimal growth conditions with CspB and CspD even belonging to the 15 most abundant proteins in the cell (Eymann *et al.*, 2004; Nicolas *et al.*, 2012). This implies a role for cold shock proteins also at optimal temperatures. Indeed, cold shock proteins are established to globally act at optimal temperatures. Global transcription profiles in *E. coli* identified sets of genes that are up- or downregulated in *cspC* or *cspE* mutants (Phadtare *et al.*, 2006). In *S. enterica*, 20% of all genes are affected in a *csp* double mutant (Michaux *et al.*, 2017). Likewise, CspA of the Gram-positive bacterium *S. aureus* was shown to have a global impact on gene expression (Caballero *et al.*, 2018). It is unclear how cold shock proteins influence the cellular physiology in such a global way. There is a variety of possibilities, as they were shown to influence transcription, RNA stability, as well as translation.

E. coli CspE associates with nascent RNA from transcription elongation complexes which suggested a role in transcription (Hanna & Liu, 1998). Localization studies in *B. subtilis* further pointed towards and implication in transcription (Weber *et al.*, 2001). In fact, *E. coli* CspA, CspE and CspC act as so-called transcriptional antiterminators by utilizing their RNA melting function (Bae *et al.*, 2000; Phadtare *et al.*, 2002). Precisely, they inhibit the termination of transcription by destabilizing intrinsic

terminator hairpins. This was shown for the expression of operon genes far away from the promoter which would otherwise experience premature transcription termination (Bae *et al.*, 2000; Phadtare *et al.*, 2002). Due to that, cold shock proteins are discussed to be a source of global antitermination activity (Holmqvist & Vogel, 2018).

Furthermore, cold shock proteins are implicated in the stability of RNAs. For example, CspE from *E. coli* impedes RNA degradation by PNPase (Feng *et al.*, 2001). A similar effect was shown for the CspC protein which stabilizes the *rpoS* transcript in *E. coli* (Phadtare & Inouye, 2001; Phadtare *et al.*, 2006; Cohen-Or *et al.*, 2010). Likewise, the *S. enterica ecnB* mRNA contains several RNase E cleavage sites that are protected by cold shock proteins *in vivo* and *in vitro* (Chao *et al.*, 2017; Michaux *et al.*, 2017). CspA from *S. aureus* also influences the stability of its own mRNA. The *cspA* transcript is processed by RNase III to form a structure that is more stable and favored in translation (Lioliou *et al.*, 2012). By inhibiting the RNase III processing of the transcripts 5'-UTR, CspA negatively autoregulates its own expression (Caballero *et al.*, 2018).

Secondary structures in RNAs increase with low temperature and inhibit efficient translation but they also form at optimal temperatures. Thus, it is believed that cold shock proteins are globally acting RNA chaperones that contribute to general translation efficiency (Jiang *et al.*, 1997; Ermolenko & Makhatadze, 2002; Holmqvist & Vogel, 2018; Budkina *et al.*, 2020). Similarly, the *B. subtilis* cold shock proteins were proposed to facilitate translation initiation at optimal and low temperatures because they influence protein expression and bind RNAs (Graumann *et al.*, 1997). Evidence from *Arabidopsis* further suggests a role of cold shock proteins in translation as they were shown to interact with ribosomes (Juntawong *et al.*, 2013). Also in *B. subtilis*, an interaction of CspB with the ribosomal RpsB protein was found in a proteome wide protein-protein interaction screen (De Jong *et al.*, 2017).

2.4 Aims of the thesis

Despite all these evidences it is unclear if cold shock proteins influence the physiology globally by shaping one or all of these processes. Explanations usually attempted to combine the observed functions. In *B. subtilis* it was proposed that they act as global translational enhancers as well as coupling transcription and translation by providing unstructured mRNAs (El-Sharoud & Graumann, 2007). However, the function of cold shock proteins as antiterminators or RNA stabilizers is restricted to a few examples. Also, the idea that they function as RNA chaperones that generally facilitate translation has mostly evolved from the fact that they unwind RNA hairpins (Jiang *et al.*, 1997; Bae *et al.*, 2000). Except for the binding of nucleotides, none of these functions was shown for the cold shock proteins of *B. subtilis*. Moreover, there is evidence suggesting they do not only promote transcription and translation. For example, the cold shock proteins from *B. subtilis, B. caldolyticus and T. maritima* suppressed transcription and translation in an *E. coli* based cell free expression system (Hofweber *et*

al., 2005). In *Thermus thermophilus*, the deletion of one of the two *csp* genes had no effect on the transcriptome but only altered the protein levels (Tanaka *et al.*, 2012). No matter which organism, the specific molecular mechanism by which cold shock proteins influence these processes is yet to be uncovered. It is further unclear, how they recognize their RNA targets *in vivo*. A recent study in *S. aureus* suggests, the cold shock proteins exhibit functional specificity that can be altered by exchange of a single amino acid (Catalan-Moreno *et al.*, 2020). Hence, it is also interesting whether cold shock proteins work redundantly or have evolved distinct functional specializations.

This study aimed to sharpen the vague definition of cold shock protein function in *B. subtilis* and contribute to a wholistic understanding. On the grounds that *B. subtilis* contains only three *csp* genes, it serves as a good model system to simplify research on that matter. To uncover the implication of cold shock proteins in various cellular processes, *csp* mutants were phenotypically characterized at optimal and low temperature. Suppressor screens gave further insights into the redundancy and cellular interrelations of the cold shock proteins. The regulation of *csp* expression was investigated by looking at reporter gene expression in *csp* mutant backgrounds and at low temperature. Pull-down experiments were used to screen for cellular RNA targets of CspD. To investigate possible functional overlaps as well as functional specializations, complementation experiments with cold shock protein variants were performed. Global transcriptome analysis of a *csp* double mutant revealed an impact on a large number of transcripts. Moreover, various putative cellular targets of cold shock proteins could be identified. *In vivo* and *in vitro* assays were used to investigate the role of cold shock proteins in the termination of transcription. Finally, the stability and processing of several mRNAs was analyzed.

3. Materials and Methods

3.1 Materials

A complete list of used materials, *i.e.* chemicals, antibodies and enzymes, commercial systems, equipment, and software can be found in the appendix Chapter 7.

3.1.1 Bacterial strains and plasmids

Bacterial strains and plasmids are listed in the appendix Chapter 7.

3.1.2 Media, buffers, and solutions

General preparation of media, buffers and solutions

Media, buffers and solutions were prepared with dH_2O (if not indicated otherwise) and autoclaved for 20 min at 121°C and 1 bar excessive pressure. Heat sensitive substances were sterilized by filtration. Recipes for buffers and solutions are listed with the respective method in Chapter 3.2.

Bacterial growth media

LB medium was used for the cultivation of bacteria. Some *B. subtilis* strains were grown on SP medium plates. Solid media were prepared by addition of 1.5% (w/v) agar.

LB medium (1 l):	Tryptone	10 g
	Yeast extract	5 g
	NaCl	10 g
10x MN medium (1 l):	$K_2HPO_4 \times 3\ H_2O$	136 g
	KH_2PO_4	60 g
	Sodium citrate × 2 H_2O	10 g
1× MNGE medium (10 ml):	10× MN medium	1 ml
	Glucose (50% (v/v))	400 µl
	Potassium glutamate (40% (v/v))	50 µl
	Ammonium iron citrate (2.2 mg ml^{-1})	50 µl
	Tryptophan (5 mg ml^{-1})	100 µl
	$MgSO_4$ (1 M)	30 µl
	+/- CAA (10% (w/v))	100 µl
	dH_2O	8.37 ml

SP medium (1 l):	Nutrient Broth	0.8 g
	$MgSO_4 \times 7\ H_2O$	0.25 g
	KCl	1 g
	Autoclave & after cooling add:	
	$CaCl_2$ (0.5 M)	1 ml
	$MnCl_2$ (10 mM)	1 ml
	Ammonium iron citrate (2.2 mg ml^{-1})	2 ml

Antibiotics

All antibiotics were prepared as 1000-fold concentrated stock solutions and dissolved in dH_2O except for chloramphenicol, erythromycin, and tetracycline, which were dissolved in 70% ethanol. The stocks were sterilized by filtration and stored at -20°C. Autoclaved medium was cooled down to approximately 50°C before addition of antibiotics.

Selective concentrations for *E. coli*:	Ampicillin	100 µg ml^{-1}
	Chloramphenicol	50 µg ml^{-1}
	Kanamycin	100 µg ml^{-1}
Selective concentrations for *B. subtilis*:	Chloramphenicol	5 µg ml^{-1}
	Erythromycin[1]	2 µg ml^{-1}
	Kanamycin	10 µg ml^{-1}
	Lincomycin[1]	25 µg ml^{-1}
	Spectinomycin	150 µg ml^{-1}
	Tetracycline	12.5 µg ml^{-1}

[1] For selection on erythromycin, combined use with lincomycin in the indicated concentration is necessary in order to exert a selective pressure.

3.2. Methods

3.2.1 General methods

The founding literature of the general methods used in this study is listed in the following table.

Table 1: General methods used in this study.

Method	Reference
Determination of optical density	Sambrook *et al.*, 1989
Determination of protein amounts	Bradford, 1976
Ethidium bromide staining of nucleic acids	Sambrook *et al.*, 1989
Gel electrophoresis of DNA	Sambrook *et al.*, 1989
Gel electrophoresis of proteins (denaturing)	Laemmli, 1970
Ligation of DNA fragments	Sambrook *et al.*, 1989
Plasmid preparation from *E. coli*	Sambrook *et al.*, 1989
Precipitation of nucleic acids	Sambrook *et al.*, 1989
Sequencing according to the chain termination method	Sambrook *et al.*, 1989

3.2.2 Cultivation and storage of bacteria

E. coli was grown in Erlenmeyer flasks or reaction tubes with LB medium over night at 37°C or 28°C with shaking at 200 rpm. If not stated otherwise, *B. subtilis* was grown in Erlenmeyer flasks or reaction tubes with LB or MNGE medium at 37°C or 28°C at 200 rpm. Growth was monitored by measuring the optical density at 600 nm. For inoculation, bacteria from cryo-stocks or single colonies were used. Cryo-stocks were prepared by mixing 400 µl glycerol (50% (v/v)) with 600 µl of an overnight culture, or 100 µl DMSO (100%) with 900 µl of an overnight culture. The stocks were snap frozen in liquid nitrogen and stored at -80°C.

Sequential evolution of strains

A cryo culture from the respective strain was used to inoculate 4 ml liquid LB medium with the corresponding antibiotics and was incubated at 37°C with shaking at 220 rpm overnight. This was counted as the first passage. The next day, 100 µl of the first passage were used to inoculate 10 ml LB medium with the appropriate antibiotics and incubated over the day at the previous conditions. In the evening, 100 µl were transferred to 10 ml LB medium with the appropriate antibiotics and incubated as described.

Biofilm analysis

To investigate biofilm-matrix production, a fresh colony of the strain of interest was used to inoculate 4 ml LB medium with the appropriate antibiotics and was incubated at 37°C and 200 rpm to an OD_{600} of 0.5 - 0.9. Then, 10 µl of the culture were dropped on an MSgg-agar plate prepared as described below. The plates incubated for 30 mins under a laminar flow cabinet until all drops were dried. The plates were incubated at 30°C for 5 days. MSgg-agar was prepared in the following order: Salts and additives were mixed as indicated below and H_2O was added to a volume of 200 ml. The solution was warmed to 55°C. Bacto-agar was prepared as indicated below with 300 ml H_2O followed by autoclaving and cooling to 55°C. Both solutions were mixed and final concentrations of 20 µg/ml Coomassie brilliant blue and 40 µg/ml Congo red were added. Plates were poured in large petri dishes or using 12 ml of MSgg-agar for a small Petri dish. Colonies were photographed a using stereo microscope (Carl Zeiss Microscopy) equipped with digital camera AxioCam MRc.

MSgg-agar

Component	**[Stock]**	**Volume [ml]**	**Final conc.**	**Sterilization**
Potassium phosphate buffer pH 7.0	1 M	2.5	5 mM	autoclave
MOPS pH 7.0	1 M	50	100 mM	filter sterilize, store in the dark at 4°C
Glycerol	50%	5	0.5%	autoclave
Thiamine	20 mM	0.05	2 µM	filter sterilize
Potassium glutamate	40%	6.25	0.5%	Autoclave, store at 4°C
L-Tryptophane	5 mg/ml	5	50 µg/µl	filter sterilize, store at 4°C
L-Phenylalanine	10 mg/ml	2.5	50 µg/µl	filter sterilize, store at 4°C
$MgCl_2$	1 M	1	2 mM	filter sterilize
$CaCl_2$	1 M	0.35	700 µM	filter sterilize
$MnCl_2$	10 mM	2.5	50 µM	filter sterilize
$FeCl_3$ - make fresh!	50 mM	0.5	50 µM	filter sterilize
$ZnCl_2$	1 mM	0.5	1 µM	filter sterilize
dH_2O		ad to 200 ml		autoclave
Bacto-agar	7.5 g	in 300 ml H_2O		autoclave

3.2.3 Genetic modification of bacteria

Fast method for preparation of competent E. coli cells

For the preparation of competent cells, the well-established $CaCl_2$ method was employed (Lederberg & Cohen, 1974). An overnight pre-culture of the required *E. coli* strain was used to inoculate 10 ml LB to an OD_{600} of 0.1 in a 100 ml shake flask. The culture was grown at 37°C to an OD_{600} of about 0.3 and harvested by centrifugation for 6 min at 5,000 rpm and 4°C. The pellet was re-suspended in 5 ml of an ice-cold 50 mM $CaCl_2$ solution and incubated for 30 min on ice. Then, harvesting as just described and re-suspension of the pellet in 1 ml of the ice-cold $CaCl_2$ solution resulted in competent cells ready for transformation.

Method for preparation of storable competent* E. coli *cells

In order to produce larger amounts of competent cells that are storable, a different method was used (Inoue *et al.*, 1990). A 20 ml LB pre-culture grown for 20 h at 28°C with shaking was used to inoculate 250 ml SOB medium supplemented with $MgCl_2$ (10 mM) and $MgSO_4$ (10 mM) in a 2 l shake flask. The culture was grown at 18°C with shaking to an OD_{600} of 0.5-0.9 (20-24 h). The whole flask was then cooled on ice for 10 min followed by harvesting *via* centrifugation for 5 min at 5,000 rpm. Re-suspension of the pellet in 20 ml ice-cold transformation buffer (TB) resulted in competent cells. Addition of DMSO to a final concentration of 7% allowed the storage of 200 µl aliquots at -80°C after snap freezing in liquid nitrogen.

SOB medium (1 l)	Tryptone	20 g
	Yeast extract	5 g
	NaCl	0.584 g
	KCl	0.188 g
	$MgCl_2$	2.032 g
	$MgSO_4$	2.064 g
	dH_2O	add to 1000 ml
TB (1 l)	PIPES	3.04 g
	$CaCl_2 \times H_2O$	2.2 g
	KCl	18.64 g
	$MnCl_2 \times H_2O$	10.84 g
	dH_2O	add to 1000 ml

Transformation of competent* E. coli *cells

Aliquots of frozen competent cells were thawed on ice before transformation. 200 µl of these, or of freshly made competent cells were mixed carefully with at least 5 ng DNA and incubated on ice for 30 min. The cells were heat-shocked by incubation at 42°C for 90 sec followed by cooling on ice for 5 min. After that, 1 ml LB was added and the cells were incubated for 1 h at 37°C with shaking. 50 µl of the cells and the remaining concentrated cells were propagated on LB agar containing the appropriate antibiotics.

Preparation of competent* B. subtilis *cells

The laboratory strain *B. subtilis* 168 easily develops natural competence under conditions of nutritional starvation within the stationary growth phase (Hamoen *et al.*, 2003). An overnight culture grown at 28°C was used to inoculate 10 ml 1× MNGE medium (see section 3.1.2) to an OD_{600} of 0.1. The culture was grown at 37°C and 220 rpm to an OD_{600} of about 1.3. Nutritional starvation is achieved by a 1:1 dilution with 10 ml pre-warmed 1× MNGE medium without CAA and incubation for 1 h under the previous conditions. The competent cells prepared in this way, could directly be used for transformation or prepared for long-term storage. Preparation for storage was done by harvesting 15 ml of the culture at 5,000 rpm for 5 min, re-suspension of the pellet in 1.8 ml of the supernatant and addition of 1.2 ml glycerol (50% (v/v)). 300 µl aliquots of competent cells were stored at -80°C after freezing in liquid nitrogen.

Transformation of competent* B. subtilis *cells

For transformation of cryo-stored competent cells, a 300 µl aliquot was thawed at room temperature and mixed with 1.7 ml 1× MN medium supplemented with 43 µl glucose (20% (v/v)) and 34 µl 1 M $MgSO_4$. 400 µl of this mix or of freshly made competent cells were incubated with 0.1 µg-1 µg DNA (2 µg plasmid DNA) for 30 min at 37°C and 220 rpm. After that, 100 µl of expression mix were added and the sample incubated for 1 h under the previous conditions. Then 100 µl and the concentrated remaining cells were propagated on LB or SP agar supplemented with the respective antibiotics.

Expression mix	Yeast extract	5 %
	CAA	10% (w/v)
	Tryptophan	5 mg ml^{-1}
	dH_2O	Solvent

3.2.4 Methods for working with DNA

Isolation of DNA

Cultures for DNA isolation were grown overnight at 37°C and 220 rpm. For isolation of chromosomal DNA, the peqGOLD Bacterial DNA Kit from PEQLAB was used. Incubation with lysozyme was prolonged to 30 min. All remaining steps were performed according to the manufacturer's instructions. Plasmid DNA was isolated with the NucleoSpin Plasmid Kit from Macherey-Nagel following the manufacturer's instructions.

Agarose gel electrophoresis for DNA

For separation of DNA fragments by size they were mixed with 5× DNA loading dye and loaded onto an agarose gel consisting of 25 ml 1% (w/v) agarose in 1× TAE buffer supplemented with 3 µl HDGreen™ Plus DNA stain (Intas). Depending on the capability of the used chamber, a voltage of 120 V or 150 V was applied for 30 min or 15 min respectively, or until the bromophenol had reached the last quarter of the gel. DNA was detected under UV light at 254 nm using a GelDoc™ XR (Biorad). As a size standard, λ-DNA cleaved by *Eco*RI and *Hind*III was used.

50× TAE buffer	Tris-base	242 g
	Acetic acid (100%)	57.1 ml
	$Na_2EDTA \times 2\ H_2O$ (0.5 M pH 8.0)	100 ml
	dH_2O	Add to 1,000 ml
5× DNA loading dye	Glycerol (100%)	5 ml
	50× TAE buffer	0.2 ml
	Bromophenol blue	10 mg
	dH_2O	4.8 ml
	Optional:	
	Xylene cyanol	10 mg
	Cresol red	25 mg

Polymerase chain reaction (PCR)

For PCR reactions, chromosomal DNA, plasmid DNA, or PCR product served as template. Fusion polymerase (Biozym) with high proofreading activity was used for cloning procedures while Dream*Taq* polymerase (ThermoScientific) was used for check PCRs. Products were purified using the PCR Purification Kit (Quiagen) following the manufacturer's instructions.

100 µl Fusion sample	
5× HF/GC buffer	20 µl
dNTPs (12.5 µmol ml^{-1})	4 µl
Forward primer (5 µM)	4 µl
Reverse primer (5 µM)	4 µl
Template DNA (10 ng $µl^{-1}$)	1 µl
Fusion DNA Polymerase	0.5 µl
dH_2O	66.5 µl

Thermocycler program for Fusion PCR

	Step	**Temperature**	**Time**
	Initial denaturation	98°C	3 min
30×	Denaturation	95°C	30 sec
	Annealing	Variable	35 sec
	Elongation	72°C	Variable (30 sec / kbp^{-1})
	Final elongation	72°C	10 min
	Hold	4°C	∞

100 µl Dream*Taq* sample	
10× *Taq* buffer	10 µl
dNTPs (12.5 µmol ml^{-1})	4 µl
Forward primer (5 µM)	4 µl
Reverse primer (5 µM)	4 µl
Template DNA (10 ng $µl^{-1}$)	1 µl
Dream*Taq* DNA Polymerase	0.5 µl
dH_2O	75.5 µl

Thermocycler program for Dream*Taq* PCR

	Step	**Temperature**	**Time**
	Initial denaturation	95°C	3 min
30×	Denaturation	95°C	30 sec
	Annealing	Variable	35 sec
	Elongation	72°C	Variable (1 min / kbp^{-1})
	Final elongation	72°C	10 min
	Hold	4°C	∞

Long flanking homology PCR (LFH-PCR)

In order to delete genes in *B. subtilis*, its native capability of homologous recombination was utilized. The long flanking homology PCR (LFH-PCR) technique that was originally developed for *S. cerevisiae* (Wach, 1996) was used for construction of a disruption cassette. The cassette consists of an antibiotic resistance gene which was fused to an up- and downstream region of ~1 kbp size that flank the target gene. The resistance genes were amplified from the plasmids pGEM-cat (chloramphenicol), pDG170 (kanamycin), pDG646 (erythromycin), pDG1726 (spectinomycin), and pDG1513 (tetracycline) (Guérout-Fleury *et al.*, 1995) with primers that attach short overhangs of 25 bp. Complementary overhangs were further generated by the primers annealing to the 3'-end of the upstream region and to the 5'-end of the downstream region. It is also to note that the 3'-end of the upstream region and

the 5'-end of the downstream region extended into the target gene as far as needed to conserve all expression signals of genes that shall remain intact. The actual LFH-PCR was two-stepped. In the first step, the three fragments were fused together to form the disruption cassette. They annealed due to the complementary overhangs attached to the primers, resulting in the upstream region fused to the 5'-end of the resistance gene and its 3'-end fused to the downstream region. In the second step, the disruption cassette was amplified by use of the forward primer of the upstream region and the reverse primer of the downstream region. The product was then used for transformation of appropriate *B. subtilis* strains where it was integrated *via* double-homologous recombination. Successful integration was checked by selection for the antibiotic resistance and check-PCR. Integrity of the up- and downstream regions was checked by Sanger sequencing with primers annealing outside of the regions.

100 µl LFH-PCR sample

5× HF buffer	20 µl
dNTPs (12.5 µmol ml^{-1})	4 µl
[Forward primer (5 µM)	8 µl]
[Reverse primer (5 µM)	8 µl]
Upstream region	200 ng
Downstream region	200 ng
Resistance gene	300 ng
Fusion DNA Polymerase	2 µl
dH_2O	Add to 100 µl

Two-step thermocycler program for LFH-PCR

	Step	Temperature	Time
	Initial denaturation	98°C	3 min
10×	Denaturation	98°C	30 sec
	Annealing	Variable	35 sec
	Elongation	72°C	Variable (1 min / kbp^{-1})
	Hold	4°C	∞
	[Addition of primers]		
	Denaturation	98°C	30 sec
25×	Annealing	Variable	35 sec
	Elongation	72°C	Variable (1 min / kbp^{-1}) + variable sec $cycle^{-1}$
	Final elongation	72°C	10 min
	Hold	4°C	∞

Combined chain reaction (CCR)

CCR allows the insertion of site-specific mutations as used for the *cspC* variant. The method uses two primers that anneal at the edges of the gene of interest, and one mutagenic primer that hybridizes more strongly to the template than the external primers. The mutagenic primer is phosphorylated at its 5'-end to enable ligation with the upstream sequence by a thermostable ligase. It is important that the used Polymerase does not exhibit 5'→3' exonuclease activity, to prevent degradation of the extended primers (Blötz *et al.,* 2017). The used reaction mix and thermocycler program are listed below.

CCR reaction mix

Forward primer (20 pmol)	2 µl
Reverse primer (20 pmol)	2 µl
Mutagenesis primer (20 pmol)	4 µl
Template DNA (plasmid or PCR product)	1 µl
5× HF buffer	10 µl
dNTPs (each 12.5 µmol ml^{-1})	2 µl
Fusion DNA Polymerase	1 µl
Ampligase	3 µl
BSA (20 mg/ml)	2 µl
dH_2O	23 µl

CCR thermocycler program

	Step	Temperature	Time
	Initial denaturation	95°C	5 min
30×	Denaturation	95°C	1 min
	Annealing	52°C	1 min
	Elongation	68°C	Variable (1 min / kbp^{-1})
	Final elongation	68°C	10 min

The product containing the desired mutation was purified using the PCR Purification Kit (Quiagen) and following the manufacturer's instructions. The mutated *cspC* variant was then used as upstream region in an LFH-PCR.

Cloning procedures

The plasmid and the insert to be integrated were digested by incubation with FastDigest endonucleases (ThermoFisher) according to the manufacturer's instructions. Incubation times ranged from 15 min to 40 min depending on star activity of the used enzyme. To prevent re-ligation of the linearized plasmid it was dephosphorylated with FastAP (alkaline phosphatase) (ThermoFisher). Hence, 1 µl of FastAP enzyme was added to the digestion mixture and incubated for at least 5 min. Subsequently, the DNA was purified using the PCR Purification Kit (Quiagen) following the manufacturer's instructions.

Ligation was done by mixing 2 µl T4 DNA ligase (ThermoFisher) with 2 µl 10× Ligation buffer (ThermoFisher) and at least 250 ng insert and 50 ng plasmid complemented with dH_2O to a total volume of 20 µl. Depending on the construct, an insert to plasmid ratio of 3:1 up to 10:1 was used. Ligation took place for at least 2 h at room temperature or overnight on ice at RT so that the ice melts until the next morning. The whole ligation sample was used to transform 200 µl of competent *E. coli* cells.

Sequencing of DNA

PCR products and plasmids were sequenced by Microsynth AG (Göttingen). Whole genome sequencing of chromosomal DNA was conducted by the Göttingen Genomics Laboratory (G2L).

3.2.5 Methods for working with RNA

Isolation of RNA

The strains of interest were cultivated in 4 ml LB medium at 37°C over the day. In the evening, 50 ml LB medium were inoculated with the overday cultures and cultivated at 28°C or 37°C (GP1971) overnight. At the next morning, 100 ml LB medium were inoculated to an OD_{600} of 0.1 and incubated to the desired OD_{600}. Cells were harvested by transferring 25 ml of the culture into a 50 ml Falcon tube with 15 ml frozen killing buffer. After melting of the killing buffer, the cells were harvested by centrifugation at 8,000 rpm and 4°C. The supernatant was removed and the cell pellet was immediately snap-frozen in liquid nitrogen and stored at -80°C if necessary.

Cells were disrupted using a Mikro-Dismembrator (Sartorius). For that, the pellets were re-suspended in 200 µl RNase-free water and transferred into the liquid nitrogen of the Mikro-Dismembrator box. The box was closed with the frozen sample and ran for 3 min at 1,800 rpm. The powder was then re-suspended in 2 ml RLT plus buffer (RNeasy Plus kit, Qiagen) with 20 µl β-mercaptoethanol and transferred into a microfuge tube. After centrifugation for 5 min at 13,000 rpm at 4°C, RNA isolation was performed with the RNeasy Plus kit (Qiagen) as described in the manufacturer's manual.

After isolation of RNA, residual DNA was eliminated using DNase I (ThermoFisher) following the manufacturer's instructions. Removal of DNA was tested *via* PCR.

Killing buffer	Tris-HCl	20 mM
	$MgCl_2$	5 mM
	dH_2O	Add to 1,000 ml
		After autoclaving add
	NaN_3	20 mM

Synthesis of cDNA

First strand cDNA was synthesized with the RevertAid First Strand cDNA Synthesis Kit (ThermoFisher) according to the manufacturer's instructions. For quantitative RT-PCR, cDNA was synthesized with the One-Step RT-PCR kit (BioRad) as described below.

Quantitative reverse transcription-PCR (qRT-PCR)

RNAs were isolated as described and the presence of residual DNA after DNase I treatment was tested *via* PCR. All used primers were designed so that they amplify ~150 bp, have a length of ~20 bp and an annealing temperature of ~60°C with as little de*via*tion as possible. All reactions used the One-Step RT-PCR kit (BioRad). The primer pairs were pre-mixed and pre-pipetted. A master mix was prepared following the recipe below and pipetted to the primers by reverse-pipetting. All qRT-PCR reactions were performed at least in technical triplicates and with a no template control. qRT-PCR was carried out on the iCycler instrument (BioRad) following the manufacturer's recommended protocol with the program adjusted as described below. The *rpsE* and *rpsJ* genes that encode constitutively expressed ribosomal proteins were used as internal controls to allow normalization of the generated Ct values. Data analysis and the calculation of expression ratios as fold changes were performed with the ΔΔCt method as follows:

$$\Delta\Delta\mathrm{Ct} = \mathrm{RNA2}(\mathrm{Ct} - \mathrm{Ct}[\mathrm{constant}]) - \mathrm{RNA1}(\mathrm{Ct} - \mathrm{Ct}[\mathrm{constant}])$$

$$\text{Fold change} = 2^{-\Delta\Delta\mathrm{Ct}}$$

Ct = Threshold cycle

Ct[constant] = Median of the *rpsE* and *rpsJ* genes in the respective strain (*e.g.* RNA1)

RNA1 = RNA of the wild type 168

RNA2 = RNA of the mutant (GP1971)

20 µl qRT-PCR reaction mix (one reaction)

2× SYBR Green reaction mix (BioRad)	10 µl
Forward primer (20 pmol)	1.2 µl
Reverse primer (20 pmol)	1.2 µl
Reverse transcriptase (BioRad)	0.2 µl
Template RNA	100 ng/ 20 µl
H_2O RNase-free	∑ 17.6 µl

qRT-PCR thermocycler program

	Step	Temperature	Time
	1	50°C	10 min
	2	95°C	1 min
40×	3	95°C	10 sec
	4	54°C	20 sec
	5	95°C	1 min
	6	55°C	1 min
81×	7	55°C	10 sec

In vitro *transcription termination assay*

The respective template was amplified *via* PCR and purified using the PCR Purification Kit (Quiagen) following the manufacturer's instructions. A reaction mixture was mixed as described below and T7 RNA polymerase (Roche) was added before CspB. The complete reaction mix was incubated for 5 min at room temperature followed by *in vitro* transcription at 37°C for 4.5 h. Then, 10 µl DNase I 50 U/µl (ThermoFisher) were added and the reaction was incubated at 37°C for 1 h. The reaction was then mixed with one volume (120 µl) Phenol:Chloroform:Isoamylaclohol (25:24:1) (PCI) and shaken vigorously by pipetting up and down for 30 sec. The mixture was transferred to a pre-spun 2 ml Phase Lock gel heavy tube (Quantabio) to allow separation of RNA, DNA and proteins. The mixture was incubated for 2 min at room temperature and centrifuged for 30 min at 14,800 rpm at 4°C. The upper phase which contains the RNA was transferred into a fresh microfuge tube and three volumes (360 µl) of ice-cold 96% EtOH:4 M LiCl (30:1) as well as 1.5 µl Glycoblue (Ambion) were added and mixed well. The RNA precipitated over night at -20°C. The next day, the mixture was centrifuged for 30 min at 14,800 rpm and 4°C. The supernatant was discarded carefully by pipetting and the RNA pellet was washed by adding 100 µl ice-cold 70% EtOH without re-suspending the pellet. The pellet was air-dried in open microfuge tubes for 20 min in a laminar flow cabinet. The RNA was dissolved by addition of 30 µl RNase-free water followed by shaking at 37°C for 1 h. Absence of residual DNA was tested *via* PCR. 25 µl of RNA were mixed with 5 µl 6× RNA loading dye and separated *via* denaturing agarose gel electrophoresis for RNA as described below.

50 µl *in vitro* transcription mix

DNA template	250 ng
1× ZAP buffer	= volume of added CspB (only add in sample without CspB!)
50% Glycerol	= volume of added CspB
NTP Mix 12.5 mM (Roche)	20 µl
10× Transcription buffer (Roche)	10 µl
RNase Inhibitor 40 U (Roche)	1 µl
DTT 1 M	2 µl
T7 RNA polymerase 80 U (Roche)	4 µl
CspB	40 µM
H_2O RNase free	Add to 100 µl

6× RNA loading dye	Glycerol	50% (v/v)
	SDS	0.075% (v/v)
	Xylene cyanole	0.075% (w/v)
	$Na_2EDTA \times 2\ H_2O$	0.15 mM (w/v)
	Formamide	Add to 100% (v/v)

Denaturing agarose gel electrophoresis for RNA

An agarose gel was prepared as described in the recipe below. Samples for Northern blotting were mixed with 2× sample buffer and samples from the *in vitro* antitermination assay were mixed with 6× RNA loading dye. All samples were heated for 10 min at 65°C. Samples were added to the gel and RNA was separated at 90 V.

10× MOPS buffer	MOPS	200 mM
	Na-Acetate	50 mM
	$Na_2EDTA \times 2\ H_2O$	10 mM
	Adjust pH with NaOH to 7.0 and filter-sterilize	

RNA agarose gel (100 ml)	Agarose	1 g
	Add 72 ml H_2O and boil	
	Let cool to 80°C and add:	
	Formaldehyde (37%)	18 ml
	10× MOPS	10 ml
	HDGreen™ Plus (Intas)	14 µl
	Cool gel to 4°C before use	

2× RNA sample buffer	Formamide	95% (v/v)
	SDS	0.025% (w/v)
	Bromophenol blue	0.025% (w/v)
	Xylene cyanole	0.025% (w/v)
	$Na_2EDTA \times 2\ H_2O$	0.05 mM (v/v)

Northern blotting

Northern probes were generated by amplifying a 200-500 bp DNA template from chromosomal DNA which served as template for *in vitro* transcription. A T7 RNA polymerase promoter sequence (CTAATACGACTCACTATAGGGAGA) was added in the 5'-extension of the reverse primer. The *in vitro* transcription was performed with the DIG RNA T7 labeling kit (Roche) following the manufacturer's instructions. Probes were tested by dropping a dilution series on a nylon membrane, followed by cross-linking and detection as described for Northern blots below.

Total RNA was extracted as described above and 5 µg RNA per lane were separated *via* denaturing agarose gel electrophoresis as described above. A positively charged nylon membrane was incubated in H_2O and placed in a vacuum blotting device with the agarose gel on top of it, excluding any air bubbles in between. Firstly, the top of the gel was covered with denaturing solution and incubated for 15 min at 60 mbar. At next, the gel was covered with neutralization solution and incubated for 15 min at 60 mbar. Final blotting proceeded for at least 4 h at 80 mbar while always keeping the top of the gel covered with 20× SSPE. After blotting, the RNA was cross-linked to the membrane by applying UV light for 90 sec to the RNA side. The membrane was then incubated for 1 h in 25 ml pre-hybridization solution at 68°C in a hybridization oven. The hybridization solution was discarded and the RNA probe diluted in 5 ml pre-hybridization solution was added and incubated over night at 68°C in a hybridization oven. The next day, the probe was removed and stored at -80°C for further uses. The membrane was then washed twice with 1× P1 for 5 min at room temperature followed by washing twice with 1× P2 for 15 min at 68°C in a hybridization oven. Then, the membrane was covered with 1× Dig P1 for 5 min and from here on incubated at gentile shaking in a plastic box at room temperature. The solution was discarded, and 45 ml 1× Dig P1 and 5 ml 10× blocking solution were added and incubated for 30 min. 5 µl of Anti-Digoxigenin-AP Fab fragments were added (1:10,000) and incubated for another 30 min. After that, the membrane was washed three times with 1× Dig P1 for 10 min. Before detection, the membrane was incubated with P3 for at least 30 min up to 3 h. Detection was started by adding 5 µl CDP star (Invitrogen) in 1 ml P3 and the signal of the chemiluminescent reaction product was detected with a ChemoCam imager (Intas).

20× SSC	NaCl	3 M
	Na_3 citrate × 2 H_2O	0.3 M
		Adjust pH with HCl to 7.0
	dH_2O	Add to 1,000 ml
20× SSPE	NaCl	3 M
	NaH_2PO_4	0.2 M
	Na_2EDTA	0.02 M
		Adjust pH with NaOH to 7.4
	dH_2O	Add to 1,000 ml
10× Dig P1	Maleic acid	1 M
	NaCl	1.5 M
	NaOH	~70 g
	dH_2O	Add to 1,000 ml
		Adjust pH with NaOH to 7.4
P1	SSC	2× (100 ml 20× SSC)
	SDS	0.1% (v/v)
	dH_2O	Add to 1,000 ml
P2	SSC	0.5× (25 ml 20× SSC)
	SDS	0.1% (v/v)
	dH_2O	Add to 1,000 ml
P3	Tris-base	0.1 M
	NaCl	0.1 M
	dH_2O	Add to 1,000 ml
		Verify pH of 9.5
10× Blocking solution	Blocking reagent (Roche)	10 g
	Dig P1	1× (10 ml 10× Dig P1)
	dH_2O	Add to 1,000 ml
		Autoclave and freeze for long-term storage
Denaturing solution	NaOH	50 mM
	NaCl	10 mM
	dH_2O	Add to 1,000 ml

Neutralization solution	Tris-base	0.1 M
		Adjust pH with HCl to 7.4
	dH_2O	Add to 1,000 ml

Pre-hybridization solution	SSC	5× (7.5 ml 20× SSC)
	Blocking solution	1× (3 ml 10× blocking solution)
	N-Laurosylsarcosine	0.3 % (v/v)
	SDS	7 % (w/v)
	Formamid	50% (v/v)
	dH_2O	Add to 30 ml

Quantification of Northern blots* via *densitometry and calculation of RNA half-life

Densitometry was performed similar to the analysis of Western blot signals using the Gel Analysis method outlined in the ImageJ manual and following the protocol of the SYBIL project (https://www.sybil-fp7.eu/node/95) (Schneider *et al.*, 2012). The Northern blot image with distinct signal formation was imported to ImageJ. The first lane was selected using the square selection tool without selecting any neighboring band while pressing Ctrl + 1 to set it as the first lane. The center of the square was clicked and dragged across to the second lane and Ctrl + 2 was pressed to mark it as the second lane. This was performed until the final lane where Ctrl + 3 was pressed to mark it as the final lane. In the pop-up window, the line tool was used to draw lines between the beginning and the ending of the peak to eliminate the background from the calculations. This was done for each peak. Calculation was started by highlighting the area underneath the peak with the magic wand tool. Each lane was measured three times with varying rectangle sizes and the mean was calculated. Percental decay of the band intensity was calculated by setting the value obtained for 0 min after addition of rifampicin to 1 and the following time points after addition of rifampicin were divided by this value. Half-logarithmic plotting of these values against the time allowed extrapolation of the decay by an exponential function: $\mathrm{f(x)} = \mathrm{e}^{-\lambda \mathrm{t}}$ whereby λ = decay constant. The half-life was calculated using: $t[half - life] = \frac{\ln(2)}{\lambda}$

Determination of RNA half-life* via *absolute quantification by qRT-PCR

Absolute quantification was performed based on the real-time PCR handbook from ThermoFisher (https://www.thermofisher.com/content/dam/LifeTech/Documents/PDFs/PG1503-PJ9169-CO019861-Update-qPCR-Handbook-branding-Americas-FLR.pdf). RNAs were isolated as described before and the presence of residual DNA after DNase I treatment was tested *via* PCR. Primers were designed as described before and the qRT-PCR was performed as described. All reactions used the One-Step RT-PCR kit (BioRad) and the iCycler instrument (BioRad) following the manufacturer's

recommended protocol with the program adjusted as already described. A standard curve was generated by using a defined DNA template amplified by the primers later used for quantification of the transcript of interest. Here, the template was generated by using primers PF228 and PF229 which amplify the *rbsR* gene. Three independent dilution series of defined template amounts were created with two technical replicates per dilution series. For each dilution, six Ct values were obtained and the highest and lowest Ct value were discarded. The remaining four Ct values were averaged. The standard curve was plotted and the resulting function was used to calculate the copy number corresponding to the Ct value in the sample of interest. Calculated copy numbers were used to calculate the RNA half-life as described for the arbitrary values obtained by densitometry.

Sequencing of RNA

RNA isolation and quality assessment were performed by the group of Ulrike Mäder (University Greifswald) as described by Nicolas *et al.*, 2012 with an additional DNase I treatment using TURBO DNase (Ambion). The RNA quality was checked by Trinean Xpose and the Agilent RNA Nano 6000 kit using an Agilent 2100 Bioanalyzer (Agilent Technologies). Ribo-Zero rRNA Removal Kit for bacteria (Illumina) was used to remove the rRNA. TruSeq Stranded mRNA Library Prep Kit (Illumina) was applied to prepare the cDNA libraries. Final libraries were sequenced by the group of Jörn Kalinowski (University Bielefeld) by paired end on an Illumina MiSeq system using 75 bp read length. Trimmed reads were mapped to the *B. subtilis* 168 genome sequence (NCBI GenBank accession number AL009126.3) using Bowtie2 (Langmead *et al.*, 2009). In order to perform differential gene expression analysis, DEseq2 (Love *et al.*, 2014) was used as a part of the software ReadXplorer(2) (Hilker *et al.*, 2016). Statistically significant expression changes (adjusted p-value ≤ 0.01) with log2 fold change >1.0 or ≤1.0 were used.

3.2.6 Methods for working with proteins

SDS-PAGE

Separation of proteins according to their molecular mass was achieved *via* Sodium dodecyl sulfate polyacrylamide gel electrophoresis (SDS-PAGE) (Laemmli, 1970). Gels were poured in a Mini-PROTEAN® (BioRad) handcasting system with 1 mm thickness. Before separation, samples were denatured by mixing with 6× SDS loading dye and heating at 95°C for 30 min. Gels ran in 1× PAGE buffer at 80 V until the bromophenol blue front had reached the running gel allowing an increase of the voltage up to 150 V.

6× SDS loading dye	Tris-HCl pH 6.8 (1 M)	3.15 ml
	Glycerol	6 ml
	SDS	1.2 g
	β-mercaptoethanol	600 µl
	Bromophenol blue	6 mg
	dH_2O	250 µl
Stacking gel	Acryl-Bisacrylamide 30%	1.3 ml
	Tris-HCl pH 6.8	870 µl
	SDS (10%)	100 µl
	APS (10%)	100 µl
	TEMED	10 µl
	dH_2O	6.83 ml
Separating gel (10%)	Acryl-Bisacrylamide 30%	3.3 ml
	Tris-HCl pH 8.8	2.5 ml
	SDS (10%)	100 µl
	APS (10%)	100 µl
	TEMED	8 µl
	dH_2O	4 ml
10× PAGE buffer	L-Glycine	144 g
	Tris-HCl pH 8.3	30.3 g
	SDS	10 g
	dH_2O	Add to 1000 ml

Silver staining

Proteins bands separated in polyacrylamide gels as described above, were silver stained according to the method of Nesterenko *et al.*, 1994. Gels were incubated on a shaker with the solutions as described in Table 2.

Table 2: Workflow for silver staining of polyacrylamide gels

Step	Reagent	Duration
Fixing	Fixer	1-24 h
Washing	Ethanol 50 %	20 min, 3x
Reducing	Thiosulfate solution	1.5 min
Washing	dH_2O	20 s, 3x
Staining	Impregnator	15-25 min
Washing	dH_2O	20 s, 3x
Development	Developer	until sufficient staining
Washing	dH_2O	20 s, 2x
Stop development	Stop solution	5 min

Fixer	Methanol	50% (v/v)
	Acetic acid	12% (v/v)
Thiosulfate solution	$Na_2S_2O_3$ x 5 H_2O	0.8 mM
Impregnator	$AgNO_3$	0.2 % (w/v)
	Formaldehyde	0.037% (v/v)
Developer	Na_2CO_3 x 5 H_2O	350 mM
	$Na_2S_2O_3$	0.016 mM
	Formaldehyde	0.05% (v/v)
Stop solution	Na_2EDTA x 2 H_2O	50 mM
		Adjust pH to 8.0

Determination of β-galactosidase activity

To test the translational activity of the various promoters, their activity was measured by fusion to a *lacZ* gene which encodes the β-galactosidase. To do so, the region of interest – encompassing the promoter with the Shine-Dalgarno (SD) sequence and a part of the open reading frame (ORF) was fused in-frame to the *lacZ* gene in the vector pAC5 (Weinrauch *et al.*, 1991). The vector integrates into the

amyE site *via* double-homologous recombination which was checked by testing α-amylase activity. For this purpose, transformants and a positive control were streaked out on starch plates and incubated overnight at 37°C. On the next day, the plate was covered with 1× Lugol's iodine. No integration or wrong integration at the *amyE* site keeps an active α-amylase that hydrolyzes the starch leading to formation of a white halo upon staining with Lugol's iodine. Correct integration disrupts the α-amylase resulting in intact stained starch. A single colony of a correct strain was used to inoculate 4 ml LB medium which was incubated at 28°C overnight. 10 ml LB medium were inoculated to an OD_{600} of 0.1 and grown at 37°C to an OD_{600} of 0.5 - 0.8. 1.5 ml of the culture were harvested *via* centrifugation at 13,000 rpm and 4°C for 5 min, the supernatant was discarded, and the pellet was stored at -20°C. Lysis of the cells was achieved by re-suspension of the pellet in 400 µl Z buffer supplemented with 20 µl LD mix and incubation for 10 min at 37°C with shaking. Cell debris was removed by centrifugation for 5 min at 13,000 rpm and 4°C and transfer of the supernatant into a new microfuge tube. 100 µl of the cell free crude extract were mixed with 700 µl Z buffer (with β-mercaptoethanol) by vortexing. This mix and 800 µl of Z buffer (with β-mercaptoethanol) as a reference were pre-incubated for 5 min at 28°C. The enzymatic reaction was started by addition of 200 µl ONPG, mixing by vortexing and incubation at 28°C. As soon as the mixture turned yellow, the reaction was stopped by addition of 500 µl 1 M Na_2CO_3. The time points where the reaction was started and stopped were noted. Absorption of the samples was determined at a wavelength of 420 nm with the reference sample serving as blank. Protein amounts in the crude extracts were determined *via* Bradford assay (Bradford, 1976). The β-galactosidase activity was determined using the following equation derived from a standard curve (Blötz *et al.,* 2017):

$$\text{Units mg}^{-1}\ \text{Protein} = \frac{2005.3 \times A_{420}}{A_{595} \times \Delta t}$$

A_{420} Absorption of *o*-nitrophenol

Δt Time difference between start and stop of reaction

V Volume of cell culture in ml

A_{595} Protein amount of cell extracts in mg ml^{-1}

LD-mix	Lysozyme	100 mg
	DNase I	10 mg
	add dH_2O	10 ml
5× Lugol's iodine	10% K-Iodide	5 g
	5% Iodine	2.5 g
	dH_2O	Add to 50 ml
ONPG	ONPG	0.4% (w/v)
	(in Z buffer without β-mercaptoethanol)	

Starch plates (1 l)	Agar	1.5% (w/v)
	Nutrient broth	7.5 g
	Starch	5 g
Stop solution	Na_2CO_3	1 M
Z buffer	Na_2HPO_4 x 2 H_2O	60 mM
	NaH_2PO_4	40 mM
	KCl	10 mM
	$MgSO_4$	1 mM
	β-mercaptoethanol (add just before use)	50 mM

Cell disruption* via *French press

The bomb was cooled to 4°C. Homogenous cell suspension was transferred into the bomb and the remaining air was squeezed out before closing the bomb. By closing the release valve, the bomb was locked and placed in the French press. Cell disruption was performed with a pressure of 18,000 psi three times.

***Overexpression of recombinant proteins in* E. coli**

4 ml LB medium were inoculated with the *E. coli* BL21 Rosetta (DE3) strain carrying the respective plasmid followed by incubation overnight at 28°C. The overnight culture was used to inoculate 1 l of LB medium to an OD_{600} of 0.1 and the culture was grown to an OD_{600} of ~0.8. Then, expression of recombinant proteins was induced by the addition of isopropyl-β-D-thiogalactopyranoside (IPTG) to a final concentration of 1 mM. Cells were cultivated for further 3 h at 37°C before harvesting by centrifugation at 5,000 rpm for 15 min at 4°C. The cells were washed with buffer W and the pellets were snap frozen on liquid nitrogen and stored at -20°C until further use.

Purification of His-tagged proteins

His-tagged proteins were purified by immobilized metal affinity chromatography using a Ni-NTA Sepharose matrix (GE Healthcare) and the ÄKTA™ pure chromatography workstation prime (GE Healthcare). Cell lysates were prepared in 1× ZAP buffer as described above and the cleared crude extracts were applied to the column at room temperature with a flow rate of 1 ml/ min. The column was washed with 1× ZAP buffer until nothing was detectable according to the absorption. Elution of the bound protein was achieved by increasing the imidazole concentration to a final concentration of

500 mM imidazole in 1× ZAP buffer over a gradient. CspB was best eluted at an imidazole concentration of 335 mM.

The elution fractions were pooled and dialyzed against 1× ZAP buffer in an excess of ~1000-fold at 4°C for ~4 h. To cleave off the His-tag, SUMO Protease which was purified beforehand was added 1:100 to the dialysis tube. Then, a second dialysis step against 1× ZAP buffer in an excess of ~1000-fold was started and incubated at 4°C overnight. Proteins with cleaved-off His-tag were purified by applying the protein solution to a gravity-flow column with 1 ml 50% Ni-NTA Sepharose matrix which was pre-equilibrated with 12.5 ml 1× ZAP buffer. The flow-through contained the protein without the tag and purity was tested via SDS-PAGE. The elution fraction was finally concentrated in a Vivaspin® Turbo centrifugal concentrator (Sartorius).

10× ZAP buffer	Tris-base	0.5 M
	NaCl	2 M
		Adjust pH with HCl to 7.5

3.2.7 Miscellaneous methods

RNA-protein co-purification

B. subtilis strains harboring the overexpression plasmids based on pGP380 or pGP382 and a knockout of the gene that is overexpressed were cultivated in 4 ml LB medium over the day at 37°C. In the evening, 50 ml LB medium were inoculated with 50 µl of the pre-culture and incubated overnight at 28°C. On the next day, 500 ml pre-warmed LB medium were inoculated with the overnight culture to an OD_{600} of 0.1 and incubated at 37°C to an OD_{600} of 2. The cultures were harvested *via* centrifugation at 5,000 rpm for 15 min at 4°C. The cells were washed with buffer W and the pellets were snap frozen on liquid nitrogen and stored at -80°C until further use. For cell disruption in the French press, the pellets were re-suspended in 10 ml buffer W cooled to 4°C. After disruption, the lysate was cleared by centrifugation at 8,500 rpm for 30 min at 4°C. 0.5 ml of Strep-Tactin matrix (for 500 ml Pellet) were applied to a column and the matrix was equilibrated by adding 2× 5 ml of buffer W. The cleared crude extract was applied to the column followed by washing four times with 5 ml cold buffer W. The fractions were collected. 2 µl Protector RNase inhibitor (Roche) were added to the elution fraction collection tubes and bound proteins were eluted in three fractions by adding 500 µl buffer E for each elution fraction. Purification of the proteins was tested via SDS-PAGE on a 17.5% acrylamide gel followed by silver staining. To extract the RNA, 400 µl of each elution fraction was mixed with one volume (400 µl) Phenol:Chloroform:Isoamylaclohol (25:24:1) (PCI). The mixture was shaken vigorously, transferred to a 2 ml Phase Lock gel heavy tube (Quantabio), incubated for 2 min at room temperature and was centrifuged for 30 min at 14,800 rpm at 15°C. The upper phase was transferred into a fresh

microfuge tube and three volumes (1200 µl) of ice-cold 96% EtOH:4 M LiCl (30:1) and 1,5 µl Glycoblue were added and mixed. RNA precipitated overnight at -20°C. The next day, the mixture was centrifuged for 30 min with 14,800 rpm at 4°C and the supernatant was carefully discarded by pipetting. The RNA pellet was washed by adding 100 µl ice-cold 70% EtOH without re-suspending the pellet and finally it was air-dried by incubation under a laminar flow cabinet. RNA was dissolved by adding 33 µl of RNase-free water and shaking at 37°C for 1 h. To prevent digestion, 0.5 µl RNase Inhibitor (Roche) were added and residual DNA was digested by addition of 3 µl DNase I (20 mg/ml), 4 µl 10X DNase I buffer, and incubation for 2 h at 37°C. Digestion of DNA was tested *via* PCR. If no DNA was left, the elution fraction RNAs 1-3 of a sample were pooled. When no DNA was left, the extraction, precipitation and washing of RNA was performed as described above to get rid of DNase I. The RNA pellet was dissolved by applying 50 µl RNase-free water and shaking at 37°C for 1 h. The final RNA concentration was determined *via* Nanodrop and Qubit. Further quality control and Illumina sequencing was performed by the Göttingen Genomics Laboratory (G2L). Sequencing data were mapped against the chromosome of *B. subtilis* 168 by the G2L and was accessed *via* the TraV software (Dietrich *et al.*, 2014). TraV represents the normalized reads as nucleotide activities per kilobase of exon model per million mapped reads (NPKM) values. These NPKM values represent the transcriptional activity or coverage on the respective genetic region.

Buffer W	Tris-HCl pH 8.0	100 mM
	NaCl	150 mM
Buffer E	Tris-HCl pH 8.0	100 mM
	NaCl	150 mM
	D-desthiobiotin	2.5 mM

Microscopy

For microscopy, cells were grown at 37°C in liquid LB medium overnight. The overnight culture was directly used for microscopy or for inoculation of LB medium, which was incubated at 37°C to an OD_{600} of 0.3-0.5. Images were acquired using an Axioskop 40 FL fluorescence microscope, equipped with digital camera AxioCam MRm and AxioVision Rel (version 4.8) software for image processing (Carl Zeiss, Göttingen, Germany) and Neofluar series objective at ×100 primary magnification.

Identification of mutations from whole genome sequencing data

To find possible differences in a sequenced genome it was compared to the in-house wild type strain 168. Single nucleotide polymorphisms or longer variations were considered as significant when the specifications of a minimum coverage of 25 reads with ≥90% variant frequency were met.

4. Results

4.1 Phenotypical characterization of *csp* mutants

Cold shock proteins are encoded by the genomes of almost all bacteria (Zhu & Stülke, 2018). They can be split into two different categories: cold-inducible and non-cold-inducible (Tanaka *et al.*, 2012). Furthermore, different cold shock proteins have been shown to serve distinct functions. For example in *S. aureus*, CspA is the only one of three cold shock proteins that indirectly controls staphyloxanthin production by regulating a sigma factor (Catalan-Moreno *et al.*, 2020). Cold shock proteins are found in very different numbers ranging from up to nine *csp* genes in *E. coli* to only two in *T. thermophilus* (Wang *et al.*, 1999; Tanaka *et al.*, 2012). Even though the activities of cold shock proteins have been extensively studied in *E. coli*, their high number and partially redundant function make it difficult to identify potential functional differences. *B. subtilis* encodes only three *csp* genes which greatly facilitates gene knockout analysis.

4.1.1 Cold shock proteins are important for growth at optimal and low temperature

Firstly, *csp* knockouts in all possible combinations were created *via* antibiotic marker substitution. Previous analysis of *B. subtilis csp* knockouts was performed in the JH642 wild type background (Graumann *et al.*, 1997). Our laboratory uses the wild type 168 and hence, all *csp* knockouts were created in that genetic background. Consistent with Graumann *et al.* (1997), presence of at least one *csp* gene is essential for *via*bility as a triple knockout could not be generated. In order to identify potential differences in the importance of the cold shock proteins, growth of the single and double knockout mutants was examined at 37°C on LB-agar. All single mutants (GP1968, GP1969, GP2614) as well as the *cspB cspC* (GP1970) and *cspC cspD* (GP1972) double mutants grew similar to the wild type 168 at optimal temperature (see Figure 5 A). In contrast, the *cspB cspD* double mutant (GP1971) exhibited a strong growth defect. Moreover, this mutant formed translucent colonies which lysed after prolonged incubation and gave rise to opaque suppressor mutants that restored growth (see section 4.2.1). It has been published that also a *cspB cspC* double mutant in the JH642 background exhibits a strong growth reduction in liquid M9 minimal medium (Graumann *et al.*, 1997). When cultivated in liquid LB complex medium or C-Glc minimal medium, the *cspB cspC* double mutant (GP1970) only exhibited very faint impairment of growth compared to the wild type (data not shown).

At 15°C, the single mutants showed no cold sensitivity and grew indistinguishable from the wild type (see Figure 5 B). However, not only the *cspB cspD* double mutant (GP1971) but also the *cspB cspC* double mutant (GP1970) exhibited a strong impairment of growth at low temperature. A small reduction of growth also for the *cspC cspD* double mutant (GP1972) became apparent when growth in

liquid culture was monitored (see Figure 5 C). The *cspB cspD* double mutant (GP1971) showed lysis and a long lag period after shift to cold.

While a *cspB cspC* double mutant exhibited the strongest impairment of growth at 15°C in the literature (Graumann *et al.*, 1997), here the *cspB cspD* double mutant (GP1971) was most severely affected at both temperatures. This suggests, CspB and CspD are most important for growth independent of the temperature. The double mutant that still harbors a *cspD* gene (GP1970) exhibits weaker growth at 15°C than at 37°C, indicating *cspD* is more important for growth at optimal temperature.

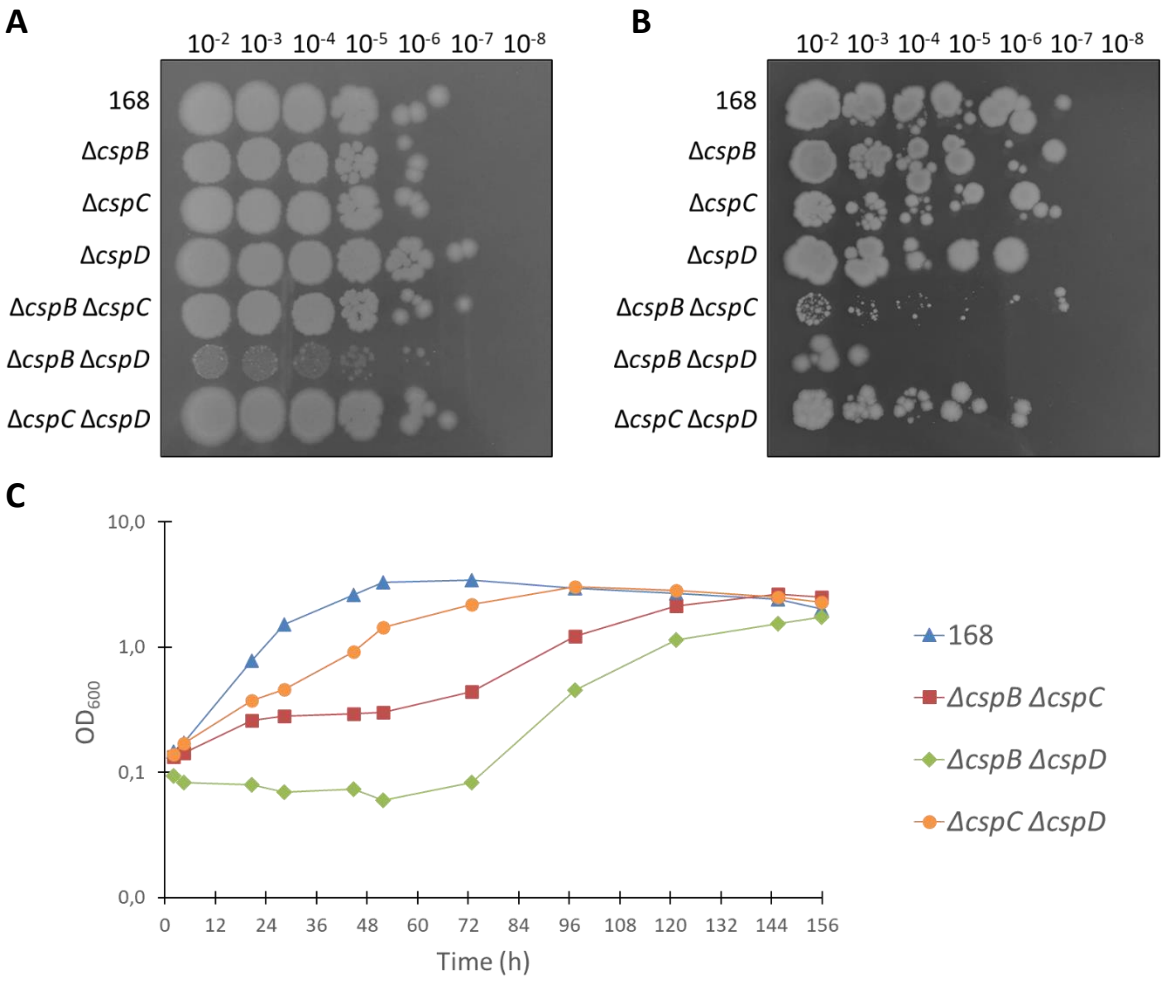

Figure 5: Growth of *csp* knockout strains. The wild type strain *B. subtilis* 168 and the *csp* mutant strains GP1968 (Δ*cspB*), GP1969 (Δ*cspC*), GP2614 (Δ*cspD*), GP1970 (Δ*cspB* Δ*cspC*), GP1971 (Δ*cspB* Δ*cspD*), and GP1972 (Δ*cspC* Δ*cspD*) were cultivated on LB-agar (**A**) at 37°C for one day and (**B**) at 15°C for 11 days. (**C**) The double knockout strains were inoculated from log-phase 37°C cultures and were directly shifted to 15°C. The OD_{600} was first measured after two hours of shift to 15°C and twice every day. All results are representative of three biological replicates.

4.1.2 CspB and CspD are essential for the physiology of *B. subtilis*

To further investigate how the loss of *csp* genes affects the physiology of *B. subtilis*, the *csp* mutants were analyzed under the microscope. Single or double *csp* mutant cells in the logarithmic growth phase did not show any obvious morphological differences except for the *cspB cspD* double mutant (GP1971) of which a few cells exhibited a curled morphology (see Figure 6 A). It has been reported that all of the *csp* double mutants exhibit reduced survival in the stationary growth phase (Graumann *et al.*, 1997). Therefore, cell morphology was also analyzed in cells grown to the stationary phase. Indeed, there were generally more lysed cells in the double mutant cultures than in the single mutant cultures. Again, the *cspB cspD* double mutant (GP1971) clearly exhibited the most severe phenotype with a majority of the cells lysed or adopting the curled morphology (see Figure 6 B). The curly morphology could stem from a disruption of the cell wall structure. Some studies have shown that high levels of Mg^{2+} can compensate cell wall defects caused by aberrant expression of proteins

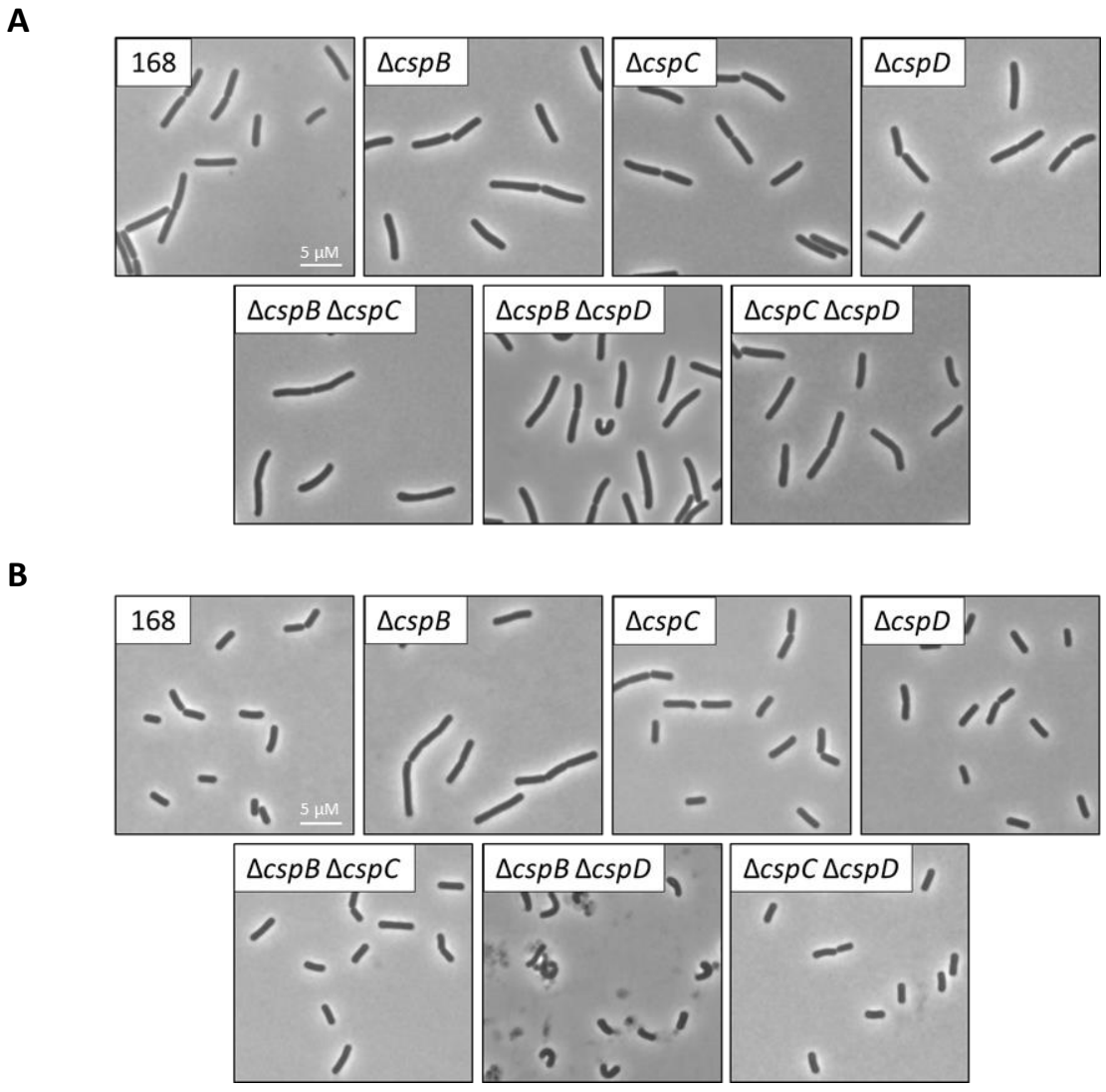

Figure 6: Morphology of *csp* knockout strains. The wild type strain *B. subtilis* 168 and the *csp* mutants GP1968 (Δ*cspB*), GP1969 (Δ*cspC*), GP2614 (Δ*cspD*), GP1970 (Δ*cspB* Δ*cspC*), GP1971 (Δ*cspB* Δ*cspD*), and GP1972 (Δ*cspC* Δ*cspD*) were analyzed for morphology by phase contrast microscopy. Scale bars, 5 µM. (**A**) Cells were grown in liquid LB medium at 37°C to an OD_{600} of 0.3 - 0.5. (**B**) Cells were grown in liquid LB medium at 37°C overnight to the stationary growth phase.

involved in cell wall homeostasis (Formstone & Errington, 2005; Mehne *et al.*, 2013). However, this was not the case for the *cspB cspD* double mutant (GP1971) indicating that the defect might be more severe, or involves other substantial proteins (see Figure 7). Nevertheless, the *cspB cspD* double mutant (GP1971) clearly exhibited strong morphological defects in agreement with the observed growth behavior.

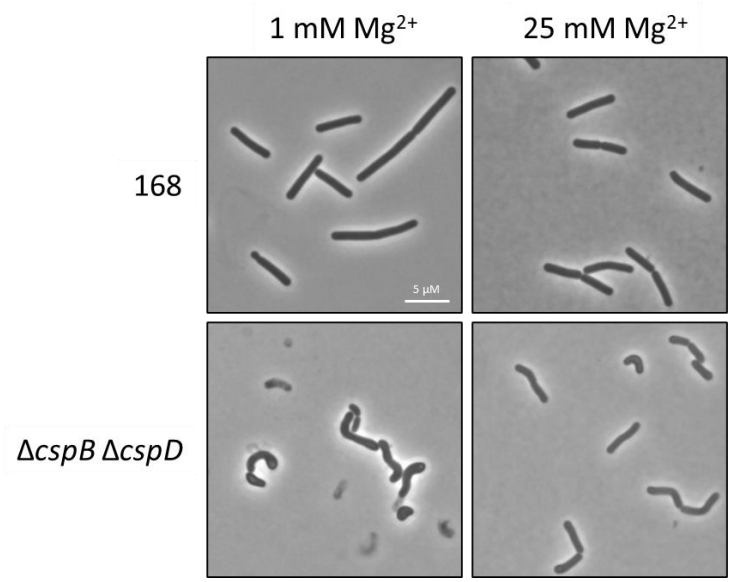

Figure 7 Morphology of *csp* knockout strains with or without addition of magnesium. The wild type strain *B. subtilis* 168 and the mutant GP1971 (Δ*cspB* Δ*cspD*) were analyzed for morphology by phase contrast microscopy. Scale bar, 5 µM. The displayed cultures were inoculated from an overnight culture and were grown to an OD_{600} of 0.7-0.8. All cells were grown in liquid LB medium with the addition of 1 mM or 25 mM $MgSO_4$ at 37°C.

Continuous work with the *csp* knockout mutants indicated that the double knockout strains exhibit reduced transformation efficiencies. Thus, genetic competence of the three *csp* double knockout strains (GP1970, GP1971, GP1972) was tested by using a modified version of the protocol for preparation of competent *B. subtilis* cells (section 3.2.3). In that, the competent cells were diluted to an OD_{600} of 0.5 before transformation proceeded as described. The cells were transformed with 500 ng chromosomal DNA of *B. subtilis* GP1966 (Δ*ynfC*::P_{alf4}-*gfp ermC*) which has no detrimental effect on fitness (Reuß *et al.*, 2019). The *cspB cspC* (GP1970) and *cspC cspD* (GP1972) double mutants indeed exhibited reduced transformation efficiencies, whereas the *cspB cspD* double mutant (GP1971) had completely lost genetic competence (see Figure 8 A). It has been reported that overexpression of the competence genes *comKS* can strongly increase transformation efficiency (Rahmer *et al.*, 2015). However, overexpression of the *comKS* genes in a *cspB cspD* double mutant (GP1995) did not restore genetic competence (data not shown). This indicates CspB and CspD are essential for genetic competence while CspC alone is not sufficient for this process.

Cold shock proteins have been shown to affect the expression of a large number of genes in several organisms (Phadtare *et al.*, 2006; Michaux *et al.*, 2017; Caballero *et al.*, 2018). An aberrant global protein expression was observed in the *cspB cspD* double mutant (GP1971) which also indicates a global effect of CspB and CspD in *B. subtilis* (see Figure 8 B). Given the global action and the pleiotropic defects observed, it is evident that CspB and CspD are essential for the physiology in *B. subtilis* at optimal temperature.

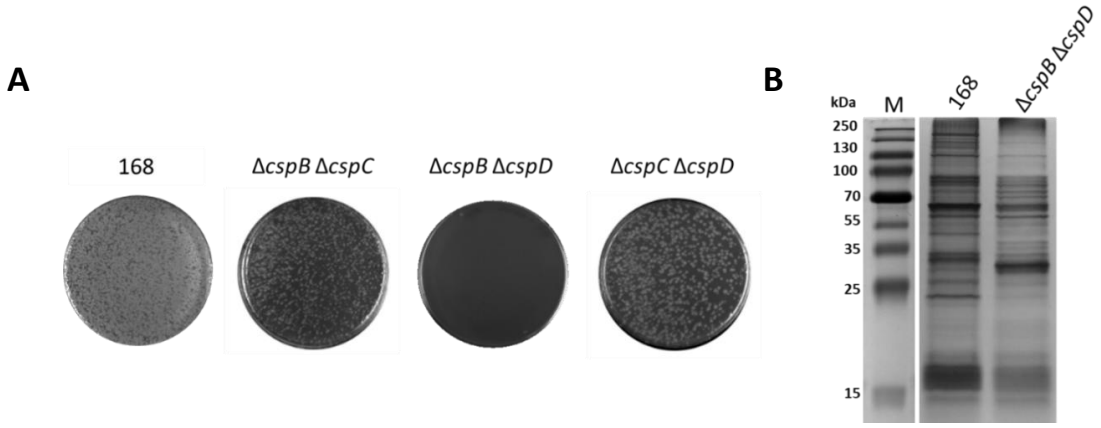

Figure 8: Genetic competence and protein expression are impaired in the *cspB cspD* double mutant. (**A**) Competent cells of the wild type strain 168 and the *csp* mutants GP1970 (Δ*cspB* Δ*cspC*), GP1971 (Δ*cspB* Δ*cspD*), and GP1972 (Δ*cspC* Δ*cspD*) were diluted to an OD of 0.5 and transformed with 500 ng chromosomal DNA from strain GP1966 (Δ*ynfC*::P_{alf4}-*gfp ermC*). The cells were selected on LB-agar plates containing erythromycin/lincomycin plus antibiotics matching the respective resistance cassettes. (**B**) Cells were grown in liquid LB medium at 37°C to an OD of 1. Cell-free crude extracts were loaded onto an 15% SDS-PA gel with 100 ng of protein per lane.

4.1.3 CspC is the only cold shock protein that is increasingly expressed at low temperature

Previous studies on the expression of the *B. subtilis* cold shock proteins showed contradicting results. Two dimensional gel electrophoresis experiments indicated that all three cold shock proteins are increased 48 hours after cold shock (Graumann *et al.*, 1997) An earlier study measured *cspB-lacZ* expression over time and found that expression is increased in the first two hours after cold shock and then gradually decreases again (Willimsky *et al.*, 1992). Another study found that transcription of *cspB* and *cspC* is increased two hours after shift to cold, but only *cspC* exhibits increased expression in translational *lacZ* fusions two hours after cold shock (Kaan *et al.*, 1999). Transcription profiles across various conditions showed that all three *csp* genes are strongly transcribed under all conditions (Nicolas *et al.*, 2012). In addition to that, the expression of the CspD protein at cold has not been analyzed so far.

To examine the definite expression of all three cold shock proteins at optimal and low temperatures, translational promoter-*lacZ* fusions (*i.e.* promoter, 5'-UTR, and ribosomal binding site) were created based on the pAC5 plasmid (Weinrauch *et al.*, 1991). The resulting strains GP3283 (P_{cspB}-*lacZ*), GP1984 (P_{cspC}-*lacZ*), and GP3286 (P_{cspD}-*lacZ*) were cultivated in LB medium for ~3 hours (37°C) or

~24 hours (15°C) to a final OD_{600} of 0.5 - 0.8. Thus, the obtained values likely represent the expression after the cells have adapted to low temperature. As shown in Table 3, expression from all three promoters was high at both temperatures. As the only promoter, *cspC* showed a significant five-fold increase of β-galactosidase expression at 15°C. The expression by the *cspB* and *cspD* promoters was not significantly increased by growth at cold.

Taken together, the expression levels fit to the observed growth behavior with CspB and CspD being equally important for cells adapted to growth at optimal or cold temperature. In contrast, increased expression of CspC indicates it is more important for growth at cold.

Table 3: Promoter activities of the *csp* genes at optimal and low temperature

Strain	Promoter	Enzyme activity in Miller units/mg of protein*	
		37°C	15°C
GP3283	*cspB*	11,750 ± 560	14,900 ± 1,680
GP1984	*cspC*	6,320 ± 280	30,950 ± 2,900
GP3286	*cspD*	19,600 ± 450	11,300 ± 1,600

*All measurements were performed in triplicate. The standard de*via*tions are indicated.

4.1.4 Modification of a single amino acid allows CspC to functionally replace CspB and CspD

As shown above, strains that express CspB or CspD have little phenotypic defects whereas strains which only express CspC exhibit strong pleiotropic defects. Furthermore, only the expression of CspC is increased at cold. The homogenous activities of CspB and CspD are also reflected by the similarity of their amino acid sequences being 81% according to SubtiList (Moszer *et al.*, 2002). In contrast, CspC only shares a similarity of 71% and 69% with CspB and CspD, respectively. It has been shown that a single proline residue at position 58 in CspA from *S. aureus* confers functional specificity (Catalan-Moreno *et al.*, 2020). For direct comparison, the *B. subtilis* cold shock protein amino acid sequences were aligned (see Figure 9). Strikingly, CspB and CspD harbor a proline residue at position 58 whereas CspC possesses an alanine residue at this position (red arrow). Thus, it seemed likely that this single amino acid residue may be responsible for the functional diversity of CspC. To test this hypothesis, a CspC(A58P) variant was created and its capability to compensate the loss of CspB and

Figure 9: Alignment of amino acid sequences of the *B. subtilis* cold shock proteins. Red arrow indicates position 58 that is critical for functional specificity of the cold shock proteins. Sequences were acquired from SubtiWiki (Zhu & Stülke, 2018)**.** Alignment was created using the Geneious software package (Kearse *et al.*, 2012).

CspD was analyzed. For that, the *cspC* gene was amplified and mutated in a combined-chain reaction (see section 3.2.4). Then, the mutated variant was fused to a spectinomycin resistance gene which was flanked by the genetic region downstream of *cspC* in a long-flanking homology PCR. Transformation of the *cspD* mutant GP2614 with this PCR product led to the strain GP3274 in which the native *cspC* gene is exchanged with the mutated variant. Final knockout of *cspB* yielded the strain GP3275. As shown in Figure 10 A, native expression of the CspC(A58P) variant in GP3275 suppressed the growth defect observed for the *cspB cspD* double mutant GP1971 which only expresses the native *cspC* gene. In addition to that, genetic competence was partially restored by the CspC(A58P) variant (see Figure 10 B). Thus, the amino acid at position 58 seems to confer functional specificity also in *B. subtilis.*

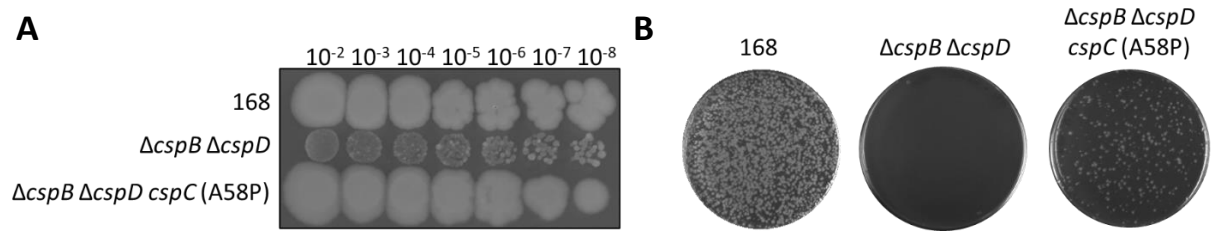

Figure 10: CspC variant A58P can functionally replace CspB and CspD. (**A**) The wild type strain 168 and the *csp* mutant strains GP1971 (Δ*cspB* Δ*cspD*), and GP3275 (*cspC::cspC*(A58P)-*aad9* Δ*cspB* Δ*cspD*) were cultivated on LB-agar at 37°C for 36 hours. (**B**) Competent cells of the wild type strain 168 and the *csp* mutants GP1971 (Δ*cspB* Δ*cspD*), and GP3275 (*cspC::cspC*(A58P)-*aad9* Δ*cspB* Δ*cspD*) were diluted to an OD of 0.5 and transformed with 200 ng chromosomal DNA from strain BKE04260 (Δ*topB*::*ermC*). The cells were selected on LB-agar plates containing erythromycin/lincomycin plus antibiotics matching the respective resistance cassettes.

4.2 Analysis of the *cspB cspD* double mutant

4.2.1 Characterization of Δ*cspB* Δ*cspD* suppressor mutants

As mentioned above, the *cspB cspD* double mutant (GP1971) exhibits translucent growth and is genetically instable. After two days of incubation on solid medium, opaque suppressor colonies appeared. In order to find out how cells cope with the loss of CspB and CspD, 20 suppressor mutants were isolated. 16 of these suppressor mutants exhibited improved growth when compared to the progenitor strain GP1971 (see Figure 11 Right Panel). The four suppressor mutants GP1989, GP1990, GP2895, and GP2900 were subjected to whole genome sequencing. GP1989 harbored a point mutation in the 5'-UTR preceding the *cspC* gene (RNA feature S179 according to Nicolas *et al.*, 2012). In GP1990, a point mutation in the ribosomal binding site of the *veg* gene was found. GP2900 carried a base exchange that leads to substitution of proline 245 by serine in the DegS protein. Surprisingly, no mutations could be identified in the GP2895 suppressor mutant. Either, the sequencing quality for this strain was not sufficient to identify the mutation, or *B. subtilis* is able to suppress the growth defect without acquisition of genetic mutations. *cspB* and *cspD* were clearly missing in all whole genome

Strain	Mutation			Growth
	cspC 5'-UTR	*veg* RBS	DegS	
168	-	-	-	
Δ*cspB* Δ*cspD* (GP1971)	-	-	-	
S1 (GP1989)*	G-65A	-	-	
S2	-	-	-	
S3	-	-	-	
S5	-	-	-	
S6 (GP3284)	-	-	-	
S7 (GP1990)*	-	G-7T	-	
S9 (GP3305)	T-99C	-	-	
S10 (GP3306)	G-96A	-	-	
S11	-	-	-	
S12 (GP2895)*	-	-	-	
S15	-	-	-	
S16	-	-	-	
S17	-	-	-	
S18	-	-	-	
S19 (GP2900)*	-	-	P245S	
S20	-	-	-	

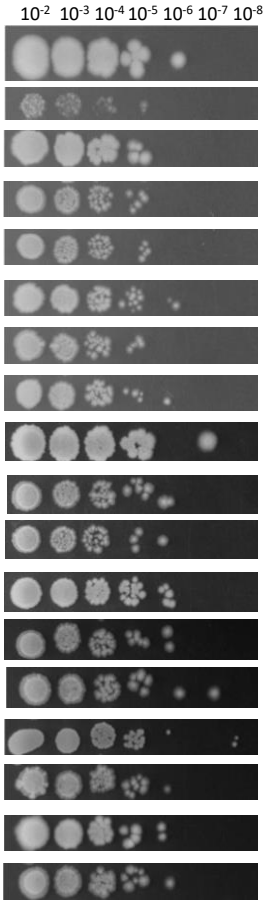

Evolved strains			
S1 (GP1989) evolved	G-65A	-	-
S6 (GP3284) evolved (=GP3304)	G-65A	-	-
S7 (GP1990) evolved	-	G-7T	-

Figure 11: Mutations and growth of Δ*cspB* Δ*cspD* suppressor strains. (**Upper Table**): Mutations in suppressor colonies of the *cspB cspD* double mutant (GP1971) identified by Sanger sequencing. *Asterisks mark strains subjected to whole genome sequencing. (**Right Panel**): Growth of suppressor strains on LB-agar at 37°C after one day. (**Lower Table**): Mutations in suppressor strains after five passages identified by Sanger sequencing. Passaging was performed at 37°C and by transferring 100 µl of the previous culture to 10 ml liquid LB medium twice a day. Absence of *cspB* and *cspD* was verified in all suppressor mutants *via* PCR. Strains that were subjected to whole genome sequencing or that acquired a suppressor mutation, were added to the strain collection as GP1989, GP3284, GP1990, GP3305, GP3306, GP2900, and GP3304.

sequenced strains. Absence of *cspB* and *cspD* was moreover verified *via* PCR in all suppressor mutants. To uncover whether the mutations are also responsible for suppression in the other isolated strains, the respective genetic regions were amplified by PCR and subjected to Sanger sequencing (see Figure 11 Upper Table). Strikingly, two more suppressor mutants (GP3305 and GP3306) carried point mutations in the 5'-UTR of *cspC* highlighting the importance of that region for suppression. The

mutations in the *veg* and *degS* genes did not reappear indicating they are less likely to occur or less efficient for suppression. On the other hand, 11 of the 16 isolated suppressors did not carry any mutation in the *cspC, veg,* or *degS* gene indicating other possibilities for suppression. In parallel, the three suppressor mutants GP1989, GP3284, and GP1990 were evolved for five passages in liquid LB medium and were checked for occurrence of suppressor mutations in the so far affected genetic regions. The suppressor strains GP1989 and GP1990 that already carried a mutation in *cspC* or *veg,* respectively, did not evolve any further mutations in the tested genetic regions (see Figure 11 Lower Table). The strain GP3284 did not harbor any mutations prior to passaging. Strikingly, its evolved variant GP3304, acquired the same point mutation in the *cspC* 5'-UTR that was already found in GP1989. Taken together, mutations in the *cspC* upstream region seem to provide the most frequent mechanism for suppression of the loss of *cspB* and *cspD*. The other mutations found in *veg* and *degS* only occur rarely. Notably, none of the three mutations restored genetic competence as judged by transformation of GP1989, GP1990, and GP2900 (see Figure 12).

Figure 12: Suppressor mutations do not restore genetic competence Competent cells of the wild type strain 168, the *csp* double knockout mutant GP1971 (Δ*cspB* Δ*cspD*), and the suppressor mutants GP1989 (Δ*cspB* Δ*cspD* P_{cspC}(G-65A)), GP1990 (Δ*cspB* Δ*cspD* P_{veg}(G-10T)), and GP2900 (Δ*cspB* Δ*cspD degS*(P245S)) were diluted to an OD of 0.5 and transformed with 500 ng chromosomal DNA from strain GP1966 (Δ*ynfC*::P_{alf4}-*gfp ermC*). The cells were selected on LB-agar plates containing erythromycin/lincomycin plus antibiotics matching the respective resistance cassettes.

4.2.2 Overexpression of CspC compensates the loss of CspB and CspD

The 5'-UTRs of *cspB* and *cspC* contain two highly conserved sequence motifs termed 'cold boxes' that likely have a regulatory function (Graumann *et al.*, 1997). Interestingly, all suppressor mutations found in the *cspC* upstream region are located in or near one of the cold boxes (see Figure 13 A). It seemed possible these mutations affect expression of *cspC*. Therefore, the *cspC* upstream regions of the wild type and of the suppressor strain GP1989 containing the G-65A base exchange were translationally fused to the promoterless *lacZ* gene in the pAC5 vector (see Figure 13 B) (Weinrauch *et al.*, 1991). Chromosomal integration of the resulting plasmids yielded the strains GP1984 (wild type) and GP1986 (G-65A mutation) which were cultivated in LB medium at 37°C to an OD_{600} of 0.5 - 0.8. As expected, the mutation in the *cspC* 5'-UTR increased expression of the reporter

gene almost two-fold, indicating that increased amounts of CspC likely suppress the loss of CspB and CspD (see Table 4). Given that mutations in the *cspC* upstream region occurred most frequently, it seems likely that increased expression of *cspC* represents the preferred suppression mechanism in a *cspB cspD* double mutant.

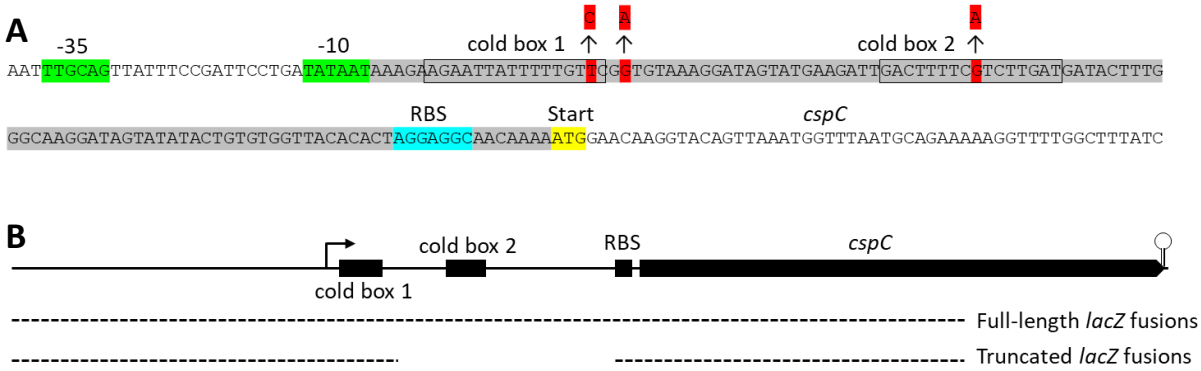

Figure 13: Organization of the *cspC* genetic region. (**A**) Mutations in the *cspC* upstream regions. Arrows point at bases that substituted the original bases. RBS: ribosomal binding site. *cspC* 5'-UTR denoted as RNA feature S179 is colored in grey. Sequence was acquired from SubtiWiki (Zhu & Stülke, 2018)**.** Positions of the cold boxes according to Graumann *et al.* 1997. (**B**) Genetic regions fused to *lacZ.* Full-length *lacZ* fusions are found in GP1984, GP1986, GP3252, GP3253, GP3254, GP3260, GP3261, GP3262. Truncated *lacZ* fusions are found in GP1988, GP3255, GP3256, GP3257.

Table 4: Promoter activities of the *cspC* gene with wild type and mutant 5'-UTR

Strain	Genetic background	Enzyme activity in Miller units/mg of protein*
GP1984	wild type	4,360 ± 210
GP1986	*cspC* (G-65A)	9,450 ± 710

*All measurements were performed in triplicate. The standard de*via*tions are indicated.

4.2.3 The *cspC* 5'-UTR is essential for efficient expression and is regulated by CspB and CspD

The mutation leading to overexpression of *cspC* is located in the cold box 2 of the *cspC* upstream region (see Figure 13 A). Similar cold boxes are found in the 5'-UTRs of *E. coli csp* genes and are involved in expression of the respective downstream gene (Jiang *et al.*, 1996). Furthermore, *E. coli cspA* expression is negatively regulated by CspA and CspE which increase transcriptional pausing at the cold box (Bae *et al.*, 1997; Bae *et al.*, 1999). Thus, it was tempting to speculate that also in *B. subtilis* the expression of *cspC* is dependent on the action of cold shock proteins. To test this hypothesis the translational *cspC-lacZ* fusion in GP1984 was combined with all *csp* knockout combinations. To furthermore test the importance of the cold box 2 for expression, a truncated *cspC* 5'-UTR which only contained the cold box 1 and the ribosomal binding site was fused to *lacZ* resulting in strain GP1988 (see Figure 13 B). As shown in Table 5, already the single deletion of *cspB* and *cspD* but not *cspC* led to

an approximately two-fold increase of β-galactosidase expression by the *cspC* promoter. Double knockout of *cspB* and *cspD* led to the strongest increase of expression, even though not significantly stronger than in the single knockouts. Truncation of the 5'-UTR and hence, loss of the cold box 2 led to a strong decrease of expression independent of the presence of *cspB* or *cspD*. Notably, expression under control of the truncated *cspC* 5'-UTR was still increased at cold. However, the increase at cold was not as strong as in the wild type.

Taken together these findings indicate that CspB and CspD but not CspC negatively regulate the expression of *cspC*. Moreover, the presence of the cold box 2 seems to be essential for efficient expression as well as for regulation by CspB and CspD. Hence, CspB and CspD likely interact with the cold box to decrease expression. Interestingly, the responsiveness of *cspC* expression to cold was not completely abolished by the truncation. This may indicate that the remaining cold box 1 still provides some regulatory potential, or that a different regulation mechanism takes action at cold shock conditions.

Table 5: Promoter activities of the *cspC* gene with wild type and truncated *cspC* 5'-UTR in *csp* knockout backgrounds and at cold

Strain	Genetic background	Enzyme activity in Miller units/mg of protein*
GP1984	wild type	5,533 ± 63
GP3252	Δ*cspB*	9,803 ± 383
GP3260	Δ*cspC*	5,313 ± 260
GP3253	Δ*cspD*	7,674 ± 534
GP3261	Δ*cspB* Δ*cspC*	7,905 ± 295
GP3254	Δ*cspB* Δ*cspD*	10,670 ± 279
GP3262	Δ*cspC* Δ*cspD*	9,641 ± 1542
GP1988	truncated 5'-UTR of *cspC*	422 ± 28
GP3255	truncated 5'-UTR of *cspC* Δ*cspB*	489 ± 3
GP3256	truncated 5'-UTR of *cspC* Δ*cspD*	584 ± 7
GP3257	truncated 5'-UTR of *cspC* Δ*cspB* Δ*cspD*	339 ± 9
	Expression at 15°C	
GP1984	wild type	19,645 ± 1,193
GP1988	truncated 5'-UTR of *cspC*	1,088 ± 32

*All measurements were performed in triplicate. The standard de*via*tions are indicated.

4.2.4 Reduced expression of *veg* suppresses the *cspB cspD* double knockout

Another suppressor mutation was found in the strain GP1990 and affected the upstream region of the *veg* gene. The mutation deteriorates the ribosomal binding site consensus sequence from GGUGGA to UGUGGA. Thus, it was tempting to speculate that the less-optimal Shine-Dalgarno sequence decreases translation efficiency of the *veg* mRNA. In order to test this hypothesis, translational fusions of the wild type and mutant upstream regions of *veg* were created using the pAC5 vector (Weinrauch *et al.*, 1991). Chromosomal integration of the resulting plasmids yielded the strains GP2898 (wild type) and GP2899 (G-7T mutation). The cultures were grown in LB medium to an OD_{600} of 0.5 - 0.8 at 37°C. As hypothesized, the mutation in the ribosomal binding site led to a strong decrease of expression (see Table 6). Thus, it seems that a reduced expression of *veg* is responsible for suppression of the *cspB cspD* double knockout. To test this hypothesis, the *veg* mutant GP2888 was created and combined with the *cspB* and *cspD* deletions yielding strain GP2897. Indeed, the knockout of *veg* suppresses the growth defect in the *cspB cspD* knockout background (GP2897) analogous to the *veg* knockdown mutation in GP1990 (see Figure 14). Unfortunately, the *veg* gene is poorly characterized and its function is unknown. It was hypothesized that Veg might negatively regulate *cspC* expression which could explain how loss of *veg* confers suppression. Therefore, the *cspC-lacZ* fusion from GP1984 was combined with the *veg* deletion yielding GP3273, as well as with the plasmid pGP3138 that constitutively overexpresses the *veg* gene. As shown in Table 7, overexpression of *veg*

Table 6: Promoter activities of the wild type and mutant *veg* upstream region

Strain	Genetic background	Enzyme activity in Miller units/ mg of protein*
GP2898	wild type	34 ± 1
GP2899	*veg* (G-7T)	2 ± 1

*All measurements were performed in triplicate. The standard de*via*tions are indicated.

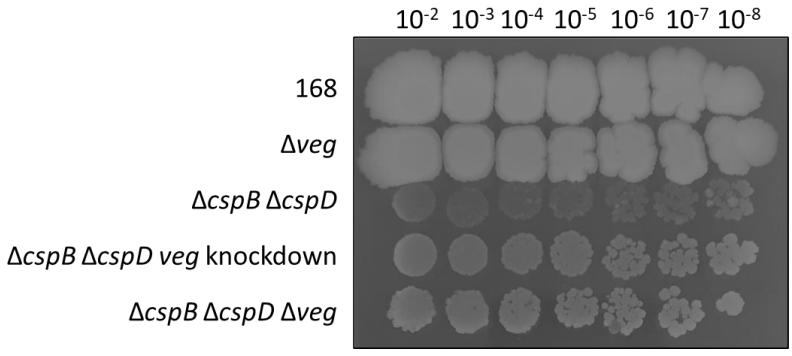

Figure 14: Decreased expression of *veg* suppresses the loss of *cspB* and *cspD*. The wild type strain 168, and the mutant strains GP2888 (Δ*veg*), GP1971 (Δ*cspB* Δ*cspD*), GP1990 (Δ*cspB* Δ*cspD veg*(G-7T)), and GP2897 (Δ*cspB* Δ*cspD* Δ*veg*) were cultivated on LB-agar at 37°C for 36 hours.

did reduce β-galactosidase expression by the *cspC* promoter. Paradoxically, deletion of *veg* also reduced the expression. This indicates that Veg does indeed influence expression of *cspC,* potentially in a dose-dependent manner.

However, the observed influence on *cspC* expression does not explain the suppression of the *cspB cspD* double knockout. Thus, these finding rather indicate that Veg plays a more general role in RNA metabolism and that it might become toxic in the absence of CspB and CspD.

Table 7: Promoter activities of the *cspC* gene at different expression levels of *veg*

Strain	Genetic background	Enzyme activity in Miller units/mg of protein*
GP1984	wild type	6337 ± 534
GP1984 + pGP3138	overexpression of *veg*	2971 ± 347
GP3273	Δ*veg*	4864 ± 171

*All measurements were performed in triplicate. The standard de*via*tions are indicated.

4.2.5 The DegS mutation affects exopolysaccharide production

The last suppressor mutation was found in the *degS* gene and leads to exchange of the proline residue at position 245 with a serine residue. It has been shown that single amino acid changes in the DegS histidine kinase domain *e.g.* at position 220 reduce the phosphorylation activity and thereby, signaling of the two-component system (Dahl *et al.*, 1992). The DegS/DegU two-component system is involved in competence regulation, and the regulation of biofilm and motility genes (Dahl *et al.*, 1992; Kobayashi, 2007). As demonstrated above, the *degS* mutation of GP2900 did not restore genetic competence (see Figure 12). It was hypothesized that loss of the cold shock proteins might influence expression of *degS* which therefore, could exert a selective pressure on DegS activity. To test this idea, a translational *lacZ* fusion of the *degS* promoter was integrated into the chromosome (GP1982), followed by deletion of *cspB* and *cspD* in that strain (GP3263). However, knockout of the cold shock proteins had no influence on the expression by the *degS* promoter (data not shown).

Another process affected by DegS as well as by Veg is the formation of biofilms. DegS/DegU negatively regulate SinR, which further represses *tasA* expression (Kobayashi, 2007). Furthermore, the Veg protein was shown to induce *tasA* expression, likely by inhibition of SinR (Lei *et al.*, 2013). Due to these cellular functions, it was tested whether the *degS, veg* and also the *cspC* suppressor mutation have an effect on biofilm formation. Problematically, the *B. subtilis* wild type 168 is a domesticated strain which is impaired in the formation of structurally complex biofilms (McLoon *et al.*, 2011). Nevertheless, 168 still produces exopolysaccharides, although on a decreased level as compared to its undomesticated version (McLoon *et al.*, 2011). Notably, the amyloid-forming biofilm gene *tasA* is

strongly transcribed in 168 in MSgg medium (Nicolas *et al.*, 2012). To visualize amyloid production in the 168 background, the strains were grown on biofilm-inducing MSgg-agar with the dyes congo red and Coomassie brilliant blue. Congo red specifically stains TasA-containing amyloid fibers of *B. subtilis* (Romero *et al.*, 2010). As shown in Figure 15, the wild type 168 formed a red halo likely representing amyloid-matrix production. The *cspB, cspD* and *veg* single mutants (GP1986, GP2614, and GP2888 respectively) grew similar to the wild type. No distinct red halo was visible in the negative control strain GP583 that contains a *ymdB* deletion and hence, is unable to express biofilm genes (Kampf *et al.*, 2018). Similar to the negative control, the *cspB cspD* double mutant GP1971 did not form a red halo. The suppressor mutants overexpressing *cspC* (GP1989) or underexpressing *veg* (GP1990) had no significant effect on halo formation. Strikingly, the *degS* mutation in GP2900 led to distinct formation of a red halo and in addition to that, the cells seemed to migrate to the colony periphery.

Taken together, the *degS* (P245S) mutation likely affects exopolysaccharide-matrix production possibly by a change of DegS phosphorylation activity. Even though biofilm formation likely poses no selective pressure for *cspB cspD* mutants, a change of DegS activity would affect many genes potentially alleviating secondary defects caused by loss of the cold shock proteins.

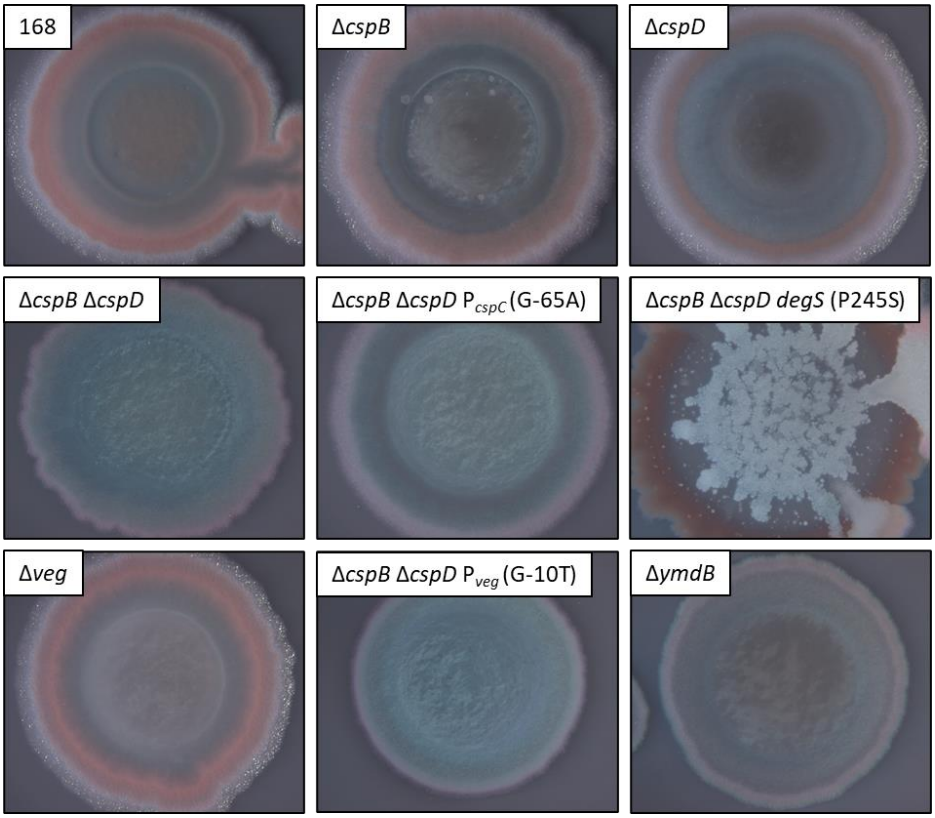

Figure 15: Matrix production on biofilm inducing medium. The wild type strain 168 and the mutant strains GP1968 (Δ*cspB*), GP2614 (Δ*cspD*), GP1971 (Δ*cspB* Δ*cspD*), GP1989 (Δ*cspB* Δ*cspD* P_{cspC}(G-65A)), GP2900 (Δ*cspB* Δ*cspD degS*(P245S)), GP2888 (Δ*veg*), GP1990 (Δ*cspB* Δ*cspD* P_{veg}(G-10T)) and GP583 (Δ*ymdB*) were cultivated at 30°C for four days on MSgg-agar with congo red and Coomassie brilliant blue. The results are representative of two biological replicates.

4.2.6 Expression of *E. coli* CspC allows deletion of all cold shock proteins in *B. subtilis*

To further understand the function of the cold shock proteins in *B. subtilis,* it was attempted to complement the *cspB cspD* double knockout with cold shock proteins from different species in which their function is better understood. Distinct cellular functions have been identified for the cold shock proteins of *E. coli* or the Gram-positive bacterium *S. aureus*. Table 8 shows the *E. coli* or *S. aureus* cold shock protein that exhibited the highest homology to the respective *B. subtilis* cold shock protein in a bi-directional homology analysis (Zhu & Stülke, 2018). The best hit for CspB was the CspC or CspA protein from *E. coli or S. aureus*, respectively. Remarkably, the best hit for *B. subtilis* CspC and CspD was always CspA from the proteomes of both species. In addition to that, there are proteins that do not share high sequence similarity but their structure closely resembles the OB fold structure of cold shock proteins. This applies for the translation initiation factor IF-1 encoded by *infA* in *E. coli* which has been reported to suppress the growth defect of a *cspB cspC* double mutant in *B. subtilis* (Weber *et al.*, 2001).

Table 8: Homologs of *B. subtilis* cold shock proteins in *E. coli* and *S. aureus*

B. subtilis protein	Best hit protein	Identity	Similarity
CspB	*E. coli:* CspC	67.2%	89.1%
	S. aureus: CspA	76.9%	95.4%
CspC	*E. coli:* CspA	72.1%	88.5%
	S. aureus: CspA	76.9%	92.3%
CspD	*E. coli:* CspA	64.1%	84.4%
	S. aureus: CspA	78.8.%	92.4%

In order to test the capability of these proteins to suppress the *cspB cspD* double knockout in *B. subtilis,* a suitable expression platform was needed. The suppressor screen showed that overexpression of *cspC* is able to suppress the growth defect (see section 4.2.2). As a proof of concept, it was firstly attempted to constitutively overexpress *cspC* with plasmid pGP3124 that drives expression by a strong *degQ* mutant promoter on pBQ200 (Martin-Verstraete *et al.*, 1994). While expression from pGP3124 was possible in the *cspD* mutant GP2614, further knockout of *cspB* was not possible. Interestingly, it was also impossible to delete *cspB* and *cspD* when the cells contained the empty vector pBQ200. This could indicate that already the empty vector becomes toxic when the major cold shock proteins are lost. In another attempt *cspC* expression was driven by a lactose-inducible promoter on pHT01 (MoBiTec, Göttingen) yielding pGP3128. Expression of *cspC* from pGP3128 was already toxic in *csp* single mutants at low amounts of inducer. Because loss of CspB and CspD increases expression of the chromosomal *cspC* gene (see section 4.2.2), it was hypothesized that a strong

increase of CspC becomes toxic as soon as *cspB* was deleted. Therefore, it was tested whether reduced *cspC* expression by a chromosomal copy driven by a xylose-inducible promoter allowed knockout of both *csp* genes. The resulting strain was GP2893. There, already the single deletion of *cspB* was not *via*ble. Other attempts to generate plasmids overexpressing *cspB* or *cspC* already failed at propagation in *E. coli* as only plasmids containing loss of function mutations could be isolated. A second copy of *cspB* was inserted into the *amyE* site under the control of its natural promoter containing the 5'-UTR. The resulting strain GP3280, showed no difference in growth as compared to the wild type (data not shown). This suggests that also *cspB* expression is regulated at its 5'-UTR. Taken together, these findings indicate that the expression of cold shock proteins has to be tightly controlled and too little or too much can become toxic for the cell.

However, it was known that the G-65A mutation which leads to increased *cspC* expression in GP1986 represents an expression level suitable for suppression of the *cspB cspD* double knockout. Therefore, the *E. coli cspA, cspC, cspD,* and *infA* genes as well as the *S. aureus cspA* gene were fused to the G-65A mutant *cspC* upstream region from GP1986 in a long flanking homology PCR. The PCR construct further included a spectinomycin resistance gene and the genetic region downstream of *cspC* which allowed substitution of the native *B. subtilis cspC* gene with the xenogenic sequences. This led to the strains GP3264 (*E. coli cspA),* GP3265 (*E. coli cspC),* GP3266 (*E. coli cspD*), GP3267 (*E. coli infA*), and GP3276 (*S. aureus cspA*). *cspB* and *cspD* were then deleted in these strains. Strikingly, only expression of the *E. coli cspC* gene allowed knockout of all three *B. subtilis csp* genes leading to strain GP3278. Expression of only *E. coli cspC* resulted in better growth compared to the *cspB cspD* double mutant GP1971 (see Figure 16 A). Nevertheless, *E. coli* CspC did not confer genetic competence (see Figure 16 B). In addition to that, GP3278 did not survive cryo conservation and was genetically instable and formed suppressors after longer storage at room temperature. Notably, also constitutive overexpression of *trans* encoded *infA* by pGP3123 did not allow deletion of *cspB* and *cspD*.

Taken together these findings demonstrate that the total amount of expressed cold shock proteins is critical for proper homeostasis. Moreover, the *E. coli* homolog CspC is able to partially replace all three *B. subtilis* cold shock proteins if expressed at a high level similar to *B. subtilis* CspC. CspC is known to be involved in transcription antitermination and RNA stability in *E. coli,* indicating a potential function of the *B. subtilis* cold shock proteins (Bae *et al.*, 2000).

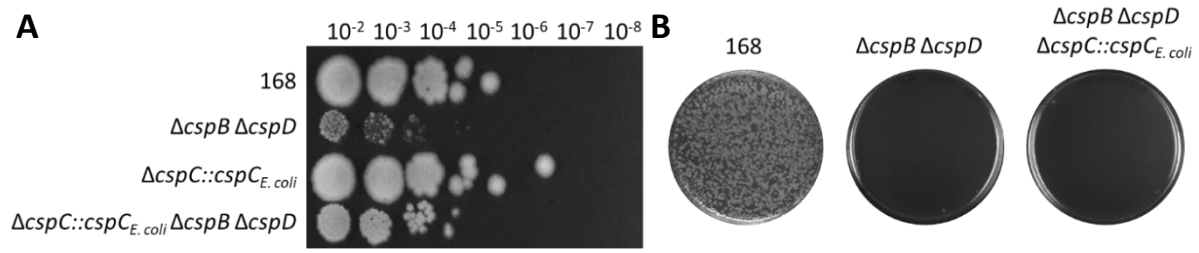

Figure 16: *E. coli* CspC allows deletion of the *B. subtilis* cold shock proteins. (**A**) The wild type strain 168 and the *csp* mutant strains GP1971 (Δ*cspB* Δ*cspD*), GP3265 (Δ*cspC*::P_{cspC}(*G-65A)-cspC*$_{E.coli}$), and GP3278 (Δ*cspC*::P_{cspC}(G-65A)-*cspC*$_{E.coli}$ Δ*cspB* Δ*cspD*) were cultivated on LB-agar at 37°C for one day. (**B**) Competent cells of the wild type strain 168 and the mutants GP1971 (Δ*cspB* Δ*cspD*) and GP3278 (Δ*cspC*::P_{cspC}(G-65A)-*cspC*$_{E.coli}$ Δ*cspB* Δ*cspD*) were diluted to an OD_{600} of 0.5 and transformed with 200 ng chromosomal DNA from strain BKE04260 (Δ*topB*::*ermC*). The cells were selected on LB-agar plates containing erythromycin/lincomycin plus antibiotics matching the respective resistance cassettes.

4.3 Identification of cellular targets of CspB and CspD

The phenotypic analysis of *csp* mutants demonstrated that cold shock proteins are essential players in the physiology of *B. subtilis* at optimal and low temperature. However, the mechanistic details on how they influence cellular processes in such a substantial way are not known. In other organisms the loss or overexpression of cold shock proteins leads to global changes in the transcriptome (Phadtare *et al.*, 2006; Michaux *et al.*, 2017; Caballero *et al.*, 2018). These changes are likely a result of numerous interactions of cold shock proteins with their RNA targets influencing transcription, RNA stability, as well as translation. To uncover how these processes are affected by the cold shock proteins in *B. subtilis* their RNA targets should be identified.

4.3.1 RNA fishing with CspD uncovers a wide range of bound RNAs

In order to identify potential RNA targets of the cold shock proteins a protein-RNA co-purification experiment was performed. Because the previous experiments showed that CspB and CspD are most important at 37°C, the targets of these proteins should be identified. To do so, the proteins were C- and N-terminally fused to a Strep-tag in the plasmids pGP380 and pGP382 which are normally used for the SPINE - Strep-protein interaction experiment (Herzberg *et al.*, 2007). The resulting plasmids were pGP3125 (Strep-CspB), pGP2164 (CspD-Strep), pGP2165 (Strep-CspD). N-terminal tagging of CspB was not possible, as observed for cloning of *cspB* into the pBQ200 overexpression plasmid which uses the same promoter as pGP380 and pGP382. Thus, it was questionable whether the Strep-tagged cold shock proteins were still functional. To test this, it was attempted to delete *cspB* and *cspD* in strains containing the respective plasmids. Similar to the *cspC* overexpression plasmids (see section 4.2.5), double knockout was not possible in the presence of a plasmid. Structural evaluation showed that the nucleotide binding site is diametrically opposed to the tagged C- and N-terminal ends and hence, the proteins likely retain their RNA binding capability (see

Figure 4). The *cspB* (GP1968) and *cspD* (GP2614) mutants were then transformed with the plasmids expressing the respective *csp* gene. As a negative control the wild type 168 was transformed with the empty vectors pGP380 or pGP382. Expression of *strep-ptsH* by pGP961 in MZ303 served as negative 'protein control' as PtsH is not known to bind RNA. Strep-tagged CsrA expressed from pGP381 in GP469 served as positive control since CsrA is known to bind the *hag* mRNA (Mukherjee *et al.*, 2011). The resulting strains were harvested at an OD_{600} of 2.0 after cultivation in LB medium at 37°C. After cell disruption, the cleared cell lysates were applied to a column in which the tagged proteins were bound to a Strep-tactin matrix. Washing and incubation with desthiobiotin resulted in eluates containing the tagged proteins and their RNA targets. The RNA was purified *via* phenol/chloroform extraction and the removal of residual DNA by DNase I was tested *via* PCR. A second round of phenol/chloroform extraction removed residual proteins and DNA and the pure RNA was subjected to RNA-sequencing after quality control.

The elution fractions after purification of the Strep-tagged proteins PtsH, CsrA, and CspD are shown in Figure 17 A. Purification of CspB was not possible in several attempts. The co-purified RNA was clearly visible as silver staining also stains nucleic acids (Blum *et al.*, 1987). Interestingly, purification of CspD led to a long smear with several bands likely indicating a high number of co-purified nucleic acids and proteins. This was also reflected by the final RNA concentrations being around 18 ng/µl for all control samples and above 1500 ng/µl for all purifications of CspD. RNA-sequencing uncovered a broad range of bound RNAs. As a proof of concept, fishing with CsrA enriched the *hag* transcript at least six-fold compared to the negative and protein control and 1.5-fold compared to the CspD sample. Fishing with CspD enriched 370 transcripts at least two-fold compared to all three control samples indicating it binds a wide range of RNAs. Of these transcripts 43 were identified as 5'-UTRs and 47 as 3'-UTRs. Figure 17 B displays some potentially interesting transcripts. The upper graph shows genes that are differentially expressed in the *cspB cspD* double mutant GP1971 (see section 4.3.2). Interestingly, CspD seemed to bind the transcripts of *cspC* and *veg* including their 5'- and 3'-UTRs indicating it may affect these RNAs as suggested by the suppressor screen. In addition to that, a lot of ribosomal protein RNAs as well as ribosomal RNAs seemed to be bound by CspD indicating a potential role in translation or a general proximity to the ribosome. Strangely, a lot of the enriched transcripts were also abundant in the purification of PtsH which is not known to bind RNA. Due to that, the experiment was only performed in one replicate. Taken together, these data show that CspD likely binds a broad range of RNAs but possibly only with low specificity.

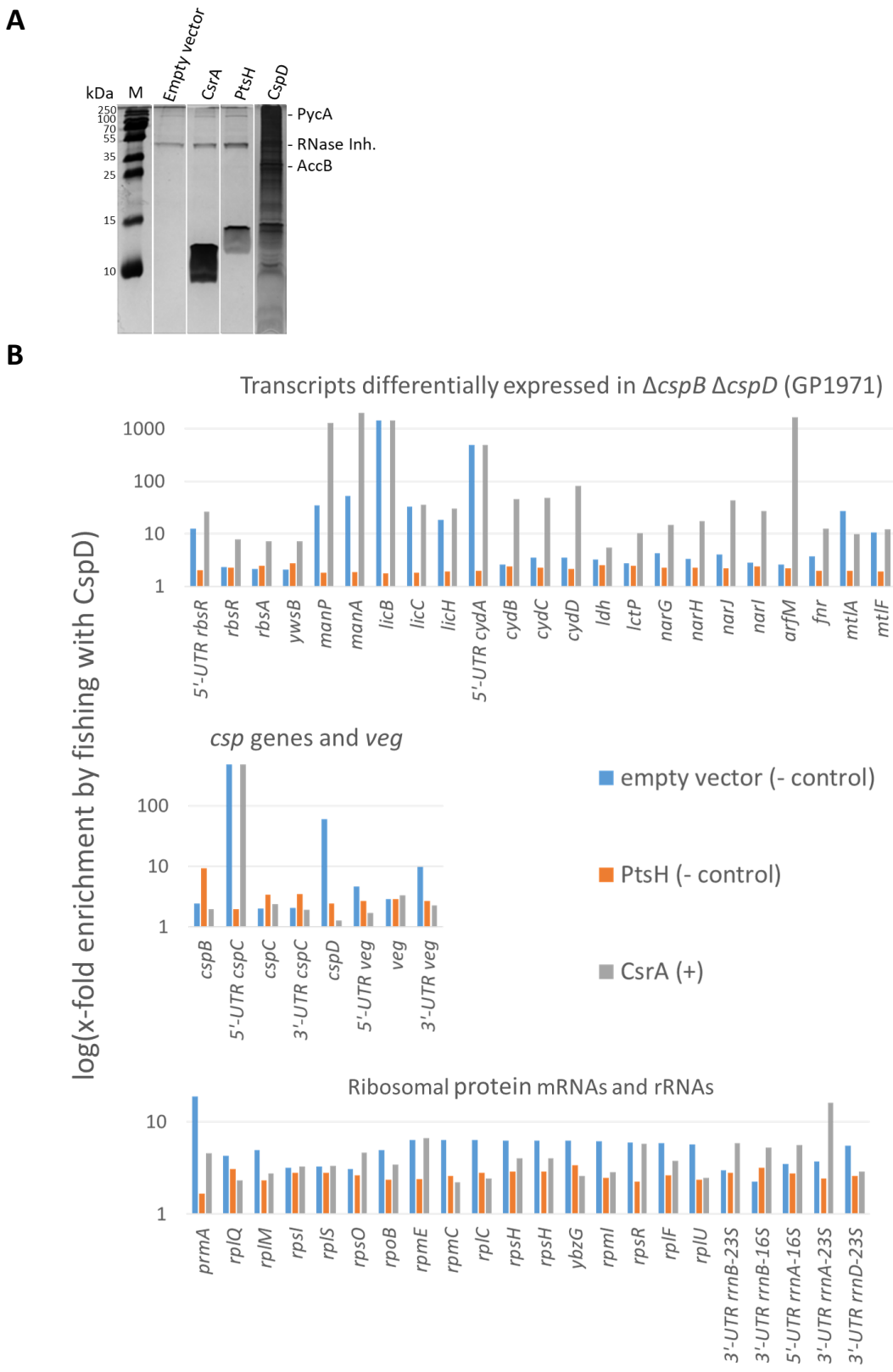

Figure 17: RNAs bound by CspD. (**A**) Silver stained elution fractions from Strep-purification. The strains GP2614+pGP382 (empty vector negative control), MZ303+pGP961 (PtsH protein control), GP469+pGP381 (CsrA positive control), and GP2614+pGP2164 (CspD sample) were harvested at an OD_{600} of 2 after cultivation in LB medium at 37°C. After Strep-purification the elution fraction were loaded on 17.5% SDS-PA gels and poteins were visualized by silver staining. RNAs of shown samples were extracted and subjected to RNA-sequencing. (**B**) x-fold enrichment by fishing with CspD compared to the control samples. The average enrichment by CspD as compared to the three control samples is at least 2-fold for all shown transcripts.

4.3.2 CspB and CspD modulate gene expression globally

The RNA-fishing experiment was not sensitive enough to clearly identify targets of CspD. Therefore, another method to identify potential RNA targets was employed. Independent of the process affected by cold shock proteins, all effects are likely a result of their interaction with RNAs. Due to that it was most reasonable to compare the transcriptomes of the wild type 168 and *cspB cspD* double mutant GP1971. The double mutant was chosen because it is clear from the data presented above that CspB and CspD have overlapping functions as only the loss of both led to severe pleiotropic defects. Both strains were grown in LB medium at 37°C to an OD_{600} of 0.2 in biological triplicates. The cells were harvested on frozen killing buffer, the pellets were snap-frozen on liquid nitrogen and stored at -80°C until extraction of total RNA. RNA-sequencing of all six replicates was performed and the generated reads were mapped to the *B. subtilis* 168 chromosome. A change of expression was set to be significant when the transcript exhibited a fold-change of at least two in GP1971 compared to 168.

In total, 846 transcripts were differentially expressed in the *cspB cspD* double mutant GP1971 corresponding to 21% of the transcriptome. Of these, 542 transcripts exhibited an increased expression and 305 transcripts exhibited a decreased expression. Table 9 shows a selection of the most strongly up- or downregulated transcripts as well as of transcripts important for the following chapters. Many of the strongly overexpressed genes but also some downregulated transcripts are involved in carbon metabolism. On the other hand, many of the downregulated transcripts are involved in the regulation of aerobic or anaerobic metabolism regulated by Rex or Fnr. A large part of the affected transcripts can be attributed to proteins involved in stress responses, carbon metabolism, nucleotide metabolism or sporulation (see Supplementary Table 1). Strikingly, many of the differentially expressed transcripts were fished by purification of CspD such as *cspC, rbsRA, ywsB, manPA, licBCH, cydABCD, ldh-lctP, narGHJI, arfM, fnr,* and *mtlAFD* (compare Table 9 and Figure 17 B Upper Panel). This was also true for a wide range of the remaining differentially expressed transcripts and include *rpoBC, spoVG, treR, groESEL, trePAR* or *bglPH* to name a few. Of all affected transcripts, 11 transcription factors (activators and repressors) were differentially expressed including *manR, liaR,* and *fnr* (see Table 9). Moreover, the sigma factor mRNAs *sigV*, *sigL* and *sigW* were upregulated four-fold, three-fold, and two-fold, respectively.

In summary, the loss of CspB and CspD has a global impact on the transcript profile which is in agreement with the observed severe pleiotropic defects in that mutant.

Table 9: Differentially expressed transcripts in the *cspB cspD* double mutant GP1971

Transcription unit	Function[1]	Regulation	Fold-change of expression upon *cspB cspD* deletion
Increased transcripts upon *cspB cspD* deletion			
liaIH	Resistance against cell wall antibiotics	Activated by LiaR	150
rbsRKDACB	Ribose utilization	Repressed by CcpA	110
maeN	Malate uptake	Activated by MalR	62
tlpA	Chemotaxis receptor	SigD regulon	47
ywsB	General stress protein	SigB regulon	45
manPA-yjdF	Mannose utilization	Activated by ManR	36
yodTSR	Spore metabolism	SigE regulon	32
licBCAH	Lichenan uptake	Repressed by CcpA and activated by LicR	21
manR	Transcriptional activator of the *manPA-yjdF* operon	Autoregulated by ManR and repressed by CcpA	18
liaGFSR	Two component system and response to bacitracin	Activated by LiaR	6
cspC	RNA chaperone	Negatively regulated by CspB and CspD (see section 4.2.2)	5
Decreased transcripts upon *cspB cspD* deletion			
cydABCD	Respiration, cytochrome bd oxidase	Repressed by CcpA and Rex	- 640
ldh-lctP	Overflow metabolism	Repressed by Rex	- 530
narGHJI	Nitrate respiration	Activated by Fnr	- 210
ywcJ	Putative nitrate channel	Repressed by Rex	- 163
arfM	Regulation of anaerobic genes	Activated by Fnr	- 90
mhqNOP	Resistance against oxidative stress	Repressed by MhqR	- 64
cotJC	Spore coat protein	SigE regulon	- 35
yflT	General stress protein	SigB regulon	- 14
fnr	Transcriptional regulator of anaerobic genes	Activated by ResD and repressed by Nsr	- 9
mtlAFD	Mannitol uptake	Activated by MtlR	- 7
pyrPB	Pyrimidine metabolism	Activated by PyrR	- 4

[1] Functional information is based on the *Subti*Wiki database (Zhu & Stülke, 2018).

4.4 CspB and CspD are involved in transcription termination and elongation

4.4.1 Loss of CspB and CspD affects transcriptional read-through at intrinsic terminators

The expression of *E. coli* CspC allowed the deletion of all three cold shock proteins in *B. subtilis.* CspC from *E. coli* was shown to antiterminate transcription at intrinsic terminators (Bae *et al.*, 2000). Hence, it was tempting to speculate that the cold shock proteins of *B. subtilis* might also act as transcriptional antiterminators. To test this idea, it was attempted to qualitatively compare the transcriptional read-through in the wild type 168 and the *cspB cspD* double mutant GP1971 *via* PCR. Both strains were grown in LB medium to an OD_{600} of 0.2 and the total RNA was converted to cDNA. During cDNA synthesis a control without reverse transcriptase was performed for both samples to control the absence of residual chromosomal DNA in the following PCR. The products then served as a template for amplification of intergenic regions harboring intrinsic terminators. If CspB and CspD have an influence on termination, the amount of read-through transcript at these sites should be altered in the *cspB cspD* double mutant. First approaches analyzed the intergenic regions of *glcT-ptsG*, *treR-hypO, dnaG-sigA, sinR-tasA, rbfA-truB,* and *mlpA-ymxH*. A reduced read-through transcript abundance was found for *dnaG-sigA* and *treR-hypO* (see Figure 18). The other intergenic regions did not exhibit any observable changes and as expected, no read-through transcript was observable for the *sinR-tasA* intergenic region (data not shown). The RNA-sequencing data of 168 and GP1971 allowed to compare transcriptional read-through and expression in the wild type and the *cspB cspD* double mutant directly. Only the *treR* and *yfkO* transcripts were upregulated. The *dnaG-sigA* and *treR-hypO* intergenic regions showed no differences in the transcript profiles between 168 and GP1971. It is possible that the number of generated reads per genetic segment is too low to visualize small changes in read-through transcription.

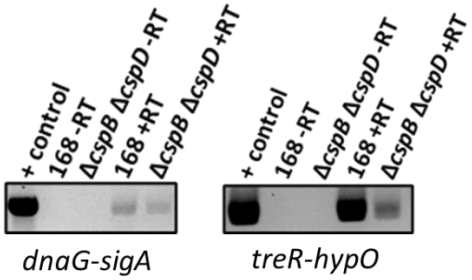

Figure 18: Qualitative PCR on read-through transcripts. Total RNA was extracted from 168 and GP1971 (Δ*cspB* Δ*cspD*). cDNA was synthesized and served as template in a PCR with primers annealing up- and downstream of the terminators between *dnaG-sigA*, *treR-hypO*. '+ control': standard PCR using chromosomal DNA of *B. subtilis* 168 as the template, '-RT': control sample without reverse transcriptase, '+RT': sample with reverse transcriptase.

Nevertheless, further direct comparison of the transcript profiles uncovered intergenic regions that clearly exhibited differences in transcriptional read-through. The intergenic regions of *manR-manP* and *liaH-liaG* exhibited an increased number of reads whereas the intergenic regions of *pyrR-pyrP and pyrP-pyrB* showed a decreased number of reads in the *cspB cspD* double mutant GP1971 (see Figure 19). All these genes were also differentially expressed in GP1971. The *manR* transcript was upregulated 18-fold while the *manP* transcript was upregulated 36-fold. *liaH* and *liaG* were upregulated 200-fold and seven-fold, respectively. The *pyrR* transcript was not affected whereas *pyrP* and *pyrB* were downregulated three-fold and four-fold, respectively. Apparently, the differential expression does not explain the observed changes in transcriptional read-through indicating that the latter is a result of the loss of CspB and CspD. The *manR-manP* and *liaH-liaG* intergenic regions contain an intrinsic terminator indicating that CspB and CspD may support termination. On the other hand, the intergenic regions of *pyrR-pyrP* and *pyrP-pyrB* can adopt a mutually exclusive terminator or antiterminator hairpin (Turner *et al.*, 1994). The reduced transcriptional read-through allows two explanations. One is that CspB and CspD act as antiterminator proteins. The other is that the loss of CspB and CspD interferes with binding of PyrR which is known to favor formation of the terminator hairpin (Turner *et al.*, 1994).

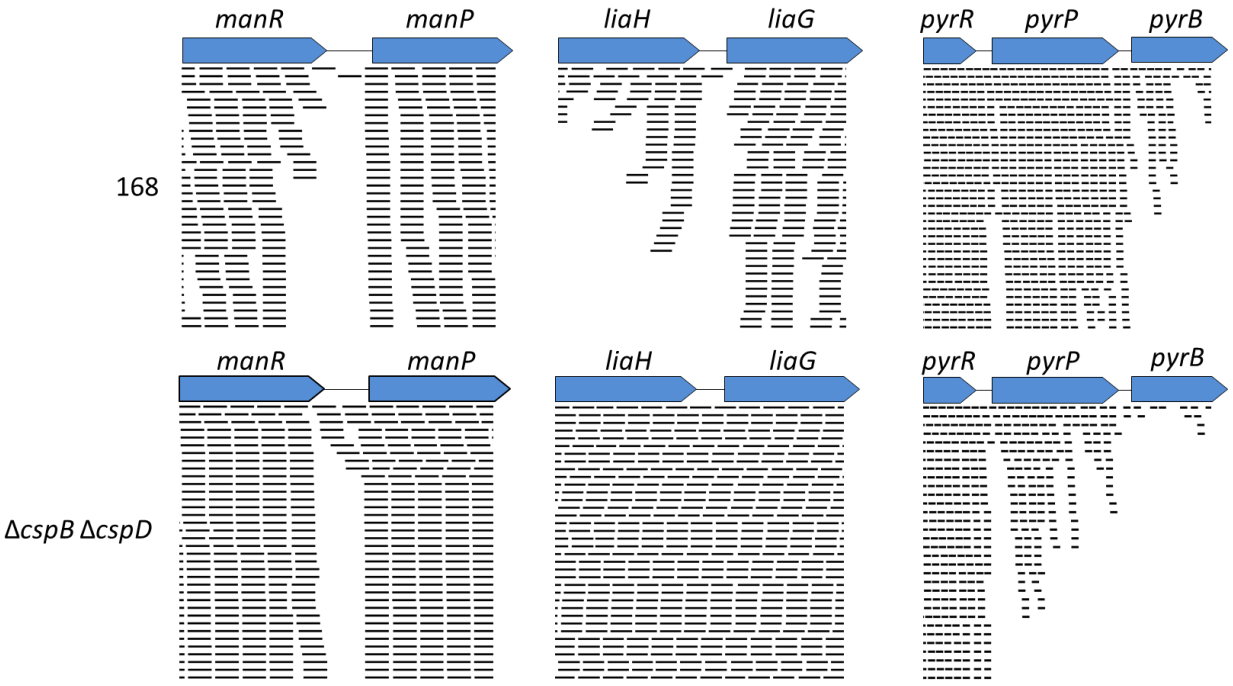

Figure 19: Differences in transcription in 168 and the *cspB cspD* double mutant. The intergenic regions between *manR-manP*, *liaH-liaG*, *pyrR-pyrP,* and *pyrP-pyrB* in the *B. subtilis* wild type 168 (upper panel) and the *cspB cspD* double mutant GP1971 (lower panel) aligned with the paired reads generated by RNA-sequencing are shown. The data are representative of three biological replicates. Pictures of aligned reads were created using the Geneious Software (Biomatters Ltd., New Zealand).

To prove the effect of CspB and CspD on the transcriptional read-through, a PCR analysis was performed as described above. 168 and GP1971 were grown to an OD_{600} of 0.2 in LB medium and the total RNA was converted to cDNA which served as template for primers that anneal 400 bp up- and downstream of the terminators. As shown in Figure 20 A, more product was detectable for the read-through transcript of *manR-manP* and *liaH-liaG* in the *cspB cspD* double mutant GP1971 which is in agreement with the observed transcription profiles. In contrast, only little effect was observable for the *pyrR-pyrP* intergenic region and only the *pyrP-pyrB* intergenic region indicated a potential decrease of read-through transcript abundance.

To quantitatively verify the observed changes of *cspB cspD* double deletion on transcriptional read-through, quantitative RT-PCR was performed. In that, 150 bp of the intergenic regions were amplified with primers that only give a product if the transcripts are elongated beyond the respective terminator hairpin. Strains 168 and GP1971 were grown to an OD_{600} of 0.2 in LB medium in biological triplicates. The quantitative RT-PCR data were in agreement with the transcription profiles and the qualitative PCR analysis (see Figure 20 B). The intergenic regions of *manR-manP* and *liaH-liaG* exhibited four-fold and 250-fold increased read-through, while the *pyrR-pyrP* and *pyrP-pyrB* intergenic regions showed a three-fold and four-fold decrease of transcriptional read-through, respectively.

In summary, these findings suggest that CspB and CspD are involved in the control of transcription elongation at intrinsic terminators in *B. subtilis.*

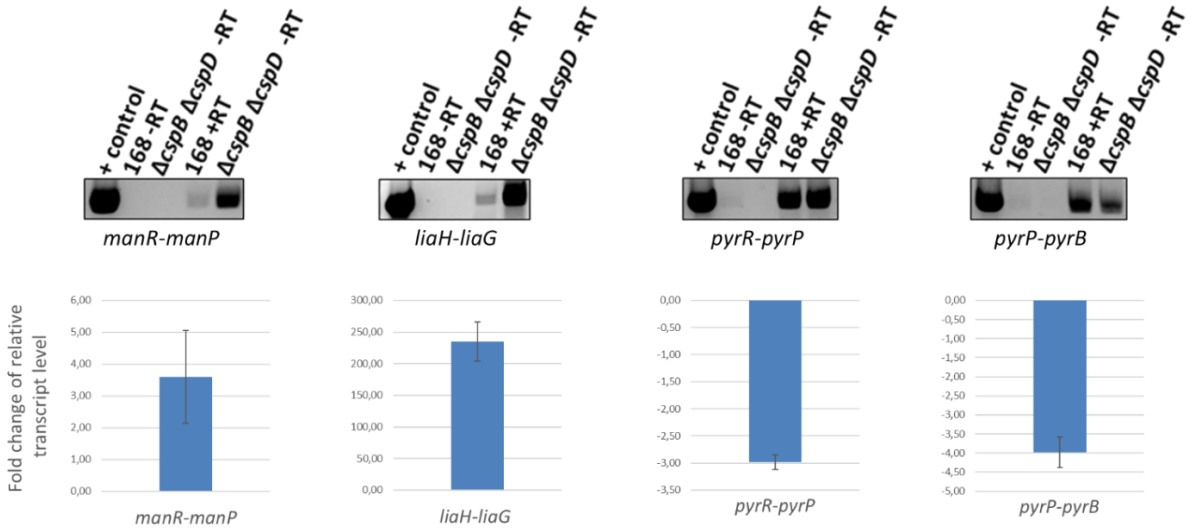

Figure 20: Transcriptional read-through in 168 and the Δ*cspB* Δ*cspD* mutant. (**A**) Qualitative PCR on read-through transcripts. Total RNA was extracted from 168 and GP1971 grown at 37°C in LB medium to an OD_{600} of 1.2. cDNA was synthesized and served as template in a PCR with primers annealing up- and downstream of the terminators between *manR-manP*, *liaH-liaG*, *pyrR-pyrP-pyrB*. '+ control': standard PCR using chromosomal DNA of *B. subtilis* 168 as the template, '-RT': control sample without reverse transcriptase, '+RT': sample with reverse transcriptase. (**B**) Fold changes in the expression of read-through transcripts in the *cspB cspD* double mutant GP1971 relative to levels in the wild type strain 168 are shown. 168 and GP1971 were grown at 37°C in LB medium to an OD_{600} of 0.2. RNA was purified from each strain and quantitative RT-PCR was performed using primer sets amplifying up- and downstream of the terminators in the indicated intergenic regions. Shown values represent the mean of three biological replicates. Errors bars indicate the standard de*via*tions.

4.4.2 CspB influences transcription by T7 RNA-polymerase *in vitro*

Phadtare *et al.* (2003) described an assay for *E. coli* CspE to test antitermination *in vitro*. They fused the T7 A1 promoter with the λ tR2-4 terminator and amplified this DNA template with reconstituted RNA-polymerase σ^{70} holoenzyme and radiolabeled nucleotides. In order to test the influence of CspB on termination of transcription, a promoter was fused to the *manR, liaH, pyrR, pyrP,* T7 and tR2-4 terminators. These constructs were further fused to a ribosomal binding site and a promoterless *lacZ* gene in pAC5 to later allow for measurement of β-galactosidase activity. The resulting plasmids were pGP3126 (*manR* terminator), pGP3130 (*liaH* terminator), pGP3135 (*pyrR* terminator), pGP3139 (*pyrP* terminator), pGP3142 (T7 terminator according to Blötz *et al.*, 2017), pGP3143 (tR2-4 terminator according to Wilson & von Hippel, 1995), and pGP3141 (no terminator). The plasmids served as template in a PCR that introduced a T7 promoter at the 5'-end. The amplicon was ~700 bp in size, started upstream of the terminator and ended ~200 bp downstream of it on the *lacZ* sequence. This served as DNA template for an *in vitro* transcription with or without the presence of CspB. His-CspB was expressed from pGP3140 in *E. coli* and purified *via* affinity chromatography. The His-tag was cleaved off using SUMO protease and was removed by a second affinity chromatography. Unfortunately, transcription assays with *B. subtilis* RNA-polymerase *in vitro* and with radiolabeled nucleotides were not possible. To circumvent this problem and to enable the visualization of RNA, T7 polymerase was used for long periods of *in vitro* transcription. While transcription with *E. coli* RNA-polymerase proceeded for 10 mins (Phadtare *et al.*, 2003), here at least 4.5 hours of transcription were needed to visualize the reaction products. The DNA template was removed by treatment with DNase I. Several experiments with different templates and varying amounts of CspB were performed. Each reaction with a DNA template containing a terminator should give two possible products: A runoff transcript where the polymerase reads through the terminator and a shorter terminated transcript (see Figure 21). The products of a representative *in vitro* transcription with the linear DNA templates amplified from pGP3140 (no terminator), pGP3142 (T7 terminator), pGP3126 (*manR* terminator) and with or without the addition of 40 µM CspB are shown in Figure 21. Unfortunately, two bands clearly indicating a runoff and a terminated transcript were not visible. However, two bands were visible in each reaction where CspB was present. Addition of CspB led to a reduction of the larger product and an increase of the smaller product as compared to the reactions without CspB. This indicates that CspB influences transcription and may lead to a general decrease of efficiency *in vitro*. The increase of the smaller product may be due to increased premature termination provoked by CspB. An effect of the terminators was not observable as the respective reactions produced even more product than the reaction containing the DNA template without a terminator.

Taken together, CspB clearly influences transcription by T7 RNA-polymerase *in vitro*. But it is unclear whether this is due to an effect on the secondary RNA structure, spatial competition with the

polymerase, or an indirect effect *e.g.* reduction of the available Mg^{2+} pool. A more specific reaction with quantifiable products and preferably the *B. subtilis* RNA-Polymerase is needed.

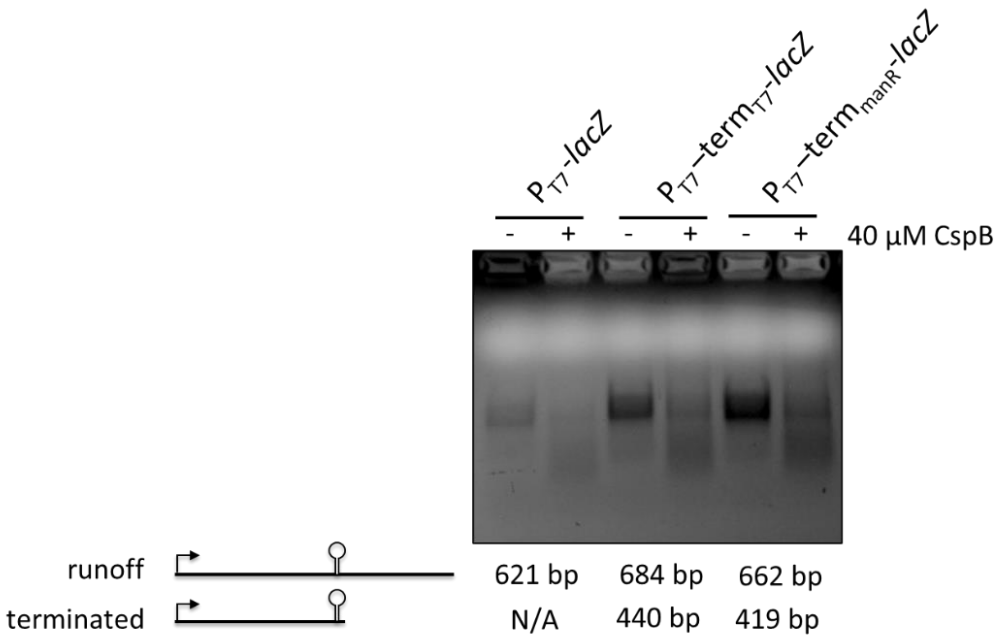

Figure 21: Effect of CspB on *in vitro* transcription by T7 RNA-polymerase. The assay was carried out as described in the methods section 3.2.5. DNA templates were amplified from pGP3140 (P_{T7}-*lacZ*), pGP3142 (P_{T7}-term$_{T7}$-*lacZ*), pGP3126 (P_{T7}-term$_{manR}$-*lacZ*). The products were analyzed by a denaturing agarose gel electrophoresis (1% agarose). Expected sizes of runoff and terminated transcripts are indicated below the gel.

4.4.3 CspB and CspD influence expression more strongly downstream of transcription

To analyze the effect of CspB and CspD on termination *in vivo*, the promoter-terminator-*lacZ* constructs mentioned above were analyzed for β-galactosidase activity in the wild type 168 and *cspB cspD* double mutant (GP1971) background. Unfortunately, the plasmids did not exhibit any β-galactosidase activity. Therefore, the plasmid pGP721 in which a translational *lacZ* fusion of the *pdhA* upstream region drives expression was used. According to the RNA-sequencing data, expression of *pdhA* was not affected in GP1971. The *pdhA* 5'-UTR contains a *Kpn*I restriction site that was used to integrate the *manR, liaH,* and *pyrR* anti-/ terminator sequences into pGP721. The resulting plasmids were pGP3144 (*manR* terminator), pGP3145 (*liaH* terminator), and pGP3146 (*pyrR* terminator/ antiterminator). Integration of the plasmids into the wild type 168 and deletion of *cspB* and *cspD* yielded the strains GP216 (P_{pdhA}-*lacZ*), GP3292 (P_{pdhA}-*lacZ* Δ*cspB* Δ*cspD*), GP3290 (P_{pdhA}-term$_{manR}$-*lacZ*), GP3291 (P_{pdhA}-term$_{manR}$-*lacZ* Δ*cspB* Δ*cspD*), GP3293 (P_{pdhA}-term$_{liaH}$-*lacZ*), GP3294 (P_{pdhA}-term$_{manR}$-*lacZ* Δ*cspB* Δ*cspD*), GP3298 (P_{pdhA}-anti-/ term$_{pyrR}$-*lacZ*), and GP3299 (P_{pdhA}-anti-/ term$_{pyrR}$-*lacZ* Δ*cspB* Δ*cspD*). The strains were cultivated in LB medium at 37°C to a final OD_{600} of 0.5 - 0.8 and β-galactosidase activities were determined (see Table 10). In contrast to the transcriptomic data, knockout of *cspB* and *cspD* already led to a two-fold reduction of *lacZ* expression driven by *pdhA*. The threshold for a change

of expression in the RNA-sequencing data was set to two which likely explains why a decreased expression of *pdhA* was not detected before. Nevertheless, insertion of the *manR* and *liaH* terminator sequences led to reduced expression as compared to the natural *pdhA* upstream region indicating they indeed have a terminating effect. The *pyrR* anti-/ terminator region had no effect on expression. This is likely because the antiterminator structure is adopted in LB medium where pyrimidines are highly abundant and hence, PyrR does not stabilize the terminator structure (Rayner *et al.*, 1990; Turner *et al.*, 1994; Hobl & Mack, 2007). As seen for the natural *pdhA* upstream region, loss of CspB and CspD reduced expression also in the presence of the anti-/ terminator regions. Strikingly, the decrease of expression was more severe when an anti-/ terminator region was present which is reflected by the fold-changes. However, these changes do not reflect the influence of CspB and CspD on read-through transcription that was observed above. This indicates that even if CspB and CspD increase or decrease the transcriptional read-through, they affect expression of these transcripts more strongly in processes downstream of transcription suggesting a potential role in RNA stability or translation.

Table 10: Promoter activities of the *pdhA* upstream region containing terminator sequences in the wild type and *cspB cspD* double mutant background

Strain	Genetic background	Enzyme activity in Miller units/mg of protein*	Fold-change
GP216	P_{pdhA}-*lacZ*	712 ± 10	2
GP3292	P_{pdhA}-*lacZ* Δ*cspB* Δ*cspD*	365 ± 67	
GP3290	P_{pdhA}-term$_{manR}$-*lacZ*	282 ± 8	3.7
GP3291	P_{pdhA}-term$_{manR}$-*lacZ* Δ*cspB* Δ*cspD*	84 ± 23	
GP3293	P_{pdhA}-term$_{liaH}$-*lacZ*	477 ± 54	5.2
GP3294	P_{pdhA}-term$_{liaH}$-*lacZ* Δ*cspB* Δ*cspD*	96 ± 13	
GP3298	P_{pdhA}-anti-/ term$_{pyrR}$-*lacZ*	750 ± 33	4.6
GP3299	P_{pdhA}-anti-/ term$_{pyrR}$-*lacZ* Δ*cspB* Δ*cspD*	165 ± 19	

*All measurements were performed in triplicate. The standard de*via*tions are indicated.

4.5 CspB and CspD do not affect RNA stability

The previous experiments and literature suggest that cold shock proteins are also involved in post-transcriptional regulation implying an effect on RNA stability and translation. It has also been reported that cold shock proteins influence the processing of RNAs *e.g.* CspA in *S. aureus* inhibits RNase III processing of the *cspA* 5'-UTR (Caballero *et al.*, 2018). Therefore, the stability and processing of various RNAs in the *cspB cspD* double mutant GP1971 were tested. For this purpose, the *rbsRKDACB* operon and the *cspC* gene that were upregulated 110-fold and five-fold, respectively, were chosen. Furthermore, it was attempted to analyze the *cydABCD* and the *gapA* operons that were

downregulated 640-fold and five-fold, respectively. All four transcription units are preceded by a 5'-UTR offering a potential site of regulation by cold shock proteins as already indicated for *cspC* (see section 4.2.2). The *gapA* operon mRNA is processed by RNase Y and thus, allows to investigate whether also cold shock proteins have an influence on processing of this RNA (Meinken *et al.*, 2003).

Firstly, processing and RNA stability were investigated by Northern blotting. A time course experiment with rifampicin which inhibits the RNA-polymerase and allowed monitoring of the RNA decay, was performed. The wild type strain 168 and the *cspB cspD* double mutant GP1971 were cultivated in LB medium at 37°C and samples were taken at 0, 3, 6, 9, and 12 minutes after addition of rifampicin. Equal amounts of extracted RNA were applied for each time point, separated by denaturing agarose gel electrophoresis, and blotted on a nylon membrane. Digoxygenin labeled probes specific for *rbsR, cspC,* and *cydA* were generated by *in vitro* transcription (see section 3.2.5). A *gapA*-specific probe was already available (Meinken *et al.*, 2003). Localization of the hybridized probe was visualized by digoxygenin specific antibodies conjugated with alkaline phosphate.

The Northern blots for *rbsR, cspC,* and *gapA* are shown in Figure 22 Left Panel. Unfortunately, the probe specific for *cydA* did not hybridize correctly and produced unspecific results (data not shown). In agreement with the RNA-sequencing data, *rbsR* and *cspC* showed an upregulation while *gapA* showed a downregulation in the *cspB cspD* double mutant as compared to the wild type. Interestingly, the *rbsR* probe uncovered several bands, likely indicating processing of this operon. However, the relative amounts were not changed in the mutant. As expected, no processing was observable for *cspC*. The two faint bands in the middle section correspond to the ribosomal RNA bands that unspecifically captured the probe. Processing of the *gapA* operon occurred as described in the literature and was also not altered by loss of CspB and CspD.

After Northern blotting, the bands corresponding to the respective transcript were quantified by densitometry. For each lane, three measurements were performed. These values were used to calculate the half-life of the respective transcript in both strains (see Figure 22 Right Panel). Densitometric quantification of the transcript *rbsR* transcript uncovered no significant differences of the half-life in both strains. The *cspC* transcript however, showed a strong increase of mRNA half-life from 30 seconds in the wild type to two minutes in the *cspB cspD* double mutant. This suggests that CspB and CspD destabilize the *cspC* transcript. Conversely, the *gapA* transcript exhibited a reduced half-life of about three minutes in the *cspB cspD* mutant compared to seven minutes in the wild type indicating CspB and CspD may be involved in stabilization of this mRNA.

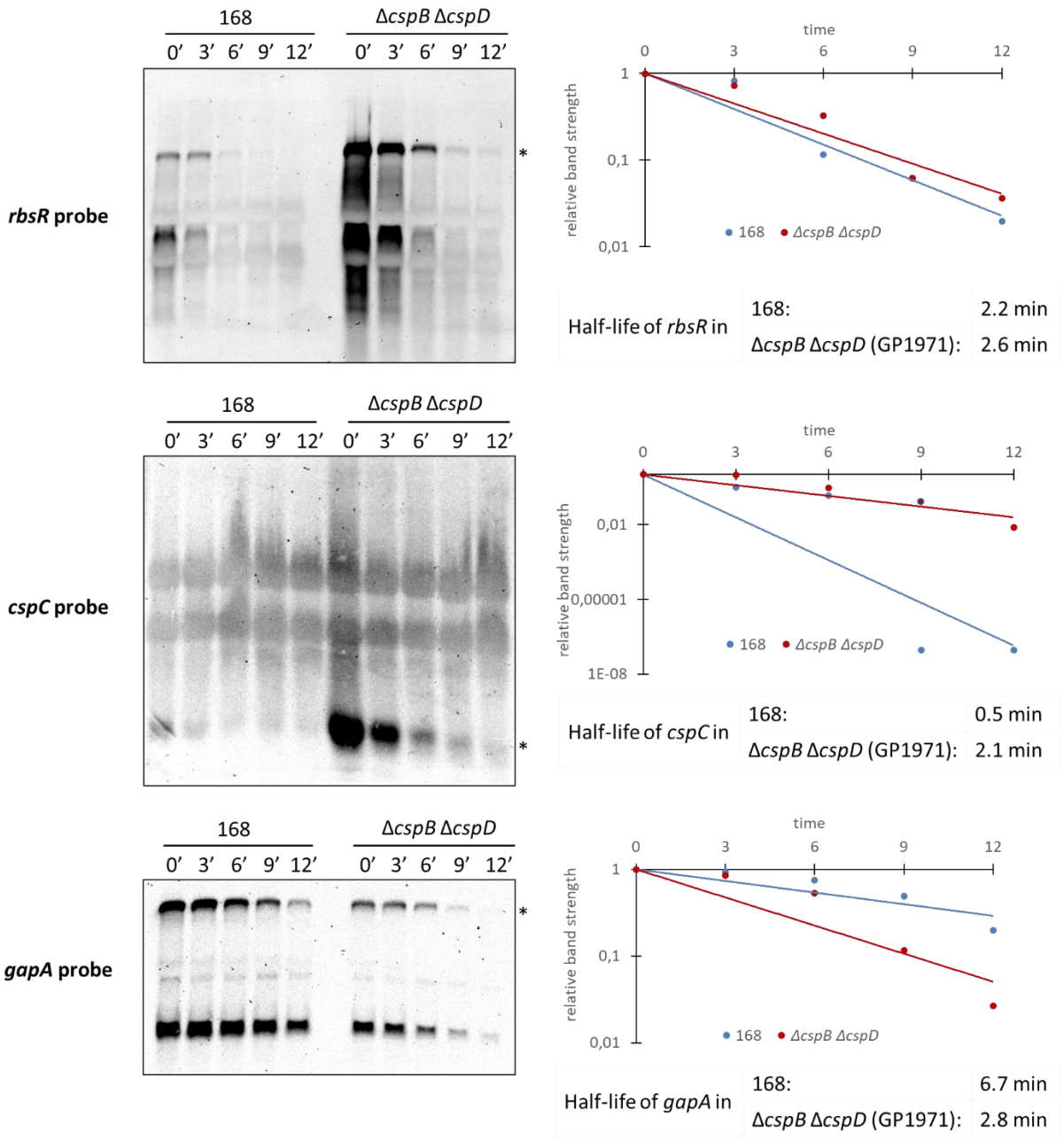

Figure 22: Processing and stability of the *rbsR, cspC,* and *gapA* transcripts in 168 and the *cspB cspD* double mutant. (**Left Panel**) Northern blot analysis with probes specific for *rbsR*, *cpsC*, and *gapA*. RNA was isolated from *B. subtilis* 168 and GP1971 (Δ*cspB* Δ*cspD*) grown in LB medium at 37°C to an OD of 1.2. Equal amounts of total RNA in each lane were separated on a 1% denaturing agarose gel, and after blotting, nylon membranes were hybridized to riboprobes specific for *rbsR, cspC,* and *gapA*. Note that the *cspC* probe cross-hybridized with 16S and 23S rRNA. Asterisks mark bands that were quantified thrice by densitometry using ImageJ. (**Right Panel**) The half-life of the *rbsR, cspC,* and *gapA* transcripts was determined in the wild type strain 168 and GP1971 (Δ*cspB* Δ*cspD*) measuring the signal strength in the Northern blot *via* densitometry as described in the methods (see section 3.2.5).

Because quantification *via* densitometry is not very reliable and quantification of chemiluminescence was not possible, the half-lives were determined *via* quantitative RT-PCR. For that, the wild type strain 168 and the *cspB cspD* double mutant GP1971 were cultivated in LB medium

at 37°C to an OD_{600} of 0.2 in biological duplicates and samples were taken at 0, 3, 6, 9, and 12 minutes after addition of rifampicin. The extracted RNA was then used for absolute quantification of the *rbsR, cspC,* and *gapA* mRNAs *via* quantitative RT-PCR in technical triplicates. In that, the transcript amount was calculated by comparing the generated Ct values with a standard curve. This was generated using a serial dilution of a defined DNA sequence as template for RT-PCR. The standard curve template was amplified with the same primers used for amplification of the *rbsR* mRNA which had the same size as the *cspC* and *gapA* amplicons. Even though, the DNA template leaves out the reaction efficiency of the reverse transcriptase reaction, it allowed for quantification of the relative transcript amounts which was sufficient to monitor the percental decay over time. In the following analysis, only the time points 0, 3, and 6 minutes after addition of rifampicin were used because the RNA amounts at later times were very low and prone to high deviation. Figure 23 shows the percental decay of the *rbsR, cspC,* and *gapA* transcripts in the wild type 168 and the *cspB cspD* double mutant GP1971. Strikingly, all three transcripts showed no significant difference in RNA half-life.

Taken together, it was shown that CspB and CspD do not influence processing of the *rbsRKDACB* and the *gapA* operon. Furthermore, both cold shock proteins do not significantly affect the RNA stabilities of the *rbsR, cspC,* and *gapA* transcripts indicating that potential differences in RNA stability are more likely a result of a different process impaired by loss of CspB and CspD as for example due to altered translation rates.

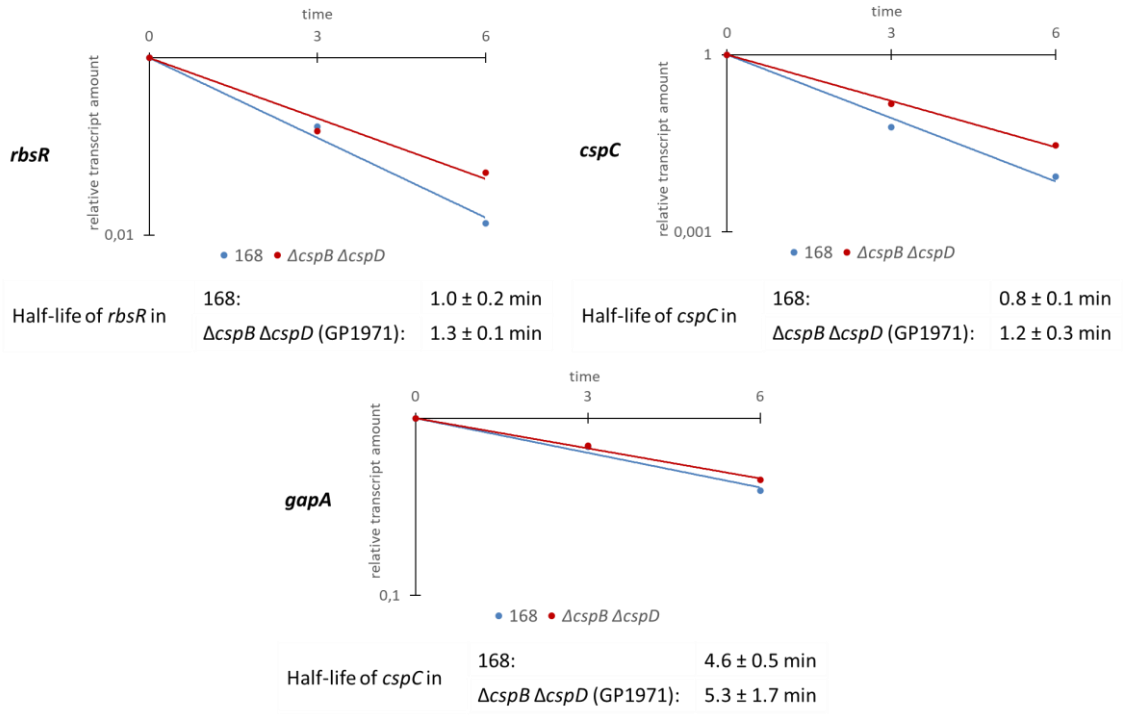

Figure 23: RNA stability of the *rbsR, cspC,* and *gapA* transcripts in 168 and the *cspB cspD* double mutant as determined by quantitative RT-PCR. RNA was isolated from *B. subtilis* 168 and GP1971 (Δ*cspB* Δ*cspD*) grown in LB medium at 37°C to an OD of 0.2. The half-lives were determined as described in the methods (see section 3.2.5). Average values obtained from biological duplicates with standard de*via*tions are shown.

5. Discussion

Cold shock domain proteins are essential for proper functioning of cells and have been shown to shape a large variety of biological processes in all kingdoms of life. Bacterial cold shock proteins consist of a single cold shock domain and all identified functions are associated with the ability to bind single stranded RNA or DNA (Budkina *et al.*, 2020). Cold shock proteins have been mostly studied in *E. coli* where they were shown to function as antiterminators, RNA stabilizers, and facilitators of translation (Jiang *et al.*, 1997; Bae *et al.*, 2000; Phadtare *et al.*, 2002; Feng *et al.*, 2001; Phadtare *et al.*, 2006; Cohen-Or *et al.*, 2010). More recent studies in other bacteria also identified implications in RNA stability, showed functional differences between cold shock proteins, and support the idea of cold shock proteins as globally acting RNA chaperones (Chao *et al.*, 2017; Michaux *et al.*, 2017; Caballero *et al.*, 2018; Zhang *et al.*, 2018; Catalan-Moreno *et al.*, 2020). In *B. subtilis,* the experimental evidence for the function(s) of cold shock proteins is thin and can basically only be inferred from other species. This work extended the knowledge on cold shock protein function in *B. subtilis* and uncovered implications in a wide range of biological processes. It was shown that the three cold shock proteins function redundantly to some extent with CspC being functionally different from CspB and CspD. It was demonstrated that the *cspC* 5'-UTR is of high importance for expression and for regulation by the other cold shock proteins. RNA-sequencing and protein-RNA co-purification experiments indicated that CspB and CspD shape the transcriptome as globally acting proteins. CspB and CspD affected transcriptional elongation positively or negatively. Further experiments suggested that CspB and CspD also affect gene expression by post-transcriptional regulation but an effect on RNA stability could not be shown.

5.1 Importance of cold shock proteins at optimal and cold temperatures

Consistent with literature, the presence of at least one *csp* gene was essential for viability and double knockouts lead to growth defects at 37°C and 15°C (Graumann *et al.*, 1997). While the strongest growth defect has been reported for the *cspB cspC* double mutant at 15°C (Graumann *et al.*, 1997), here the loss of *cspB* and *cspD* was most severe at both temperatures. Given the genetic instability of the *cspB cspD* double mutant, it is well conceivable that differences in growth behavior reported by Graumann *et al.* (1997) are due to unrecognized suppressor formation.

Only expression by the *cspC* promoter exhibited a clear increase at 15°C in this study whereas two dimensional gel electrophoresis experiments indicated that all three *B. subtilis* cold shock proteins are increased 48 h after cold shock (Graumann *et al.*, 1997). Different translation efficiencies at cold and the varied ^{35}S-methionine labeling times among the compared samples may have led to a distortion of the detected protein amounts by Graumann *et al.* (1997). An older study measured *cspB-lacZ* expression over time and found that CspB expression increases in the first two hours after cold shock and then quickly decreases again (Willimsky *et al.*, 1992). Northern blotting and transcriptional

lacZ fusions showed that the transcripts of *cspB* and *cspC* are transiently induced at 15°C whereas this induction was negligible in translational *cspB-lacZ* fusions (Kaan *et al.*, 1999). In *E. coli*, the cold-induction of *cspA* expression a is also only transient and returns to a basal level (Goldstein *et al.*, 1990; Jiang *et al.*, 1996). Therefore, it is possible that *cspB* expression is indeed transiently increased at cold but it returns to a basal level shortly after adaption to cold. Following this, transient overexpression of *cspB* could be important for adaptation to cold. More importantly, constitutive overexpression of *cspC* is clearly needed for adaptation and persisted growth at cold. This study further showed that *cspD* expression is slightly reduced at cold indicating that CspD is more important at optimal temperature. The differential expression of the *csp* genes is also reflected by the long 5'-UTRs harboring the cold boxes. These are only found for *cspB* and *cspC* and upstream of cold-induced *csp* genes in *E. coli* (Lopez *et al.*, 2001). Genes that are not cold-inducible only have a short 5'-UTR such as *cspD* in *B. subtilis* or *cspC, cspD,* and *cspE* in *E. coli* (Lopez *et al.*, 2001). Cold induction of the *E. coli cspA* gene is mediated by its 5'-UTR which upon temperature shift folds into a different structure that is less susceptible to degradation and is more efficiently translated (Giuliodori *et al.*, 2010). Likewise, the *cspB* and *cspC* 5'-UTRs from *S. aureus* adopt a structure which is more efficiently translated at low temperature (Catalan-Moreno *et al.*, 2021). This work highlighted the importance of the 5'-UTR for *B. subtilis cspC* expression suggesting a potentially similar regulatory mechanism at cold. It will be interesting for future studies to investigate the stability and translation of the *cspC* and *cspB* RNAs at low temperature.

Furthermore, it would be interesting to analyze whether the cold shock proteins contribute to cold adaption similarly as in *E. coli*. There, CspA utilizes its RNA melting activity to globally reduce secondary structures to adjust the translation rate while RNase R ensures the correct RNA levels (Zhang *et al.*, 2018). It is well possible that a similar mechanism takes place in *B. subtilis.*

5.2 Functional specialization of cold shock proteins

The high structural similarity of the cold shock proteins indicates that all of them bind nucleic acids and that they might function redundantly. However, their diversity in sequence (CspC shares ~70% identity with CspB and CspD) suggests that they do not share the same biological function. For example, the two cold shock proteins from *T. thermophilus* also share 69% sequence similarity and have different functions and only one is cold-induced (Tanaka *et al.*, 2012). The differential expression of the *cspC* gene at cold as well as its inability to sustain genetic competence and overall fitness when the other paralogs are missing, indicates functional specialization of CspC in *B. subtilis*. It could be argued that this is because of the lower overall expression of *cspC* compared to *cspB* and *cspD* (Nicolas *et al.*, 2012; see Table 3). On the other hand, while increased expression of *cspC* by the suppressor mutation did enhance overall fitness, the genetic competence was not restored. This shows that the cold shock proteins exhibit partial redundancy but also specific biological functions can be attributed

to the different paralogs. Similarly, knockout studies in *E. coli, S. enterica,* and *L. monocytogenes* showed that the loss of cold shock proteins can be functionally compensated by some but not all of the remaining paralogs (Xia *et al.*, 2001; Michaux *et al.*, 2017; Eshwar *et al.*, 2017). Taken together, the cold shock proteins have different biological functions with CspC being more important for growth at cold and CspB and CspD conferring genetic competence. To further examine the functional specialization of the different cold shock proteins in *B. subtilis* it would be interesting to compare expression levels in different conditions such as temperature or growth phase. It has been reported that CspB and CspC together are important for growth in the stationary phase even though this was not observable in this work (Weber, *et al.*, 2001). Also in *E. coli* and *S. aureus,* the expression of *csp* genes was shown to be dependent on nutritional conditions and growth phase (Czapski & Trun, 2014; Brandi *et al.*, 2016; Uppalapati *et al.*, 2017; Kram *et al.*, 2020).

This study further demonstrated that the proline at position 58 is responsible for the specific control of genetic competence and overall fitness by CspB and CspD. Likewise, in CspA from *S. aureus* the proline at position 58 is essential for the regulation of staphyloxanthin production (Catalan-Moreno *et al.*, 2020). According to *in vitro* studies with *B. subtilis* CspB, proline 58 is located within the RNA-binding motif and its backbone carbonyl group forms water mediated contact with the nucleic acid (Sachs *et al.*, 2012). Therefore, it has been suggested that proline 58 might be responsible for selection of specific RNA targets (Catalan-Moreno *et al.*, 2020). Interestingly, an alignment of the *B. subtilis, S. aureus*, *E. coli,* and *L. monocytogenes* cold shock protein amino acid sequences shows that most of them contain a proline residue (red arrow) which is flanked by highly conserved amino acid residues (see Figure 24). Earlier studies on *B. subtilis* CspB and *E. coli* CspA showed that mutation of single aromatic amino acids impairs nucleic acid binding (Schröder *et al.*, 1995; Hillier *et al.*, 1998; Rennella *et al.*, 2017). Moreover, different amino acids seem to be responsible for RNA binding or RNA melting (Phadtare *et al.*, 2002; Zeeb *et al.*, 2006; Sachs *et al.*, 2012). Hence, the highly conserved amino acid residues seem to be important for nucleic acid binding in general and the less conserved proline residue is likely important for target selection. This is supported by the fact that all cold shock proteins that do not contain the proline in the respective sequence motif, do indeed exhibit distinct biological functions. In contrast to CspA, CspB and CspC are not able to positively regulate staphyloxanthin production in *S. aureus* (Catalan-Moreno *et al.*, 2020). *E. coli* CspD is the only cold shock protein that is not able to suppress cold sensitivity and is expressed at different conditions than the other *csp* genes (Xia *et al.*, 2001). Also, the *L. monocytogenes* CspD protein lacks a proline residue at position 58 and was shown to be important for biological functions that are different from the other cold shock proteins (Schmid *et al.*, 2009; Eshwar *et al.*, 2017). Finally, this has been demonstrated for the *B. subtilis* CspC protein in this work.

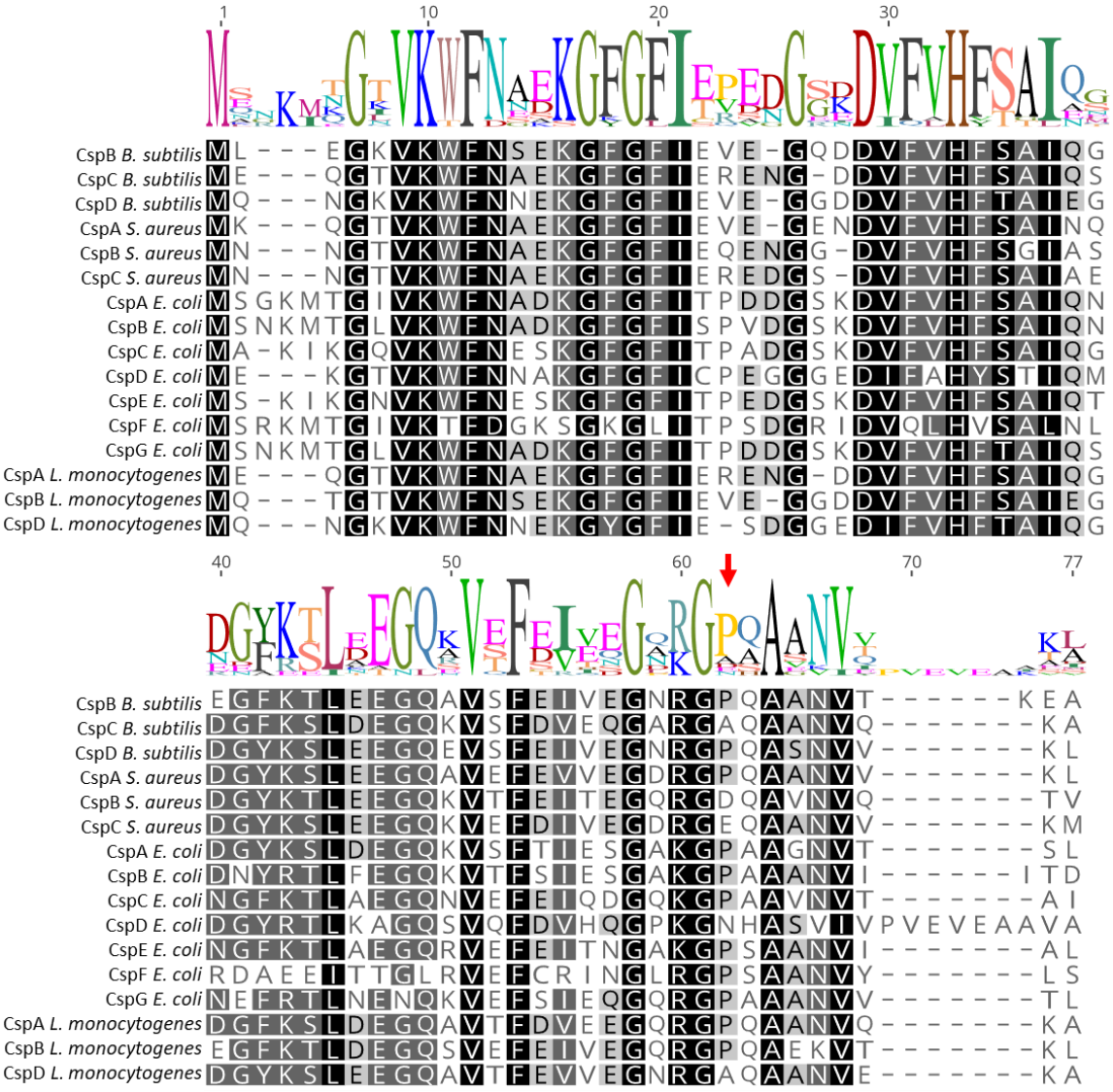

Figure 24: Alignment of the *B. subtilis, S. aureus, E. coli,* and *L. monocytogenes* cold shock protein amino acid sequences. Darker shading indicates higher conservation. Red arrow indicates position of the proline residue that is critical for functional specificity. Sequences were acquired from SubtiWiki and ListiWiki (Zhu & Stülke, 2018)**,** or EcoCyc (Keseler *et al.*, 2017)**.** Alignment was created using the Geneious software package (Kearse *et al.*, 2012).

However, the target specificity does not seem to solely depend on the proline residue. For example, cold shock proteins which all contain the proline residue have also been shown to exhibit different target specificites *in vitro. E. coli* CspB preferentially binds the UUUUU sequence, whereas CspC prefers the AGGGAGGGA motif, and CspE selects for AU-rich sequences (Jiang *et al.*, 1997; Phadtare & Inouye, 1999). *E. coli* CspE has moreover been shown to specifically interact with ribosome-free RNAs encoding inner membrane proteins (Benhalevy *et al.*, 2015; Benhalevy *et al.*, 2017). In *B. subtilis*, it is known that even though the CspB protein has an overall low sequence specificity, it preferentially binds T-rich single stranded DNA sequences (Lopez *et al.*, 2001; Max *et al.*, 2006). Nevertheless, a different target specificity of CspC is further supported by the finding that *cspC*

expression was responsive to the CspB and CspD but not the CspC levels. In addition to that, regulation by the cold shock proteins was dependent on the presence of a cold box. The importance of other amino acid residues than proline for the functional specificity was further demonstrated by the complementation of a *csp* triple knockout with CspC from *E. coli.* Even though the *E. coli* CspC protein contains the proline residue, it was not able to restore genetic competence. In addition to that, other cold shock proteins with less similarity to CspB such as CspA from *E. coli* and *S. aureus* were not able to allow a triple knockout of the *csp* genes in *B. subtilis*. This is likely a consequence of the different target specificities. It has been stated that for analysis of the functional diversity of cold shock proteins, comparable protein levels are needed (Catalan-Moreno *et al.*, 2020). Thus, it is well possible that even more cold shock protein homologs can replace the *B. subtilis* paralogs dependent on the expression level. The observed toxicity of *cspB* or *cspC* overexpression further supports this idea. Likewise, overexpression of *cspD* results in a lethal phenotype in *E. coli* (Yamanaka & Inouye, 1997). The toxicity of high CspC levels could also explain why no genetic amplifications of the *cspC* region were found in suppressors of the *cspB cspD* double mutant. Because *cspC* is upregulated when CspB and CspD are missing, this could lead to toxic amounts when a duplication of the *cspC* gene is present.

The protein-RNA co-purification did not allow clear identification of preferential targets of CspD. However, CspD likely also binds RNAs in a selective manner. This is supported by the observation that many RNAs that were enriched by purification of CspD, were also found to be differentially expressed in the *cspB cspD* double mutant. Using a different protein than PtsH as a control that does not bind RNA, could increase the significance of enriched RNAs compared to this control. More stringent washing to remove unspecific interactions as well as additional replicates should allow refinement of the CspD target profile. Future analyses could also employ target profiling for the individual cold shock proteins as it has been performed in *S. enterica* (Michaux *et al.*, 2017). A systematic evolution of ligands by exponential enrichment (SELEX) approach could additionally identify potential target sequence preferences as it has been performed for some *E. coli* cold shock proteins (Phadtare & Inouye, 1999).

5.3 Cellular targets of CspB and CspD

This work identified various cellular targets of the cold shock proteins. As described above, CspC occupies a functionally different role from CspB and CspD which seemed to have more overlapping activities. This was reflected by the strong phenotype observed only for the *cspB cspD* double mutant. Phenotypic defects were found in genetic competence, cell wall morphology, exopolysaccharide matrix production on biofilm inducing medium, as well as a strong deregulation of the transcriptome and proteome.

There are no reports of cold shock protein involvement in genetic competence or cell wall morphology. Neither genes important for genetic competence such as the *com* or *rec* genes, nor important cytoskeletal genes such as the *mre, min,* or *fts* genes were differentially expressed in the *cspB cspD* double mutant in the exponential growth phase. Because the competence and morphological defects were only observed in the late-exponential or stationary phase, it is possible that the involved genes are only differentially expressed in these growth phases. Differential expression of the *csp* genes as found in other species could play a role (Brandi *et al.*, 2016; Uppalapati *et al.*, 2017; Kram *et al.*, 2020). The observed loss of genetic competence may also be a consequence of the strongly reduced overall fitness which does not allow for sufficiently fast integration of external DNA in the stringent transformation protocol fitted to wild type cells. A role of cold shock proteins in genetic competence is also conceivable because they are known to bind single stranded DNA (Graumann *et al.*, 1997; Lopez *et al.*, 2001; Max *et al.*, 2006; Zeeb *et al.*, 2006; von König *et al.*, 2020) whose secondary structure is important during genetic recombination (reviewed by Lenhart *et al.*, 2012). Interestingly, CspB even preferentially binds single stranded DNA over RNA (Sachs *et al.*, 2012). *In vivo* cross-linking of proteins after induction of DNA repair may uncover spatial proximity of cold shock proteins to the proteins involved in homologous recombination. The observation that double-knockout of *cspB* and *cspD* was not possible in the presence of a plasmid (empty pBQ200) could further suggest a function on DNA. Interestingly, CspD from *E. coli* has been reported to inhibit DNA replication and tightly packs single stranded DNA distinguishable from SSB-coated DNA (Yamanaka *et al.*, 2001; Kim *et al.*, 2010).

Another defect of the *cspB cspD* double mutant was the decreased exopolysaccharide formation on biofilm inducing MSgg-agar. The cold shock proteins of *S. enterica* and *S. typhimurium* are implicated in biofilm formation and motility (Michaux *et al.*, 2017; Ray *et al.*, 2020). Also in *E. coli,* several *csp* genes were among the major induced genes in early biofilms (Domka *et al.*, 2007). A similar involvement of CspB and CspD in *B. subtilis* could explain the reduced formation of exopolysaccharides. Indeed, the biofilm associated genes *bslA*, *ywcA*, *yxaB, ydaM, epsK* and *epsM* were deregulated in the *cspB cspD* double mutant. The downregulated EpsM protein is directly involved in exopolysaccharide production (Kaundinya *et al.*, 2018; Arnaouteli *et al.*, 2021). Moreover, two suppressor mutations of the *cspB cspD* double mutant were found in the *veg* and *degS* gene which both are implicated in biofilm formation and/ or motility (Lei *et al.*, 2013; Belas, 2013). DegS is also involved in the regulation of late competence genes but the suppressor mutation did not restore the ability for genetic transformation (Msadek *et al.*, 1991; Mäder *et al.*, 2002). Because the Veg protein is poorly characterized it is interesting to mention that it influenced expression by the *cspC* promoter (see Table 7). This is the third promoter which was shown to be influenced by Veg besides *tapA* and *eps* (Lei *et al.*, 2013), suggesting a regulatory function potentially in RNA metabolism. Notably, the overall expression was

very low for the wild type *veg* upstream region. The *veg* gene is known to be strongly transcribed in the vegetative growth phase – hence its name (Nicolas *et al.*, 2012). Transcriptional *lacZ* fusions in the vegetative growth phase showed much higher activities (Fukushima *et al.*, 2003), indicating that *veg* expression may undergo strong post-transcriptional regulation. Future experiments could investigate the effect of *csp* loss on the formation of complex biofilms in the DK1042 wild type background. Motility assays and microscopy of flagella in *csp* mutant backgrounds could further uncover the importance of cold shock proteins for motility. Nevertheless, the *veg* and *degS* mutations likely only alleviate secondary defects caused by loss of *cspB* and *cspD* which would explain their low frequency.

Aside from these specific phenotypic defects, the loss of CspB and CspD had a much broader effect as their loss ultimately led to deregulation of 21% of the transcriptome in the exponential growth stage. This was also reflected by the total protein expression consistent with a previous study (Graumann *et al.*, 1997). Notably, the discovered regulon of CspB and CspD overlaps with the regulon of cold shock proteins in other bacteria including genes involved in stress response, carbon metabolism, and nucleotide metabolism (Phadtare *et al.*, 2006; Michaux *et al.*, 2017; Caballero *et al.*, 2018). These changes could be a consequence of globally acting proteins deregulated by the loss of CspB and CspD. In fact, several sigma factors such as *sigV, sigL,* and *sigW* were deregulated. However, these three sigma factors together regulate 123 genes at most and cannot explain the differential expression of at least 846 transcripts in the *cspB cspD* double mutant (Zhu & Stülke, 2018). The same holds true for the affected activators and repressors which usually only have very few targets in the chromosome. Other globally acting deregulated proteins are the RNA polymerase subunit mRNAs *rpoB* and *rpoC* which were downregulated two-fold in the *cspB cspD* double mutant. Yet, a decrease of the overall RNA polymerase level would not explain the higher abundance of 542 transcripts. Other RNA binding proteins that act as global post-transcriptional regulators such as RNases or proteins with potentially large targetomes such as Hfq or CsrA were not differentially expressed in the *cspB cspD* double mutant (Van Assche *et al.*, 2015). Taken together, the changes of transcript abundance must be a consequence of a global function of CspB and CspD. Also in other organisms the loss or overexpression of cold shock proteins leads to extensive changes in the transcriptome (Phadtare *et al.*, 2006; Wang *et al.*, 2016; Michaux *et al.*, 2017; Caballero *et al.*, 2018). It would be interesting to investigate the targetomes of the single cold shock proteins by constructing a mild overexpression platform that does not lead to toxic protein levels.

Lastly, a very probable target of CspB and CspD is the *cspC* 5'-UTR since loss of the two proteins only affected *cspC* expression when the full length 5'-UTR was present. The *cspC* gene was also upregulated in the *cspB cspD* double mutant. In *E. coli,* the CspE protein was shown to negatively regulate *cspA* expression by increasing pause recognition near the cold box in the 5'-UTR (Bae *et al.*, 1999). CspA further mediates a conformational switch of the 5'-UTR at low temperature to increase

the RNA stability (Zhang *et al.*, 2018). Also the 5'-UTRs of *cspA* in *S. aureus* was shown to be important for autoregulation by the CspA protein which inhibits RNase III processing (Caballero *et al.*, 2018). It is well possible that regulation by cold shock protein in *B. subtilis* functions in a comparable way. It would be interesting for future studies to investigate the effect of CspB and CspD on the *cspC* 5'-UTR. Also, an effect on the 5'-UTR of *cspB* or other genes could be tested. A closer identification of the structural determinants for regulation in the 5'-UTR could be explored by mutational probing.

5.4 Mechanism(s) of regulation by CspB and CspD

This work identified a multifold of cold shock protein targets but it is unclear which mechanism leads to positive or negative regulation. *E. coli* CspC was able to replace all *B. subtilis* cold shock proteins at least with respect to viability. CspC as well as CspE from *E. coli* act as transcriptional antiterminators which utilize their RNA melting activity to destabilize terminator structures (Bae *et al.*, 2000; Phadtare *et al.*, 2002; Phadtare & Severinov, 2005). Also the *E. coli* and *S. aureus* CspA proteins were shown to have nucleic acid melting activity (Rennella *et al.*, 2017; Caballero *et al.*, 2018). Mutated variants of *E. coli* CspE have lost nucleic acid melting activity and cannot antiterminate transcription but they further regulate the expression of genes *via* their RNA binding activity (Phadtare *et al.*, 2002). It is not known whether also *B. subtilis* cold shock proteins have RNA melting capabilities and it is unclear whether the *E. coli* CspC nucleic acids melting activity is essential for replacement of the *B. subtilis* proteins. Hence, future research should investigate the RNA melting as well as RNA binding capability of the different cold shock proteins. Binding could easily be tested by electrophoretic mobility shift assays. Melting could be investigated by advanced real time NMR spectroscopy, or by analysis of quenching using a double stranded RNA beacon system with fluorescent and quenching dyes at the strand ends (Rennella *et al.*, 2017; Caballero *et al.*, 2018).

Nevertheless, this study clearly observed an effect of CspB and CspD on transcription. The intergenic regions of *manR-manP* and *liaH-liaG* exhibited increased transcriptional read-through when CspB and CspD were absent. The *manR* and *liaH* genes possess intrinsic terminators according to the ARNold Rho-independent terminator prediction tool or global transcription profiles (Naville *et al.*, 2011; Nicolas *et al.*, 2012). Following this, CspB and CspD reduce transcription at these sites. Assuming they have RNA melting capability, it would not be utilized to destabilize the terminator structure. This is supported by the fact that transcriptional read-through was not affected at the vast majority of intrinsic terminator sites in the *cspB cspD* double mutant. It can be hypothesized that CspB and CspD reduce transcription by increasing transcriptional attenuation at these sites. In *E. coli,* CspA and CspE have been proposed to increase pause recognition efficiency by binding the nascent RNA of the *cspA* 5'-UTR cold box region (Bae *et al.*, 1999). Interestingly, the hairpin structure in the *E. coli cspA* 5'-UTR mRNA is reminiscent of the transcriptional pausing site of intrinsic terminators (Bae *et al.*, 1997). As

described above, a similar mechanism may occur at the *cspC* 5'-UTR which was only responsive to CspB and CspD when the cold box 2 was present. Noteworthy, CspB preferentially binds T-rich single stranded DNA or U-rich RNA sequences as found in the cold boxes or in intrinsic terminators (Wilson & von Hippel, 1995; Graumann *et al.*, 1997; Lopez *et al.*, 2001; Max *et al.*, 2006).

The *B. subtilis pyr* gene cluster is regulated by a transcriptional attenuation mechanism in which PyrR stabilizes an anti-antiterminator hairpin and thereby, stabilizes the terminator structure (Turner *et al.*, 1994; Hobl & Mack, 2007). This work demonstrated that the intergenic regions of *pyrR-pyrP* and *pyrP-pyrB* exhibited decreased transcriptional read-through in the *cspB cspD* double mutant. This finding allows several explanations. Firstly, CspB and CspD could destabilize the terminator specifically by utilizing a putative RNA melting function. Secondly, they could counteract PyrR by inhibiting formation of the anti-antiterminator structure and hence, stabilization of the antiterminator. Lastly, CspB and CspD may directly hinder binding of PyrR an hence, stabilize the antiterminator. Even though deletion of *pyrR* was not possible in this study, future *in vivo* experiments should try to analyze read-through transcription in a *pyrR cspB cspD* triple mutant to rule out an effect of PyrR. Mutational probing and *in vitro* transcription assays could uncover the structural elements involved in regulation by the cold shock proteins at this region.

This work attempted to analyze read-through transcription of the isolated terminator or antiterminator structures by *in vitro* transcription. Unfortunately, the assay was not suited as no termination was observable. It is possible that the chosen terminators do not terminate transcription of T7 polymerase. Future studies should test the influence of cold shock proteins at intrinsic terminators which have been shown to terminate in *in vitro* transcription termination assays previously (Jeng *et al.*, 1992). Another solution could be the use of purified *B. subtilis* RNA polymerase as done with *E. coli* RNA polymerase for *in vitro* antitermination assays of *E. coli* cold shock proteins (Phadtare *et al.*, 2003). Nevertheless, CspB exerted an effect on transcription and reduced the amount of product. This recapitulates the results of another study in which *B. subtilis* CspB suppressed transcription in an *E. coli* based cell free expression system (Hofweber *et al.*, 2005). Opposingly, a study with *E. coli* cold shock proteins reported that the nucleic acid melting activity can also facilitate reactions hindered by secondary structures such as RT-PCR or RNA cleavage (Phadtare *et al.*, 2009). The observed detrimental effect on transcription could also be a consequence of the very high CspB concentration leading to spatial blockage of the T7 RNA polymerase. Nevertheless, the cold shock proteins' low affinity for RNA is said to likely pose no obstacle at least for ribosome movement (Budkina *et al.*, 2020). Future research with an optimized assay that uses *B. subtilis* RNA polymerase elongation complexes stalled before the terminator, radiolabeled nucleotides, and much shorter incubation time as performed for *E. coli* should allow to uncover the action of cold shock proteins on intrinsic terminators *in vitro* (Phadtare *et al.*, 2003).

In vivo termination assays showed that the *manR* and *liaH* terminators reduce expression, while the *pyrR* antiterminator region missing the terminator sequence did not. Loss of CspB and CspD led to a decrease of expression downstream of the *pdhA* 5'-UTR which was even more severe in the presence of the terminator and antiterminator regions. The regulatory function of the *pdhA* 5'-UTR has not been elucidated except for the importance of a single base in the transcription initiation site during the stringent response (Tojo *et al.*, 2010). It cannot be elucidated from the current data whether the stronger decrease of expression in the absence of CspB and CspD is due to an effect on transcription termination or due to a post-transcriptional effect. The fact that expression was also more strongly decreased when the antiterminator region was present suggests a regulatory role of CspB and CspD independent from termination and thus, downstream of transcription. However, the effect of CspB and CspD on the respective region is likely encoded in the secondary structure of the *pdhA* 5'-UTR and the inserted anti-/ terminator structure. The complexity and interplay of both sequences makes functional prediction by the secondary structure impossible. Future *in vivo* assays should employ artificial promoters without regulatory upstream regions to rule out secondary effects of a 5'-UTR.

Many of the differentially expressed genes in the *cspB cspD* double mutant are preceded by 5'-UTRs which can be regulated at the level of transcriptional attenuation, RNA stability, or translation (Naville & Gautheret, 2010; Bouloc & Repoila, 2016; Millman *et al.*, 2017; Jia *et al.*, 2020). This work investigated RNA processing and stability of the *rbsR*, *cspC,* and *gapA* operon mRNAs which all contain a 5'-UTR and which were deregulated in the *cspB cspD* double mutant. No differences were visible in RNA processing and no mRNA exhibited a significantly altered stability in the *cspB cspD* double mutant. Yet, an effect of cold shock proteins on RNA stability cannot be ruled out fully because too few RNAs were tested and the employed techniques suffer from high deviation. Future experiments should use a narrower time frame with more sampled time points to investigate the RNA decay over time. Quantification of the chemiluminescent signal in the Northern blots should help to produce more reliable results. The literature suggests that an effect on RNA stability is likely as cold shock proteins act as RNase E or RNase III antagonists in *E. coli, S. enterica,* and *S. aureus* (Phadtare & Inouye, 2001; Lioliou *et al.*, 2012; Barria *et al.*, 2013; Chao *et al.*, 2017; Michaux *et al.*, 2017; Caballero *et al.*, 2018). A recent study reported that the *E. coli* RNase E can functionally replace *B. subtilis* RNase Y (Laalami *et al.*, 2021). It is tempting to speculate that the *B. subtilis* cold shock proteins also bind to RNase Y cleavage sites and protect the respective RNA from degradation. Even though the *cggR-gapA* transcript stability which is regulated by RNase Y was not affected by loss of CspB and CspD, it is possible that other RNase Y cleavage sites are targets of cold shock proteins (Lehnik-Habrink *et al.*, 2011). Recent work in *B. subtilis* identified a loss-of function mutation in *cspD* after deletion of *rny* suggesting a functional connection (Benda *et al.*, 2020). The identification of RNase Y cleavage sites as performed

for 5'-UTRs in *E. coli* will allow to test the effect of cold shock proteins as potential RNase Y antagonists on different RNAs (Chao *et al.*, 2017). The *B. subtilis* cold shock proteins have been proposed to facilitate translation by providing linear mRNAs for the ribosome after unwinding by the helicases CshA and CshB (Hunger *et al.*, 2006). Bacterial two hybrid experiments uncovered interactions of CspD but not CspB or CspC with CshA and CshB (Tödter, 2011). CshA has been proposed to be a component of a potential *B. subtilis* degradosome (Lehnik-Habrink *et al.*, 2010). It would be interesting to further analyze potential functional dependencies of the DEAD-box helicases and cold shock proteins in genetic mutants of the respective genes.

The translational *lacZ* fusions in the *in vivo* anti-/ termination assay suggested that regulation by cold shock proteins occurs more strongly downstream of transcription. Because no effect on RNA stability was observable, it is well possible that cold shock proteins affect the rate of translation. Therefore, changes of RNA stability could also be a product of altered translation rates. Studies showed that mRNAs contain regulatory elements that block the ribosomal binding site and *E. coli* cold shock proteins are thought to assist in unwinding of these elements (Kudla *et al.*, 2009; Barria *et al.*, 2013; Pop *et al.*, 2014). During cold shock, the *E. coli* CspA protein facilitates translation together with RNase III (Zhang *et al.*, 2018). Similarly, it has been speculated that CspA in *S. aureus* enhances translation by disrupting ribosome stalling sites (Caballero *et al.*, 2018). The observation that the *B. subtilis* cold shock proteins are localized around nucleoids when the cells experience intensive transcription and translation, and that they are homogenously distributed at phases with less intensive transcription and translation suggests they act near the respective enzyme complexes (Weber *et al.*, 2001; Mascarenhas *et al.*, 2001). CspB interacted with the ribosomal RpsB protein in a proteome wide protein-protein interaction screen (De Jong *et al.*, 2017). It will be interesting for future research to investigate the effect of cold shock proteins on translation. This could be done by performing *in vitro* translation experiments that use mRNAs with structural elements that influence translatability.

In summary, CspB and CspD are potentially involved in transcriptional attenuation but also regulation at the level of RNA stability or translation is conceivable. This study provided interesting targets that allow more detailed research on cold shock protein function. Many genes that were differentially regulated in the *cspB cspD* double mutant are subject to known RNA-based regulation systems and RNA binding proteins. These include the *pyrP and pyrB* genes, the *bglPH* operon, the *licBCAH* operon, the *trp* operon, as well as the *glpFK* and *glpTQ* operons (Shimotsu *et al.*, 1986; Turner *et al.*, 1994; Krüger & Hecker, 1995; Darbon *et al.*, 2002; Stülke, 2002). It is well possible cold shock proteins are important for proper functioning of these regulatory systems.

6. References

Adhya, S., & Gottesman, M. 1978. Control of transcription termination. *Annu. Rev. Biochem.*, *47*, 967–996.

Akanuma, G., Nanamiya, H., Natori, Y., Yano, K., Suzuki, S., *et al.* 2012. Inactivation of ribosomal protein genes *in Bacillus subtilis* reveals importance of each ribosomal protein for cell proliferation and cell differentiation. *J. Bacteriol.*, *194*, 6282–6291.

Alén, C., & Sonenshein, A. L. 1999. *Bacillus subtilis* aconitase is an RNA-binding protein. *Proc. Natl. Acad. Sci. U. S. A.*, *96*, 10412–10417.

Amir, M., Kumar, V., Dohare, R., Rehman, M. T., Hussain, A., *et al.* 2019. Investigating architecture and structure-function relationships in cold shock DNA-binding domain family using structural genomics-based approach. *Int. J. Biol. Macromol.*, *133*, 484–494.

Amster-Choder, O. 2005. The *bgl* sensory system: A transmembrane signaling pathway controlling transcriptional antitermination. *Curr. Opin. Microbiol.*, *8*, 127–134.

Arnaouteli, S., Bamford, N. C., Stanley-Wall, N. R., & Kovács, Á. T. 2021. *Bacillus subtilis* biofilm formation and social interactions. *Nat. Rev. Microbiol.*, Epub ahead of print.

Arnaud, M., Vary, P., Zagorec, M., Klier, A., Debarbouille, M., *et al.* 1992. Regulation of the *sacPA* operon of *Bacillus subtilis*: Identification of phosphotransferase system components involved in SacT activity. *J. Bacteriol.*, *174*, 3161–3170.

Aymerich, S., & Steinmetz, M. 1992. Specificity determinants and structural features in the RNA target of the bacterial antiterminator proteins of the BglG/SacY family. *Proc. Natl. Acad. Sci. U. S. A.*, *89*, 10410–10414.

Babitzke, P., Stults, J. T., Shire, S. J., & Yanofsky, C. 1994. TRAP, the *trp* RNA-binding attenuation protein of *Bacillus subtilis*, is a multisubunit complex that appears to recognize G/UAG repeats in the *trpEDCFBA* and *trpG* transcripts. *J. Biol. Chem.*, *269*, 16597–16604.

Bae, W, Xia, B., Inouye, M., & Severinov, K. 2000. *Escherichia coli* CspA-family RNA chaperones are transcription antiterminators. *Proc. Natl. Acad. Sci. U. S. A.*, *97*, 7784–7789.

Bae, W., Jones, P. G., & Inouye, M. 1997. CspA, the major cold shock protein of *Escherichia coli*, negatively regulates its own gene expression. *J. Bacteriol.*, *179*, 7081–7088.

Bae, W., Phadtare, S., Severinov, K., & Inouye, M. 1999. Characterization of *Escherichia coli cspE*, whose product negatively regulates transcription of *cspA*, the gene for the major cold shock protein. *Mol. Microbiol.*, *31*, 1429–1441.

Baker, C. S., Morozov, I., Suzuki, K., Romeo, T., & Babitzke, P. 2002. CsrA regulates glycogen biosynthesis by preventing translation of *glgC* in *Escherichia coli*. *Mol. Microbiol.*, *44*, 1599–1610.

Barria, C., Malecki, M., & Arraiano, C. M. 2013. Bacterial adaptation to cold. *Microbiol. (United Kingdom)*, *159*, 2437–2443.

Bechhofer, D. H., & Deutscher, M. P. 2019. Bacterial ribonucleases and their roles in RNA metabolism. *Crit. Rev. Biochem. Mol. Biol.*, *54*, 242–300.

Belas, R. 2013. When the swimming gets tough, the tough form a biofilm. *Mol. Microbiol.*, *90*, 1-5.

Belogurov, G. A., & Artsimovitch, I. 2015. Regulation of transcript elongation. *Annu. Rev. Microbiol.*, *69*, 49–69.

Benda, M., Woelfel, S., Gunka, K., Klumpp, S., Poehlein, A., *et al.* 2020. Quasi-essentiality of RNase Y in *Bacillus subtilis* is caused by its critical role in the control of mRNA homeostasis. *bioRxiv*. 106237 doi: https://doi.org/10.1101/2020.05.20.106237

Benhalevy, D., Biran, I., Bochkareva, E. S., Sorek, R., & Bibi, E. 2017. Evidence for a cytoplasmic pool of ribosome-free mRNAs encoding inner membrane proteins in *Escherichia coli*. *PLoS One*, *12*, 1–28.

Benhalevy, D., Bochkareva, E. S., Biran, I., & Bibi, E. 2015. Model uracil-rich RNAs and membrane protein mRNAs interact specifically with cold shock proteins in *Escherichia coli*. *PLoS One*, *10*, 1–18.

Berger, F., Normand, P., & Potier, P. 1997. *capA*, a *cspA*-like gene that encodes a cold acclimation protein in the psychrotrophic bacterium *Arthrobacter globiformis* SI55. *J. Bacteriol.*, *179*, 5670–5676.

Bidnenko, V., Nicolas, P., Grylak-Mielnicka, A., Delumeau, O., Auger, S., *et al.* 2017. Termination factor Rho: From the control of pervasive transcription to cell fate determination in *Bacillus subtilis*. *PLoS Genet.*, *13*, e1006909.

Bienert, R., Zeeb, M., Dostál, L., Feske, A., Magg, C., *et al.* 2004. Single-stranded DNA bound to bacterial cold-shock proteins: Preliminary crystallographic and Raman analysis. *Acta Crystallogr. Sect. D Biol. Crystallogr.*, *60*, 755–757.

Bisht, S. C., Joshi, G. K., & Mishra, P. K. 2014. CspA encodes a major cold shock protein in Himalayan psychrotolerant *Pseudomonas* strains. *Interdiscip. Sci. Comput. Life Sci.*, *6*, 140–148.

Blötz, C., Commichau, F. M., Stülke, J. 2017. *Methods in Molecular Biology of Bacteria*. Dept. of General Microbiology. University of Göttingen.

Blum, H., Beier, H., & Gross, H. J. 1987. Improved silver staining of plant proteins, RNA and DNA in polyacrylamide gels. *Electrophoresis*, *8*, 93–99.

Bohn, C., Rigoulay, C., & Bouloc, P. 2007. No detectable effect of RNA-binding protein Hfq absence in *Staphylococcus aureus*. *BMC Microbiol.*, *7*, 1–9.

Bouloc, P., & Repoila, F. 2016. Fresh layers of RNA-mediated regulation in Gram-positive bacteria. *Curr. Opin. Microbiol.*, *30*, 30–35.

Bradford, M. M. 1976. A rapid and sensitive method for the quantitation of microgram quantities of protein utilizing the principle of protein-dye binding. *Anal. Biochem.*, *72*, 248–254.

Brandi, A., Giangrossi, M., Giuliodori, A. M., & Falconi, M. 2016. An interplay among FIS, H-NS, and guanosine tetraphosphate modulates transcription of the *Escherichia coli cspA* gene under physiological growth conditions. *Front. Mol. Biosci.*, *3*, 1–12.

Budkina, K. S., Zlobin, N. E., Kononova, S. V., Ovchinnikov, L. P., & Babakov, A. V. 2020. Cold shock domain proteins: Structure and interaction with nucleic acids. *Biochemistry. (Mosc).*, *85*, S1–S19.

Burd, C. G., & Dreyfuss, G. 1994. Conserved structures and diversity of functions of RNA-binding proteins. *Science*, *265*, 615–621.

Bycroft, M., Hubbard, T. J. P., Proctor, M., Freund, S. M. V., & Murzin, A. G. 1997. The solution structure of the S1 RNA binding domain: A member of an ancient nucleic acid-binding fold. *Cell*, *88*, 235–242.

Caballero, C. J., Menendez-Gil, P., Catalan-Moreno, A., Vergara-Irigaray, M., García, B., *et al.* 2018. The regulon of the RNA chaperone CspA and its auto-regulation in *Staphylococcus aureus*. *Nucleic Acids Res.*, *46*, 1345–1361.

Cardinale, C. J., Washburn, R. S., Tadigotla, V. R., Brown, L. M., Gottesman, M. E., & Nudler, E. 2008. Termination factor Rho and its cofactors NusA and NusG silence foreign DNA in *E. coli*. *Science 320*, 935–938.

Catalan-Moreno, A., Caballero, C. J., Irurzun, N., Cuesta, S., López-Sagaseta, J., & Toledo-Arana, A. 2020. One evolutionarily selected amino acid variation is sufficient to provide functional specificity in the cold shock protein paralogs of *Staphylococcus aureus*. *Mol. Microbiol. 113*, 826–840.

Catalan-Moreno, A., Cela, M., Menendez-Gil, P., Irurzun, N., Caballero, C. J., Caldelari, I., & Toledo-Arana, A. 2021. RNA thermoswitches modulate *Staphylococcus aureus* adaptation to ambient temperatures . *Nucleic Acids Res.*, *49*, 3409–3426.

Cech, T. R. 2012. The RNA worlds in context. *Cold Spring Harb. Perspect. Biol.*, *4*, 1–5.

Chaikam, V., & Karlson, D. T. 2010. Comparison of structure, function and regulation of plant cold shock domain proteins to bacterial and animal cold shock domain proteins. *BMB Rep. 43,* 1-8.

Chao, Y., Li, L., Girodat, D., Förstner, K. U., Said, N., Corcoran, C., *et al.* 2017. *In vivo* cleavage map illuminates the central role of RNase E in coding and non-coding RNA pathways. *Mol. Cell*, *65*, 39–51.

Chaulk, S. G., Smith-Frieday, M. N., Arthur, D. C., Culham, D. E., Edwards, R. A., *et al.* 2011. ProQ is an RNA chaperone that controls ProP levels in *Escherichia coli*. *Biochemistry*, *50*, 3095–3106.

Cohen-Or, I., Shenhar, Y., Biran, D., & Ron, E. Z. 2010. CspC regulates *rpoS* transcript levels and complements *hfq* deletions. *Res. Microbiol.*, *161*, 694–700.

Commichau, F. M., Rothe, F. M., Herzberg, C., Wagner, E., Hellwig, D., *et al.* 2009. Novel activities of glycolytic enzymes in *Bacillus subtilis*: Interactions with essential proteins involved in mRNA processing. *Mol. Cell. Proteomics*, *8*, 1350–1360.

Commichau, F. M., & Stülke, J. 2012. A Mystery Unraveled: Essentiality of RNase III in *Bacillus subtilis* Is caused by resident prophages. *PLoS Genet.*, *8*, 8–9.

Condon, C. 2010. What is the role of RNase J in mRNA turnover? *RNA Biol.*, *7*, 316-21.

Condon, C., & Putzer, H. 2002. The phylogenetic distribution of bacterial ribonucleases. *Nucleic Acids Res.*, *30*, 5339–5346.

Czapski, T. R., & Trun, N. 2014. Expression of *csp* genes in *E. coli* K-12 in defined rich and defined minimal media during normal growth, and after cold-shock. *Gene*, *547*, 91–97.

Dahl, M. K., Msadek, T., Kunst, F., & Rapoport, G. 1992. The phosphorylation state of the DegU response regulator acts as a molecular switch allowing either degradative enzyme synthesis or expression of genetic competence in *Bacillus subtilis*. *J. Biol. Chem.*, *267*, 14509–14514.

Darbon, E., Servant, P., Poncet, S., & Deutscher, J. 2002. Antitermination by GlpP, catabolite repression via CcpA and inducer exclusion triggered by P∼GlpK dephosphorylation control *Bacillus subtilis glpFK* expression. *Mol. Microbiol.*, *43*, 1039–1052.

De Hoon, M. J. L., Makita, Y., Nakai, K., & Miyano, S. 2005. Prediction of transcriptional terminators in *Bacillus subtilis* and related species. *PLoS Comput. Biol.*, *1*, e25.

De Jong, L., De Koning, E. A., Roseboom, W., Buncherd, H., Wanner, M. J., *et al.* 2017. In-culture cross-linking of bacterial cells reveals large-scale dynamic protein-protein interactions at the peptide level. *J. Proteome Res.*, *16*, 2457–2471.

Dietrich, S., Wiegand, S., & Liesegang, H. 2014. TraV: A genome context sensitive transcriptome browser. *PLoS One*, *9*, e93677.

Dimastrogiovanni, D., Fröhlich, K. S., Bandyra, K. J., Bruce, H. A., Hohensee, S., Vogel, J., & Luisi, B. F. 2014. Recognition of the small regulatory RNA *rydC* by the bacterial Hfq protein. *Elife*, *3*, 1–19.

Domka, J., Lee, J., Bansal, T., & Wood, T. K. 2007. Temporal gene-expression in *Escherichia coli* K-12 biofilms. *Environ. Microbiol.*, *9*, 332–346.

Dubey, A. K., Baker, C. S., Romeo, T., & Babitzke, P. 2005. RNA sequence and secondary structure participate in high-affinity CsrA-RNA interaction. *RNA*, *11*, 1579–1587.

Durand, S., & Condon, C. 2018. RNases and helicases in Gram-positive bacteria. *Regul. with RNA Bact. Archaea*, *6*, 37–53.

Durand, S., Gilet, L., & Condon, C. 2012. The essential function of *B. subtilis* RNase III is to silence foreign toxin genes. *PLoS Genet.*, *8*, e1003181.

Duval, M., Korepanov, A., Fuchsbauer, O., Fechter, P., Haller, A., *et al.* 2013. *Escherichia coli* ribosomal protein S1 unfolds structured mRNAs onto the ribosome for active translation initiation. *PLoS Biol.*, *11*, 12–14.

El-Sharoud, W. M., & Graumann, P. L. 2007. Cold shock proteins aid coupling of transcription and translation in bacteria. *Sci. Prog.*, *90*, 15–27.

Ermolenko, D. N., & Makhatadze, G. I. 2002. Bacterial cold-shock proteins. *Cell. Mol. Life Sci.*, *59*, 1902–1913.

Eshwar, A. K., Guldimann, C., Oevermann, A., & Tasara, T. 2017. Cold-shock domain family proteins (Csps) are involved in regulation of virulence, cellular aggregation, and flagella-based motility in *Listeria monocytogenes*. *Front. Cell. Infect. Microbiol.*, *7*, 1–15.

Eymann, C., Dreisbach, A., Albrecht, D., Bernhardt, J., Becher, D., *et al.* 2004. A comprehensive proteome map of growing *Bacillus subtilis* cells. *Proteomics*, *4*, 2849–2876.

Fang, L., Jiang, W., Bae, W., & Inouye, M. 1997. Promoter-independent cold-shock induction of *cspA* and its derepression at 37°C by mRNA stabilization. *Mol. Microbiol.*, *23*, 355–364.

Fang, M., Zeisberg, W. M., Condon, C., Ogryzko, V., Danchin, A., & Mechold, U. 2009. Degradation of nanoRNA is performed by multiple redundant RNases in *Bacillus subtilis*. *Nucleic Acids Res.*, *37*, 5114–5125.

Farnham, P. J., & Platt, T. 1981. Rho-independent termination: dyad symmetry in DNA causes RNA polymerase to pause duringtranscription in vitro. *Nucleic Acids Res.*, *9*, 563–577.

Fender, A., Elf, J., Hampel, K., Zimmermann, B., & Wagner, E. G. H. 2010. RNAs actively cycle on the Sm-like protein Hfq. *Genes Dev.*, *24*, 2621–2626.

Feng, Y., Huang, H., Liao, J., & Cohen, S. N. 2001. *Escherichia coli* poly(A)-binding proteins that interact with components of degradosomes or impede RNA decay mediated by polynucleotide phosphorylase and RNase E. *J. Biol. Chem.*, *276*, 31651–31656.

Figueroa-Bossi, N., Schwartz, A., Guillemardet, B., D'Heygère, F., Bossi, L., & Boudvillain, M. 2014. RNA remodeling by bacterial global regulator CsrA promotes Rho-dependent transcription termination. *Genes Dev.*, *28*, 1239–1251.

Formstone, A., & Errington, J. 2005. A magnesium-dependent *mreB* null mutant: Implications for the role of *mreB* in *Bacillus subtilis*. *Mol. Microbiol.*, *55*, 1646–1657.

Fox, G. E. 2010. Origin and evolution of the ribosome. *Cold Spring Harb. Perspect. Biol.*, *2*, 1–19.

Franze De Fernandez, M. T., Eoyang, L., & August, J. T. 1968. Factor fraction required for the synthesis of bacteriophage Qβ-RNA. *Nature*, *219*, 588–590.

Fröhlich, K. S., & Vogel, J. 2009. Activation of gene expression by small RNA. *Curr. Opin. Microbiol.*, *12*, 674–682.

Fukushima, T., Ishikawa, S., Yamamoto, H., Ogasawara, N., & Sekiguchi, J. 2003. Transcriptional, functional and cytochemical analyses of the *veg* gene in *Bacillus subtilis*. *J. Biochem.*, *133*, 475–483.

Gerwig, J., Kiley, T. B., Gunka, K., Stanley-Wall, N., & Stülke, J. 2014. The protein tyrosine kinases EpsB and PtkA differentially affect biofilm formation in *Bacillus subtilis*. *Microbiol. (United Kingdom)*, *160*, 682–691.

Ghosh, S., & Deutscher, M. P. 1999. Oligoribonuclease is an essential component of the mRNA decay pathway. *Proc. Natl. Acad. Sci. U. S. A.*, *96*, 4372–4377.

Giuliodori, A. M., Di Pietro, F., Marzi, S., Masquida, B., Wagner, R., *et al.* 2010. The *cspA* mRNA is a thermosensor that modulates translation of the cold-shock protein CspA. *Mol. Cell*, *37*, 21–33.

Glatz, E., Nilsson, R.-P., Rutberg, L., & Rutberg, B. 1996. A dual role for the *Bacillus subtilis glpD* leader and the GlpP protein in the regulated expression of *glpD*: antitermination and control of mRNA stability. *Mol. Microbiol.*, *19*, 319–328.

Goldstein, J., Pollitt, N. S., & Inouye, M. 1990. Major cold shock protein of *Escherichia coli*. *Proc. Natl. Acad. Sci. U. S. A.*, *87*, 283–287.

Gonzalez, G. M., Durica-Mitic, S., Hardwick, S. W., Moncrieffe, M. C., Resch, M., *et al.* 2017. Structural insights into RapZ-mediated regulation of bacterial amino-sugar metabolism. *Nucleic Acids Res.*, *45*, 10845–10860.

Gonzalez, G. M., Hardwick, S. W., Maslen, S. L., Mark Skehel, J., Holmqvist, E., *et al.* 2017. Structure of the *Escherichia coli* ProQ RNA-binding protein. *RNA*, *23*, 696–711.

Goodall, E. C. A., Robinson, A., Johnston, I. G., Jabbari, S., Turner, K. A., *et al.* 2018. The essential genome of *Escherichia coli* K-12. *MBio*, *9*, e02096-17.

Göpel, Y., Papenfort, K., Reichenbach, B., Vogel, J., & Görke, B. 2013. Targeted decay of a regulatory small RNA by an adaptor protein for RNase E and counteraction by an anti-adaptor RNA. *Genes Dev.*, *27*, 552–564.

Gopinath, S. C. B., Balasundaresan, D., Kumarevel, T., Misono, T. S., Mizuno, H., & Kumar, P. K. R. 2008. Insights into anti-termination regulation of the *hut* operon in *Bacillus subtilis*: Importance of the dual RNA-binding surfaces of HutP. *Nucleic Acids Res.*, *36*, 3463–3473.

Graumann, P. L., & Marahiel, M. A. 1998. A superfamily of proteins that contain the cold-shock domain. *Trends Biochem. Sci.*, *23*, 286–290.

Graumann, P., & Marahiel, M. A. 1996. Some like it cold: Response of microorganisms to cold shock. *Arch. Microbiol.*, *166*, 293–300.

Graumann, P., Schröder, K., Schmid, R., & Marahiel, M. A. 1996. Cold shock stress-induced proteins in *Bacillus subtilis*. *J. Bacteriol.*, *178*, 4611–4619.

Graumann, P., Wendrich, T. M., Weber, M. H. W., Schröder, K., & Marahiel, M. A. 1997. A family of cold shock proteins in *Bacillus subtilis* is essential for cellular growth and for efficient protein synthesis at optimal and low temperatures. *Mol. Microbiol.*, *25*, 741–756.

Guérout-Fleury, A. M., Shazand, K., Frandsen, N., & Stragier, P. 1995. Antibiotic-resistance cassettes for *Bacillus subtilis*. *Gene*, *167*, 335–336.

Guerrier-Takada, C., Subramanian, A. R., & Cole. 1983. The activity of discrete fragments of ribosomal protein S1 in Qβ replicase function. *J. Biol. Chem.*, *258*, 13649–13652.

Hajnsdorf, E., & Boni, I. V. 2012. Multiple activities of RNA-binding proteins S1 and Hfq. *Biochimie*, *94*, 1544–1553.

Hämmerle, H., Amman, F., Večerek, B., Stülke, J., Hofacker, I., & Bläsi, U. 2014. Impact of Hfq on the *Bacillus subtilis* transcriptome. *PLoS One*, *9*, e98661.

Hamoen, L. W., Venema, G., & Kuipers, O. P. 2003. Controlling competence in *Bacillus subtilis*: Shared use of regulators. *Microbiology*, *149*, 9-17.

Hanna, M. M., & Liu, K. 1998. Nascent RNA in transcription complexes interacts with CspE, a small protein in *E. coli* implicated in chromatin condensation. *J. Mol. Biol.*, *282*, 227–239.

Hardin, J. W., Hu, Y. X., & McKay, D. B. 2010. Structure of the RNA binding domain of a DEAD-box helicase bound to its ribosomal RNA target reveals a novel mode of recognition by an RNA recognition motif. *J. Mol. Biol.*, *402*, 412–427.

Heidrich, N., Moll, I., & Brantl, S. 2007. *In vitro* analysis of the interaction between the small RNA SR1 and its primary target *ahrC* mRNA. *Nucleic Acids Res.*, *35*, 4331–4346.

Heinemann, U., & Roske, Y. 2021. Cold-shock domains—abundance, structure, properties, and nucleic-acid binding. *Cancers (Basel).*, *13*, 190.

Herschlag, D. 1995. RNA chaperones and the RNA folding problem. *J. Biol. Chem.*, *270*, 20871–20874.

Herskovitz, M. A., & Bechhofer, D. H. 2000. Endoribonuclease RNase III is essential in *Bacillus subtilis*. *Mol. Microbiol.*, *38*, 1027–1033.

Herzberg, C., Weidinger, L. A. F., Dörrbecker, B., Hübner, S., Stülke, J., & Commichau, F. M. 2007. SPINE: A method for the rapid detection and analysis of protein-protein interactions in vivo. *Proteomics*, *7*, 4032–4035.

Hilker, R., Stadermann, K. B., Schwengers, O., Anisiforov, E., Jaenicke, S., *et al.* 2016. ReadXplorer 2-detailed read mapping analysis and visualization from one single source. *Bioinformatics*, *32*, 3702–3708.

Hillier, B. J., Rodriguez, H. M., & Gregoret, L. M. 1998. Coupling protein stability and protein function in *Escherichia coli* CspA. *Fold. Des.*, *3*, 87–93.

Hobl, B., & Mack, M. 2007. The regulator protein PyrR of *Bacillus subtilis* specifically interacts *in vivo* with three untranslated regions within *pyr* mRNA of pyrimidine biosynthesis. *Microbiology*, *153*, 693–700.

Hofweber, R., Horn, G., Langmann, T., Balbach, J., Kremer, W., *et al.* 2005. The influence of cold shock proteins on transcription and translation studied in cell-free model systems. *FEBS J.*, *272*, 4691–4702.

Holmqvist, E., Li, L., Bischler, T., Barquist, L., & Vogel, J. 2018. Global maps of ProQ binding *in vivo* reveal target recognition via RNA structure and stability control at mRNA 3' ends. *Mol. Cell*, *70*, 971-982.

Holmqvist, E., & Vogel, J. 2018. RNA-binding proteins in bacteria. *Nat. Rev. Microbiol.*, *16*, 601-615.

Holmqvist, E., Wright, P. R., Li, L., Bischler, T., Barquist, L., *et al.* 2016. Global RNA recognition patterns of post-transcriptional regulators Hfq and CsrA revealed by UV crosslinking *in vivo*. *EMBO J.*, *35*, 991–1011.

Horn, G., Hofweber, R., Kremer, W., & Kalbitzer, H. R. 2007. Structure and function of bacterial cold shock proteins. *Cell. Mol. Life Sci., 64,* 1457-1470.

Hübner, S., Declerck, N., Diethmaier, C., Le Coq, D., Aymerich, S., & Stülke, J. 2011. Prevention of cross-talk in conserved regulatory systems: Identification of specificity determinants in RNA-binding anti-termination proteins of the BglG family. *Nucleic Acids Res.*, *39*, 4360–4372.

Hui, M. P., Foley, P. L., & Belasco, J. G. 2014. Messenger RNA degradation in bacterial cells. *Annu. Rev. Genet.*, *48*, 537–559.

Hunger, K., Beckering, C. L., Wiegeshoff, F., Graumann, P. L., & Marahiel, M. A. 2006. Cold-induced putative DEAD box RNA helicases CshA and CshB are essential for cold adaptation and interact with cold shock protein B in *Bacillus subtilis*. *J. Bacteriol.*, *188*, 240–248.

Inoue, H., Nojima, H., & Okayama, H. 1990. High efficiency transformation of *Escherichia coli* with plasmids. *Gene*. *96,* 23-28-

Jagtap, C. B., Kumar, P., & Rao, K. K. 2016. *Bacillus subtilis* Hfq: A role in chemotaxis and motility. *J. Biosci.*, *41*, 347–358.

Jeng, S. T., Gardner, J. F., & Gumport, R. I. 1992. Transcription termination *in vitro* by bacteriophage T7 RNA polymerase. The role of sequence elements within and surrounding a ρ-independent transcription terminator. *J. Biol. Chem.*, *267*, 19306–19312.

Jia, L., Mao, Y., Ji, Q., Dersh, D., Yewdell, J. W., & Qian, S. B. 2020. Decoding mRNA translatability and stability from the 5′ UTR. *Nat. Struct. Mol. Biol.*, *27*, 814–821.

Jiang, W., Fang, L., & Inouye, M. 1996. The role of the 5'-end untranslated region of the mRNA for CspA, the major cold-shock protein of *Escherichia coli*, in cold-shock adaptation. *J. Bacteriol.*, *178*, 4919–4925.

Jiang, W., Hou, Y., & Inouye, M. 1997. CspA, the major cold-shock protein of *Escherichia coli*, is an RNA chaperone. *J. Biol. Chem.*, *272*, 196–202.

Jones, P. G., VanBogelen, R. A., & Neidhardt, F. C. 1987. Induction of proteins in response to low temperature in *Escherichia coli*. *J. Bacteriol.*, *169*, 2092–2095.

Jousselin, A., Metzinger, L., & Felden, B. 2009. On the facultative requirement of the bacterial RNA chaperone, Hfq. *Trends Microbiol.*, *17*, 399–405.

Juntawong, P., Sorenson, R., & Bailey-Serres, J. 2013. Cold shock protein 1 chaperones mRNAs during translation in *Arabidopsis thaliana*. *Plant J.*, *74*, 1016–1028.

Kaan, T., Jürgen, B., & Schweder, T. 1999. Regulation of the expression of the cold shock proteins CspB and CspC in *Bacillus subtilis*. *Mol. Gen. Genet.*, *262*, 351–354.

Kampf, J., Gerwig, J., Kruse, K., Cleverley, R., Dormeyer, M., *et al.* 2018. Selective pressure for biofilm formation in *Bacillus subtilis*: Differential effect of mutations in the master regulator *sinR* on bistability. *MBio*, *9*, 1–15.

Kaundinya, C. R., Savithri, H. S., Rao, K. K., & Balaji, P. V. 2018. EpsM from *Bacillus subtilis* 168 has UDP-2,4,6-trideoxy-2-acetamido-4-amino glucose acetyltransferase activity *in vitro*. *Biochem. Biophys. Res. Commun.*, *505*, 1057–1062.

Kavita, K., de Mets, F., & Gottesman, S. 2018. New aspects of RNA-based regulation by Hfq and its partner sRNAs. *Curr. Opin. Microbiol.*, *42*, 53–61.

Kearse, M., Moir, R., Wilson, A., Stones-Havas, S., Cheung, M., Sturrock, S., … Drummond, A. 2012. Geneious Basic: An integrated and extendable desktop software platform for the organization and analysis of sequence data. *Bioinformatics*, *28*, 1647–1649.

Keseler, I. M., Mackie, A., Santos-Zavaleta, A., Billington, R., Bonavides-Martínez, C., *et al.* 2017. The EcoCyc database: Reflecting new knowledge about *Escherichia coli* K-12. *Nucleic Acids Res.*, *45*, D543–D550.

Kibbe, W. A. 2007. OligoCalc: An online oligonucleotide properties calculator. *Nucleic Acids Res.*, *35*, 43–46.

Kim, Y., Wang, X., Zhang, X. S., Grigoriu, S., Page, R., *et al.* 2010. *Escherichia coli* toxin/antitoxin pair MqsR/MqsA regulate toxin CspD. *Environ. Microbiol.*, *12*, 1105–1121.

Kobayashi, K. 2007. Gradual activation of the response regulator DegU controls serial expression of genes for flagellum formation and biofilm formation in *Bacillus subtilis*. *Mol. Microbiol.*, *66*, 395–409.

Koo, B.-M., Kritikos, G., Farelli, J. D., Todor, H., Tong, K., *et al.* 2017. Construction and analysis of two genome-scale deletion libraries for *Bacillus subtilis*. *Cell Syst.*, *4*, 291-305.

Kram, K. E., Henderson, A. L., & Finkel, S. E. 2020. *Escherichia coli* has a unique transcriptional program in long-term stationary phase allowing identification of genes important for survival . *mSystems*, *5*, e00364-20

Krebs, J. E., Goldstein, E. S., & Kilpatrick, S. T. 2014. *Lewin's Genes XI* (11th ed.). Burlington, Massachusetts: Jones & Bartlett Publishers.

Kremer, W., Schuler, B., Harrieder, S., Geyer, M., Gronwald, W., *et al.* 2001. Solution NMR structure of the cold-shock protein from the hyperthermophilic bacterium *Thermotoga maritima*. *Eur. J. Biochem.*, *268*, 2527–2539.

Krüger, S., & Hecker, M. 1995. Regulation of the putative *bglPH* operon for aryl-β-glucoside utilization in *Bacillus subtilis*. *J. Bacteriol.*, *177*, 5590–5597.

Kudla, G., Murray, A. W., Tollervey, D., & Plotkin, J. B. 2009. Coding-sequence determinants of gene expression in *Escherichia coli*. *Science*, *324*, 255–259.

Kumarevel, T., Mizuno, H., & Kumar, P. K. R. 2005. Structural basis of HutP-mediated anti-termination and roles of the Mg^{2+} ion and L-histidine ligand. *Nature*, *434*, 183–191.

Laalami, S., Cavaiuolo, M., Roque, S., Chagneau, C., & Putzer, H. 2021. *Escherichia coli* RNase E can efficiently replace RNase Y in *Bacillus subtilis*. *Nucleic Acids Res. 49,* 4643-4654.

Laemmli, U. K. 1970. Cleavage of structural proteins during the assembly of the head of bacteriophage T4. *Nature*, *227*, 680–685.

Landsman, D. 1992. RNP-1, an RNA-binding motif is conserved in the DNA-binding cold shock domain. *Nucleic Acids Res.*, *20*, 2861–2864.

Langmead, B., Trapnell, C., Pop, M., & Salzberg, S. L. 2009. Ultrafast and memory-efficient alignment of short DNA sequences to the human genome. *Genome Biol.*, *10,* R25.

Le Coq, D., Lindner, C., Krüger, S., Steinmetz, M., & Stülke, J. 1995. New β-glucoside (*bgl*) genes in *Bacillus subtilis*: The *bglP* gene product has both transport and regulatory functions similar to those of BglF, its *Escherichia coli* homolog. *J. Bacteriol.*, *177*, 1527–1535.

Lederberg, E. M., & Cohen, S. N. 1974. Transformation of *Salmonella typhimurium* by plasmid deoxyribonucleic acid. *J. Bacteriol.*, *119*, 1072–1074.

Lehnik-Habrink, M., Lewis, R. J., Mäder, U., & Stülke, J. 2012. RNA degradation in *Bacillus subtilis*: An interplay of essential endo- and exoribonucleases. *Mol. Microbiol.*, *84*, 1005–1017.

Lehnik-Habrink, M., Pförtner, H., Rempeters, L., Pietack, N., Herzberg, C., & Stülke, J. 2010. The RNA degradosome in *Bacillus subtilis*: Identification of CshA as the major RNA helicase in the multiprotein complex. *Mol. Microbiol.*, *77*, 958–971.

Lehnik-Habrink, M., Rempeters, L., Kovács, Á. T., Wrede, C., Baierlein, C., *et al.* 2013. Dead-box RNA helicases in *Bacillus subtilis* have multiple functions and act independently from each other. *J. Bacteriol.*, *195*, 534–544.

Lehnik-Habrink, M., Schaffer, M., Mäder, U., Diethmaier, C., Herzberg, C., & Stülke, J. 2011. RNA processing in *Bacillus subtilis*: Identification of targets of the essential RNase Y. *Mol. Microbiol.*, *81*, 1459–1473.

Lei, Y., Oshima, T., Ogasawara, N., & Ishikawa, S. 2013. Functional analysis of the protein *veg*, which stimulates biofilm formation in *Bacillus subtilis*. *J. Bacteriol.*, *195*, 1697–1705.

Lenhart, J. S., Schroeder, J. W., Walsh, B. W., & Simmons, L. A. 2012. DNA repair and genome maintenance in *Bacillus subtilis*. *Microbiol. Mol. Biol. Rev.*, *76*, 530–564.

Link, T. M., Valentin-Hansen, P., & Brennana, R. G. 2009. Structure of *Escherichia coli* Hfq bound to polyriboadenylate RNA. *Proc. Natl. Acad. Sci. U. S. A.*, *106*, 19292–19297.

Lioliou, E., Sharma, C. M., Caldelari, I., Helfer, A. C., Fechter, P., *et al.* 2012. Global regulatory functions of the *Staphylococcus aureus* endoribonuclease III in gene expression. *PLoS Genet.*, *8*, e1002782.

Liu, M. Y., & Romeo, T. 1997. The global regulator CsrA of *Escherichia coli* is a specific mRNA- binding protein. *J. Bacteriol.*, *179*, 4639–4642.

Lopez, M. M., Yutani, K., & Makhatadze, G. I. 2001. Interactions of the cold shock protein CspB from *Bacillus subtilis* with single-stranded DNA. Importance of the T base content and position within the template. *J. Biol. Chem.*, *276*, 15511–15518.

Love, M. I., Huber, W., & Anders, S. 2014. Moderated estimation of fold change and dispersion for RNA-seq data with DESeq2. *Genome Biol.*, *15*, 1–21.

Luciano, J., Foulquier, E., Fantino, J. R., Galinier, A., & Pompeo, F. 2009. Characterization of YvcJ, a conserved P-loop-containing protein, and its implication in competence in *Bacillus subtilis*. *J. Bacteriol.*, *191*, 1556–1564.

Mäder, U., Antelmann, H., Buder, T., Dahl, M. K., Hecker, M., & Homuth, G. 2002. *Bacillus subtilis* functional genomics: Genome-wide analysis of the DegS-DegU regulon by transcriptomics and proteomics. *Mol. Genet. Genomics*, *268*, 455–467.

Manival, X., Yang, Y., Strub, M. P., Kochoyan, M., Steinmetz, M., & Aymerich, S. 1997. From genetic to structural characterization of a new class of RNA-binding domain within the SacY/BgIG family of antiterminator proteins. *EMBO J.*, *16*, 5019–5029.

Mark Glover, J. N., Chaulk, S. G., Edwards, R. A., Arthur, D., Lu, J., & Frost, L. S. 2015. The FinO family of bacterial RNA chaperones. *Plasmid*, *78*, 79–87.

Martin-Verstraete, I., Débarbouillé, M., Klier, A., & Rapoport, G. 1994. Interactions of wild-type and truncated LevR of *Bacillus subtilis* with the upstream activating sequence of the levanase operon. *J. Mol. Biol.*, *241*, 178–192.

Mascarenhas, J., Weber, M. H. W., & Graumann, P. L. 2001. Specific polar localization of ribosomes in *Bacillus subtilis* depends on active transcription. *EMBO Rep.*, *2*, 685–689.

Mathy, N., Bénard, L., Pellegrini, O., Daou, R., Wen, T., & Condon, C. 2007. 5'-to-3' Exoribonuclease activity in bacteria: Role of RNase J1 in rRNA maturation and 5' stability of mRNA. *Cell*, *129*, 681–692.

Max, K. E. A., Zeeb, M., Bienert, R., Balbach, J., & Heinemann, U. 2006. T-rich DNA single strands bind to a preformed site on the bacterial cold shock protein *Bs*-CspB. *J. Mol. Biol.*, *360*, 702–714.

Mayr, B., Kaplan, T., Lechner, S., & Scherer, S. 1996. Identification and purification of a family of dimeric major cold shock protein homologs from the psychrotrophic *Bacillus cereus* WSBC 10201. *J. Bacteriol.*, *178*, 2916–2925.

McAdams, N. M., & Gollnick, P. 2014. The *Bacillus subtilis* TRAP protein can induce transcription termination in the leader region of the tryptophan biosynthetic (*trp*) operon independent of the *trp* attenuator RNA. *PLoS One*, *9*, e88097.

McLoon, A. L., Guttenplan, S. B., Kearns, D. B., Kolter, R., & Losick, R. 2011. Tracing the domestication of a biofilm-forming bacterium. *J. Bacteriol.*, *193*, 2027–2034.

Mechold, U., Fang, G., Ngo, S., Ogryzko, V., & Danchin, A. 2007. YtqI from *Bacillus subtilis* has both oligoribonuclease and pAp-phosphatase activity. *Nucleic Acids Res.*, *35*, 4552–4561.

Mega, R., Manzoku, M., Shinkai, A., Nakagawa, N., Kuramitsu, S., & Masui, R. 2010. Very rapid induction of a cold shock protein by temperature downshift in Thermus thermophilus. *Biochem. Biophys. Res. Commun.*, *399*, 336–340.

Mehne, F. M. P., Gunka, K., Eilers, H., Herzberg, C., Kaever, V., & Stülke, J. 2013. Cyclic di-AMP homeostasis in *Bacillus subtilis*: Both lack and high level accumulation of the nucleotide are detrimental for cell growth. *J. Biol. Chem.*, *288*, 2004–2017.

Meinken, C., Blencke, H. M., Ludwig, H., & Stülke, J. 2003. Expression of the glycolytic *gapA* operon in *Bacillus subtilis*: Differential syntheses of proteins encoded by the operon. *Microbiology*, *149*, 751–761.

Michaux, C., Holmqvist, E., Vasicek, E., Sharan, M., Barquist, L., *et al*. 2017. RNA target profiles direct the discovery of virulence functions for the cold-shock proteins CspC and CspE. *Proc. Natl. Acad. Sci.*, *114*, 6824–6829.

Mikulecky, P. J., Kaw, M. K., Brescia, C. C., Takach, J. C., Sledjeski, D. D., & Feig, A. L. 2004. *Escherichia coli* Hfq has distinct interaction surfaces for DsrA, *rpoS* and poly(A) RNAs. *Nat. Struct. Mol. Biol.*, *11*, 1206–1214.

Millman, A., Dar, D., Shamir, M., & Sorek, R. 2017. Computational prediction of regulatory, premature transcription termination in bacteria. *Nucleic Acids Res.*, *45*, 886–893.

Mitra, P., Ghosh, G., Hafeezunnisa, M., & Sen, R. 2017. Rho protein: Roles and mechanisms. *Annu. Rev. Microbiol.*, *71*, 687–709.

Mohanty, B. K., & Kushner, S. R. 2016. Regulation of mRNA Decay in Bacteria. *Annu. Rev. Microbiol.*, *70*, 25–44.

Moll, I., Afonyushkin, T., Vytvytska, O., Kaberdin, V. R., & Bläsi, U. 2003. Coincident Hfq binding and RNase E cleavage sites on mRNA and small regulatory RNAs. *Rna*, *9*, 1308–1314.

Mondal, S., Yakhnin, A. V., Sebastian, A., Albert, I., & Babitzke, P. 2016. NusA-dependent transcription termination prevents misregulation of global gene expression. *Nat. Microbiol.*, *1*, 1–8.

Morgan, H. P., Estibeiro, P., Wear, M. A., Max, K. E. A., Heinemann, U., *et al*. 2007. Sequence specificity of single-stranded DNA-binding proteins: A novel DNA microarray approach. *Nucleic Acids Res.*, *35*.

Morita, T., Maki, K., & Aiba, H. 2005. RNase E-based ribonucleoprotein complexes: Mechanical basis of mRNA destabilization mediated by bacterial noncoding RNAs. *Genes Dev.*, *19*, 2176-2186.

Moszer, I., Jones, L. M., Moreira, S., Fabry, C., & Danchin, A. 2002. SubtiList: The reference database for the *Bacillus subtilis* genome. *Nucleic Acids Res.*, *30*, 62–65.

Msadek, T., Kunst, F., Klier, A., & Rapoport, G. 1991. DegS-DegU and ComP-ComA modulator-effector pairs control expression of the *Bacillus subtilis* pleiotropic regulatory gene *degQ*. *J. Bacteriol.*, *173*, 2366–2377.

Mueller, U., Perl, D., Schmid, F. X., & Heinemann, U. 2000. Thermal stability and atomic-resolution crystal structure of the *Bacillus caldolyticus* cold shock protein. *J. Mol. Biol.*, *297*, 975–988.

Mukherjee, S., Yakhnin, H., Kysela, D., Sokoloski, J., Babitzke, P., & Kearns, D. B. 2011. CsrA-FliW interaction governs flagellin homeostasis and a checkpoint on flagellar morphogenesis in *Bacillus subtilis*. *Mol. Microbiol.*, *82*, 447–461.

Müller, P., Gimpel, M., Wildenhain, T., & Brantl, S. 2019. A new role for CsrA: promotion of complex formation between an sRNA and its mRNA target in *Bacillus subtilis*. *RNA Biol. 16*, 972-987.

Mura, C., Randolph, P. S., Patterson, J., & Cozen, A. E. 2013. Archaeal and eukaryotic homologs of Hfq: A structural and evolutionary perspective on Sm function. *RNA Biol.*, *10*, 636–651.

Naville, M., & Gautheret, D. 2010. Premature terminator analysis sheds light on a hidden world of bacterial transcriptional attenuation. *Genome Biol.*, *11*, R79.

Naville, M., Ghuillot-Gaudeffroy, A., Marchais, A., & Gautheret, D. 2011. ARNold: A web tool for the prediction of Rho-independent transcription terminators. *RNA Biol.*, *8*, 11-13.

Nesterenko, M. V., Tilley, M., & Upton, S. J. 1994. A simple modification of Blum's silver stain method allows for 30 minute detection of proteins in polyacrylamide gels. *J. Biochem. Biophys. Methods*, *28*, 239–242.

Newman, J. A., Hewitt, L., Rodrigues, C., Solovyova, A. S., Harwood, C. R., & Lewis, R. J. 2012. Dissection of the network of interactions that links RNA processing with glycolysis in the *Bacillus subtilis* degradosome. *J. Mol. Biol.*, *416*, 121–136.

Nicolas, P., Mäder, U., Dervyn, E., Rochat, T., Leduc, A., *et al*. 2012. Condition-dependent transcriptome reveals high-level regulatory architecture in *Bacillus subtilis*. *Science 335,* 1103-1106.

Nielsen, J. S., Lei, L. K., Ebersbach, T., Olsen, A. S., Klitgaard, J. K., *et al*. 2009. Defining a role for Hfq in Gram-positive bacteria: Evidence for Hfq-dependent antisense regulation in *Listeria monocytogenes*. *Nucleic Acids Res.*, *38*, 907–919.

Nudler, E., Kashlev, M., Nikiforov, V., & Goldfarb, A. 1995. Coupling between transcription termination and RNA polymerase inchworming. *Cell*, *81*, 351–357.

Oda, M., Kobayashi, N., Fujita, M., Miyazaki, Y., Sadaie, Y., *et al*. 2004. Analysis of HutP-dependent transcription antitermination in the *Bacillus subtilis* hut operon: identification of HutP binding sites on hut antiterminator RNA and the involvement of the N-terminus of HutP in binding of HutP to the antiterminator RNA. *Mol. Microbiol.*, *51*, 1155–1168.

Oda, M., Kobayashi, N., Ito, A., Kurusu, Y., & Taira, K. 2000. cis-Acting regulatory sequences for antitermination in the transcript of the *Bacillus subtilis hut* operon and histidine-dependent binding of HutP to the transcript containing the regulatory sequences. *Mol. Microbiol.*, *35*, 1244–1254.

Oussenko, I. A., Abe, T., Ujiie, H., Muto, A., & Bechhofer, D. H. 2005. Participation of 3′-to-5′ exoribonucleases in the turnover of *Bacillus subtilis* mRNA. *J. Bacteriol.*, *187*, 2758–2767.

Panja, S., Schu, D. J., & Woodson, S. A. 2013. Conserved arginines on the rim of Hfq catalyze base pair formation and exchange. *Nucleic Acids Res.*, *41*, 7536–7546.

Papenfort, K., Sun, Y., Miyakoshi, M., Vanderpool, C. K., & Vogel, J. 2013. Small RNA-mediated activation of sugar phosphatase mRNA regulates glucose homeostasis. *Cell*, *153*, 426–437.

Papenfort, K., & Vanderpool, C. K. 2015. Target activation by regulatory RNAs in bacteria. *FEMS Microbiol. Rev.*, *39*, 362–378.

Papenfort, K., & Vogel, J. 2010. Regulatory RNA in bacterial pathogens. *Cell Host & Microbe*. *8,* 116-127.

Pechter, K. B., Meyer, F. M., Serio, A. W., Stülke, J., & Sonenshein, A. L. 2013. Two roles for aconitase in the regulation of tricarboxylic acid branch gene expression in *Bacillus subtilis*. *J. Bacteriol.*, *195*, 1525–1537.

Peng, Y., Curtis, J. E., Fang, X., & Woodson, S. A. 2014. Structural model of an mRNA in complex with the bacterial chaperone Hfq. *Proc. Natl. Acad. Sci. U. S. A.*, *111*, 17134–17139.

Perl, D., Welker, C., Schindler, T., Schröder, K., Marahiel, M. A., *et al*. 1998. Conservation of rapid two-state folding in mesophilic, thermophilic and hyperthermophilic cold shock proteins. *Nat. Struct. Biol.*, *5*, 229–235.

Peters, J. M., Vangeloff, A. D., & Landick, R. 2011. Bacterial transcription terminators: The RNA 3′-end chronicles. *J. Mol. Biol. 412*, 793-813.

Phadtare, S., & Inouye, M. 2001. Role of CspC and CspE in regulation of expression of RpoS and UspA, the stress response proteins in *Escherichia coli*. *J. Bacteriol.*, *183*, 1205–1214.

Phadtare, S., & Inouye, M. 1999. Sequence-selective interactions with RNA by CspB, CspC and CspE, members of the CspA family of *Escherichia coli*. *Mol. Microbiol.*, *33*, 1004–1014.

Phadtare, S., Inouye, M., & Severinov, K. 2002. The nucleic acid melting activity of *Escherichia coli* CspE is critical for transcription antitermination and cold acclimation of cells. *J. Biol. Chem.*, *277*, 7239–7245.

Phadtare, S., & Severinov, K. 2005. Nucleic acid melting by *Escherichia coli* CspE. *Nucleic Acids Res.*, *33*, 5583–5590.

Phadtare, S., Severinov, K., & Inouye, M. 2003. Assay of Transcription Antitermination by Proteins of the CspA Family. *Methods Enzymol.*, *371*, 460–471.

Phadtare, S., Tadigotla, V., Shin, W. H., Sengupta, A., & Severinov, K. 2006. Analysis of *Escherichia coli* global gene expression profiles in response to overexpression and deletion of CspC and CspE. *J. Bacteriol.*, *188*, 2521–2527.

Phadtare, S., Zhu, L., Uemori, T., Mukai, H., Kato, I., & Inouye, M. 2009. Applications of nucleic acid chaperone activity of CspA and its homologues. *J. Mol. Microbiol. Biotechnol.*, *17*, 110–117.

Pop, C., Rouskin, S., Ingolia, N. T., Han, L., Phizicky, E. M., Weissman, J. S., & Koller, D. 2014. Causal signals between codon bias, mRNA structure, and the efficiency of translation and elongation. *Mol. Syst. Biol.*, *10*, 770.

Potts, A. H., Vakulskas, C. A., Pannuri, A., Yakhnin, H., Babitzke, P., & Romeo, T. 2017. Global role of the bacterial post-transcriptional regulator CsrA revealed by integrated transcriptomics. *Nat. Commun.*, *8*, 1–15.

Qayyum, M. Z., Dey, D., & Sen, R. 2016. Transcription elongation factor NusA is a general antagonist of Rho-dependent termination in *Escherichia coli*. *J. Biol. Chem.*, *291*, 8090–8108.

Quirk, P. G., Dunkley, E. A., Lee, P., & Krulwich, T. A. 1993. Identification of a putative *Bacillus subtilis* Rho gene. *J. Bacteriol.*, *175*, 647–654.

Rahmer, R., Heravi, K. M., & Altenbuchner, J. 2015. Construction of a super-competent *Bacillus subtilis* 168 using the P_{mtlA}-*comKS* inducible cassette. *Front. Microbiol.*, *6*, 1–11.

Rajkowitsch, L., Chen, D., Stampfl, S., Semrad, K., Waldsich, *et al*. 2007. RNA chaperones, RNA annealers and RNA helicases. *RNA Biol.*, *4*, 118–130.

Rajkowitsch, L., & Schroeder, R. 2007. Dissecting RNA chaperone activity. *RNA*, *13*, 2053–2060.

Ray-Soni, A., Bellecourt, M. J., & Landick, R. 2016. Mechanisms of bacterial transcription termination: All good things must end. *Annu. Rev. Biochem.*, *85*, 319–347.

Ray, S., Da Costa, R., Thakur, S., & Nandi, D. 2020. *Salmonella typhimurium* encoded cold shock protein E is essential for motility and biofilm formation. *Microbiol., 166*, 460–473.

Rayner, M. H., Sadler, P. J., & Scawen, M. D. 1990. NMR studies of a bacterial cell culture medium (LB Broth): cyclic nucleosides in yeast extracts. *FEMS Microbiol. Lett.*, *68*, 217–221.

Redder, P., Hausmann, S., Khemici, V., Yasrebi, H., & Linder, P. 2015. Bacterial versatility requires DEAD-box RNA helicases. *FEMS Microbiol. Rev.*, *39*, 392–412.

Rennella, E., Sára, T., Juen, M., Wunderlich, C., Imbert, L., *et al*. 2017. RNA binding and chaperone activity of the *E. coli* cold-shock protein CspA. *Nucleic Acids Res.*, *45*, 4255–4268.

Reuß, D. R., Faßhauer, P., Mroch, P. J., Ul-Haq, I., Koo, B.-M., *et al*. 2019. Topoisomerase IV can functionally replace all type 1A topoisomerases in *Bacillus subtilis*. *Nucleic Acids Res., 47,* 5231–5242.

Rochat, T., Delumeau, O., Figueroa-Bossi, N., Noirot, P., Bossi, L., *et al*. 2015. Tracking the Elusive Function of *Bacillus subtilis* Hfq. *PLoS One*, *10*, e0124977.

Romeo, T., Gong, M., Mu Ya Liu, & Brun-Zinkernagel, A. M. 1993. Identification and molecular characterization of *csrA*, a pleiotropic gene from *Escherichia coli* that affects glycogen biosynthesis, gluconeogenesis, cell size, and surface properties. *J. Bacteriol.*, *175*, 4744–4755.

Romero, D., Aguilar, C., Losick, R., & Kolter, R. 2010. Amyloid fibers provide structural integrity to *Bacillus subtilis* biofilms. *Proc. Natl. Acad. Sci. U. S. A.*, *107*, 2230–2234.

Sachs, R., Max, K. E. A., Heinemann, U., & Balbach, J. 2012. RNA single strands bind to a conserved surface of the major cold shock protein in crystals and solution. *RNA*, *18*, 65–76.

Sahr, T., Rusniok, C., Impens, F., Oliva, G., Sismeiro, O., *et al*. 2017. The *Legionella pneumophila* genome evolved to accommodate multiple regulatory mechanisms controlled by the CsrA-system. *PLoS Genet.*, *13,* e1006629.

Salah, P., Bisaglia, M., Aliprandi, P., Uzan, M., Sizun, C., & Bontems, F. 2009. Probing the relationship between Gram-negative and Gram-positive S1 proteins by sequence analysis. *Nucleic Acids Res.*, *37*, 5578–5588.

Sambrook, J., Fritsch, E. F., & Maniatis, T. 1989. *Molecular cloning: a laboratory manual.* Cold Spring Harbor, NY: Cold Spring Harbor Laboratory Press.

Santiago-Frangos, A., Kavita, K., Schu, D. J., Gottesman, S., & Woodson, S. A. 2016. C-terminal domain of the RNA chaperone Hfq drives sRNA competition and release of target RNA. *Proc. Natl. Acad. Sci. U. S. A.*, *113*, e6089–e6096.

Sauer, E., & Weichenrieder, O. 2011. Structural basis for RNA 3'-end recognition by Hfq. *Proc. Natl. Acad. Sci. U. S. A.*, *108*, 13065–13070.

Schindelin, H., Jiang, W., Inouye, M., & Heinemann, U. 1994. Crystal structure of CspA, the major cold shock protein of *Escherichia coli*. *Proc. Natl. Acad. Sci. U. S. A.*, *91*, 5119–5123.

Schindelin, H., Marahiel, M. A., & Heinemann, U. 1993. Universal nucleic acid-binding domain revealed by crystal structure of the *B. subtilis* major cold-shock protein. *Nature*, *364*, 164–168.

Schindelin, J., Arganda-Carreras, I., Frise, E., Kaynig, V., Longair, M., *et al*. 2012. Fiji: An open-source platform for biological-image analysis. *Nat. Methods*, *9*, 676–682.

Schmid, B., Klumpp, J., Raimann, E., Loessner, M. J., Stephan, R., & Tasara, T. 2009. Role of cold shock proteins in growth of *Listeria monocytogenes* under cold and osmotic stress conditions. *Appl. Environ. Microbiol.*, *75*, 1621–1627.

Schneider, C. A., Rasband, W. S., & Eliceiri, K. W. 2012. NIH Image to ImageJ: 25 years of image analysis. *Nat. Methods*, *9*, 671–675.

Schnetz, K., Stülke, J., Gertz, S., Krüger, S., Krieg, M., Hecker, M., & Rak, B. 1996. LicT, a *Bacillus subtilis* transcriptional antiterminator protein of the BglG family. *J. Bacteriol.*, *178*, 1971–1979.

Schnuchel, A., Wiltscheck, R., Czisch, M., Herrler, M., G. Willimsky, G., *et al*. 1993. Structure in solution of the major cold-shock protein from *Bacillus subtilis*. *Nature*, *364*, 169–171.

Schröder, K., Graumann, P., Schnuchel, A., Holak, T. A., & Marahiel, M. A. 1995. Mutational analysis of the putative nucleic acid-binding surface of the cold-shock domain, CspB, revealed an essential role of aromatic and basic residues in binding of single-stranded DNA containing the Y-box motif. *Mol. Microbiol.*, *16*, 699–708.

Schubert, M., Edge, R. E., Lario, P., Cook, M. A., Strynadka, N. C. J., *et al*. 2004. Structural characterization of the RNase E S1 domain and identification of its oligonucleotide-binding and dimerization interfaces. *J. Mol. Biol.*, *341*, 37–54.

Schuergers, N., Ruppert, U., Watanabe, S., Nürnberg, D. J., Lochnit, G., *et al*. 2014. Binding of the RNA chaperone Hfq to the type IV pilus base is crucial for its function in *Synechocystis sp.* PCC 6803. *Mol. Microbiol.*, *92*, 840–852.

Schumacher, M. A., Pearson, R. F., Møller, T., Valentin-Hansen, P., & Brennan, R. G. 2002. Structures of the pleiotropic translational regulator Hfq and an Hfq-RNA complex: A bacterial Sm-like protein. *EMBO J.*, *21*, 3546–3556.

Semrad, K. 2011. Proteins with RNA chaperone activity: A world of diverse proteins with a common task-impediment of RNA misfolding. *Biochem. Res. Int.* 532908. doi: 10.1155/2011/532908.

Shahbabian, K., Jamalli, A., Zig, L., & Putzer, H. 2009. RNase Y, a novel endoribonuclease, initiates riboswitch turnover in *Bacillus subtilis*. *EMBO J.*, *28*, 3523–3533.

Shimotsu, H., Kuroda, M. I., Yanofsky, C., & Henner, D. J. 1986. Novel form of transcription attenuation regulates expression of the *Bacillus subtilis* tryptophan operon. *J. Bacteriol.*, *166*, 461–471.

Skordalakes, E., & Berger, J. M. 2003. Structure of the Rho transcription terminator: Mechanism of mRNA recognition and helicase loading. *Cell*, *114*, 135–146.

Smirnov, A., Förstner, K. U., Holmqvist, E., Otto, A., Günster, R., *et al*. 2016. Grad-seq guides the discovery of ProQ as a major small RNA-binding protein. *Proc. Natl. Acad. Sci. U. S. A.*, *113*, 11591–11596.

Sobrero, P., & Valverde, C. 2012. The bacterial protein Hfq: Much more than a mere RNA-binding factor. *Crit. Rev. Microbiol.*, *38*, 276–299.

Someya, T., Baba, S., Fujimoto, M., Kawai, G., Kumasaka, T., & Nakamura, K. 2012. Crystal structure of Hfq from *Bacillus subtilis* in complex with SELEX-derived RNA aptamer: Insight into RNA-binding properties of bacterial Hfq. *Nucleic Acids Res.*, *40*, 1856–1867.

Sorokin, A., Serror, P., Pujic, P., Azevedo, V., & Ehrlich, S. D. 1995. The *Bacillus subtilis* chromosome region encoding homologues of the *Escherichia coli mssA* and *rpsA* gene products. *Microbiology*, *141*, 311–319.

Stülke, J. 2002. Control of transcription termination in bacteria by RNA-binding proteins that modulate RNA structures. *Arch. Microbiol. 177,* 433-440.

Stülke, J., Martin-Verstraete, I., Zagorec, M., Rose, M., Klier, A., & Rapoport, G. 1997. Induction of the *Bacillus subtilis ptsGHI* operon by glucose is controlled by a novel antiterminator, GlcT. *Mol. Microbiol.*, *25*, 65–78.

Subramanian, A. R. 1983. Structure and functions of ribosomal protein S1. *Prog. Nucleic Acid Res. Mol. Biol.*, *28*, 101–142.

Tanaka, T., Mega, R., Kim, K., Shinkai, A., Masui, R., *et al*. 2012. A non-cold-inducible cold shock protein homolog mainly contributes to translational control under optimal growth conditions. *FEBS J.*, *279*, 1014–1029.

Tödter, D. 2011. Interaktionspartner von RNA-Helikasen in *Bacillus subtilis*. *Bachelor thesis.* Dept. of General Microbiology. University of Göttingen.

Tojo, S., Kumamoto, K., Hirooka, K., & Fujita, Y. 2010. Heavy involvement of stringent transcription control depending on the adenine or guanine species of the transcription initiation site in glucose and pyruvate metabolism in *Bacillus subtilis*. *J. Bacteriol.*, *192*, 1573–1585.

Tree, J. J., Granneman, S., McAteer, S. P., Tollervey, D., & Gally, D. L. 2014. Identification of Bacteriophage-Encoded Anti-sRNAs in Pathogenic *Escherichia coli*. *Mol. Cell*, *55*, 199–213.

Turner, R. J., Lu, Y., & Switzer, R. L. 1994. Regulation of the *Bacillus subtilis* pyrimidine biosynthetic (*pyr*) gene cluster by an autogenous transcriptional attenuation mechanism. *J. Bacteriol.*, *176*, 3708–3722.

Updegrove, T. B., Zhang, A., & Storz, G. 2016. Hfq: The flexible RNA matchmaker. *Curr. Opin. Microbiol.*, *30*, 133–138.

Uppalapati, C. K., Gutierrez, K. D., Buss-Valley, G., & Katzif, S. 2017. Growth-dependent activity of the cold shock *cspA* promoter + 5′ UTR and production of the protein CspA in *Staphylococcus aureus* Newman. *BMC Res. Notes*, *10*, 1–10.

Vakulskas, C. A., Leng, Y., Abe, H., Amaki, T., Okayama, A., *et al* 2016. Antagonistic control of the turnover pathway for the global regulatory sRNA CsrB by the CsrA and CsrD proteins. *Nucleic Acids Res.*, *44*, 7896–7910.

Van Assche, E., Van Puyvelde, S., Vanderleyden, J., & Steenackers, H. P. 2015. RNA-binding proteins involved in post-transcriptional regulation in bacteria. *Front. Microbiol.*, *6*, 1–16.

Vogel, J., & Luisi, B. F. 2011. Hfq and its constellation of RNA. *Nat. Rev. Microbiol.*, *9*, 578–589.

Von König, K., Kachel, N., Kalbitzer, H. R., & Kremer, W. 2020. RNA and DNA binding epitopes of the cold shock protein *Tm*Csp from the hyperthermophile *Thermotoga maritima*. *Protein J.*, *39*, 487–500.

Wach, A. 1996. PCR-synthesis of marker cassettes with long flanking homology regions for gene disruptions in *S. cerevisiae*. *Yeast*, *12*, 259–265.

Wang, N., Yamanaka, K., & Inouye, M. 1999. CspI, the ninth member of the CspA family of *Escherichia coli*, is induced upon cold shock. *J. Bacteriol.*, *181*, 1603–1609.

Wang, W., & Bechhofer, D. H. 1996. Properties of a *Bacillus subtilis* polynucleotide phosphorylase deletion strain. *J. Bacteriol.*, *178*, 2375–2382.

Wang, Z., Liu, W., Wu, T., Bie, P., & Wu, Q. 2016. RNA-seq reveals the critical role of CspA in regulating *Brucella melitensis* metabolism and virulence. *Sci. China Life Sci.*, *59*, 417–424.

Waters, S. A., McAteer, S. P., Kudla, G., Pang, I., Deshpande, N. P., *et al*. 2017. Small RNA interactome of pathogenic *E. coli* revealed through crosslinking of RNase E . *EMBO J.*, *36*, 374–387.

Weber, M. H. W., Beckering, C. L., & Mohamed, A. 2001. Complementation of cold shock proteins by translation initiation factor IF1 *in vivo*. *J. Bacteriol.*, *183*, 7381–7386.

Weber, M. H. W., & Marahiel, M. A. 2003. Bacterial cold shock responses, *Science Progress 86,* 9-75.

Weber, M. H. W., Volkov, A. V., Fricke, I., Marahiel, M. A., & Graumann, P. L. 2001. Localization of cold shock proteins to cytosolic spaces surrounding nucleoids in *Bacillus subtilis* depends on active transcription. *J. Bacteriol.*, *183*, 6435–6443.

Weilbacher, T., Suzuki, K., Dubey, A. K., Wang, X., Gudapaty, S., *et al*. 2003. A novel sRNA component of the carbon storage regulatory system of *Escherichia coli*. *Mol. Microbiol.*, *48*, 657–670.

Weinrauch, Y., Msadek, T., Kunst, F., & Dubnau, D. 1991. Sequence and properties of *comQ*, a new competence regulatory gene of *Bacillus subtilis*. *J. Bacteriol.*, *173*, 5685–5693.

Wen, T., Oussenko, I. A., Pellegrini, O., Bechhofer, D. H., & Condon, C. 2005. Ribonuclease PH plays a major role in the exonucleolytic maturation of CCA-containing tRNA precursors in *Bacillus subtilis*. *Nucleic Acids Res.*, *33*, 3636–3643.

Wickiser, J. K., Winkler, W. C., Breaker, R. R., & Crothers, D. M. 2005. The speed of RNA transcription and metabolite binding kinetics operate an FMN riboswitch. *Mol. Cell*, *18*, 49–60.

Willimsky, G., Bang, H., Fischer, G., & Marahiel, M. A. 1992. Characterization of *cspB*, a *Bacillus subtilis* inducible cold shock gene affecting cell viability at low temperatures. *J. Bacteriol.*, *174*, 6326–6335.

Wilson, K. S., & von Hippel, P. H. 1995. Transcription termination at intrinsic terminators: the role of the RNA hairpin. *Proc. Natl. Acad. Sci. U. S. A.*, *92*, 8793–8797.

Wilusz, C. J., & Wilusz, J. 2005. Eukaryotic Lsm proteins: Lessons from bacteria. *Nat. Struct. Mol. Biol.*, *12*, 1031–1036.

Worbs, M., Bourenkov, G. P., Bartunik, H. D., Huber, R., & Wahl, M. C. 2001. An extended RNA binding surface through arrayed S1 and KH domains in transcription factor NusA. *Mol. Cell*, *7*, 1177–1189.

Wray, L. V., & Fisher, S. H. 1994. Analysis of *Bacillus subtilis* hut operon expression indicates that histidine-dependent induction is mediated primarily by transcriptional antitermination and that amino acid repression is mediated by two mechanisms: Regulation of transcription initiation . *J. Bacteriol.*, *176*, 5466–5473.

Xia, B., Ke, H., & Inouye, M. 2001. Acquirement of cold sensitivity by quadruple deletion of the *cspA* family and its suppression by PNPase S1 domain in *Escherichia coli*. *Mol. Microbiol.*, *40*, 179–188.

Yakhnin, H., Pandit, P., Petty, T. J., Baker, C. S., Romeo, T., & Babitzke, P. 2007. CsrA of *Bacillus subtilis* regulates translation initiation of the gene encoding the flagellin protein (*hag*) by blocking ribosome binding. *Mol. Microbiol.*, *64*, 1605–1620.

Yakhnin, A. V., & Babitzke, P. 2002. NusA-stimulated RNA polymerase pausing and termination participates in the *Bacillus subtilis trp* operon attenuation mechanism *in vitro*. *Proc. Natl. Acad. Sci. U. S. A.*, *99*, 11067–11072.

Yakhnin, A. V., & Babitzke, P. 2010. Mechanism of NusG-stimulated pausing, hairpin-dependent pause site selection and intrinsic termination at overlapping pause and termination sites in the *Bacillus subtilis* trp leader. *Mol. Microbiol.*, *76*, 690–705.

Yakhnin, A. V., Baker, C. S., Vakulskas, C. A., Yakhnin, H., Berezin, I., Romeo, T., & Babitzke, P. 2013. CsrA activates *flhDC* expression by protecting *flhDC* mRNA from RNase E-mediated cleavage. *Mol. Microbiol.*, *87*, 851–866.

Yamanaka, K., Fang, L., & Inouye, M. 1998. The CspA family in *Escherichia coli*: Multiple gene duplication for stress adaptation. *Mol. Microbiol.*, *27*, 247–255.

Yamanaka, K., & Inouye, M. 1997. Growth-phase-dependent expression of *cspD*, encoding a member of the CspA family in *Escherichia coli*. *J. Bacteriol.*, *179*, 5126–5130.

Yamanaka, K., Zheng, W., Crooke, E., Wang, Y. H., & Inouye, M. 2001. CspD, a novel DNA replication inhibitor induced during the stationary phase in *Escherichia coli*. *Mol. Microbiol.*, *39*, 1572–1584.

Zeeb, M., Max, K. E. A., Weininger, U., Löw, C., Sticht, H., & Balbach, J. 2006. Recognition of T-rich single-stranded DNA by the cold shock protein *Bs*-CspB in solution. *Nucleic Acids Res.*, *34*, 4561–4571.

Zere, T. R., Vakulskas, C. A., Leng, Y., Pannuri, A., Potts, A. H., *et al*. 2015. Genomic targets and features of BarA-UvrY (-SirA) signal transduction systems. *PLoS One*, *10*, e0145035.

Zhang, A., Wassarman, K. M., Ortega, J., Steven, A. C., & Storz, G. 2002. The Sm-like Hfq Protein Increases OxyS RNA Interaction with Target mRNAs. *Mol. Cell*, *9*, 11–22.

Zhang, J., & Landick, R. 2016. A two-way street: Regulatory interplay between RNA polymerase and nascent RNA structure. *Trends Biochem. Sci.*, *41*, 293–310.

Zhang, Y., Burkhardt, D. H., Rouskin, S., Li, G. W., Weissman, J. S., & Gross, C. A. 2018. A stress response that monitors and regulates mRNA Structure Is central to cold shock adaptation. *Mol. Cell*, *70*, 274-286.

Zheng, A., Panja, S., & Woodson, S. A. 2016. Arginine patch predicts the RNA annealing activity of Hfq from Gram-negative and Gram-positive bacteria. *J. Mol. Biol.* 428, 2259-2264

Zhu, B., & Stülke, J. 2018. SubtiWiki in 2018: From genes and proteins to functional network annotation of the model organism *Bacillus subtilis*. *Nucleic Acids Res.*, *46*, D743–D748.

7. Appendix

7.1 Supplementary information

Supplementary Table 1: Functional categories of deregulated RNAs in the *cspB cspD* double mutant GP1971.

Amount	Category Name	Percentage
	Transcripts with higher expression	
70	Proteins of unknown function	13.01%
66	Coping with stress	12.27%
46	Phosphoproteins	8.55%
45	Essential genes	8.36%
45	Membrane proteins	8.36%
44	Transporters	8.18%
39	Prophages	7.25%
36	Carbon metabolism	6.69%
23	Exponential and early post-exponential lifestyles	4.28%
20	Poorly characterized/ putative enzymes	3.72%
19	Additional metabolic pathways	3.53%
16	Regulation of gene expression	2.97%
15	Sporulation	2.79%
14	Amino acid/ nitrogen metabolism	2.60%
11	Protein synthesis, modification and degradation	2.04%
6	Homeostasis	1.12%
4	Genetics	0.74%
3	Cell envelope and cell division	0.56%
3	Electron transport and ATP synthesis	0.56%
2	Nucleotide metabolism	0.37%
2	Lipid metabolism	0.37%
1	Short peptides	0.19%
1	RNA synthesis and degradation	0.19%
1	Targets of second messengers	0.19%
	Transcripts with lower expression	
40	Transporters	13.16%
35	Proteins of unknown function	11.51%
34	Membrane proteins	11.18%
34	Coping with stress	11.18%
24	Phosphoproteins	7.89%
18	Sporulation	5.92%
16	Essential genes	5.26%

Amount	Category Name	Percentage
15	Nucleotide metabolism	4.93%
13	Poorly characterized/ putative enzymes	4.28%
12	Amino acid/ nitrogen metabolism	3.95%
9	Genetics	2.96%
9	Regulation of gene expression	2.96%
8	Additional metabolic pathways	2.63%
7	Electron transport and ATP synthesis	2.30%
7	Protein synthesis, modification and degradation	2.30%
6	Homeostasis	1.97%
4	Carbon metabolism	1.32%
3	RNA synthesis and degradation	0.99%
3	Exponential and early post-exponential lifestyles	0.99%
3	Cell envelope and cell division	0.99%
2	Detoxification reactions	0.66%
2	Lipid metabolism	0.66%

7.2 Bacterial strains

Bacterial strains constructed in this study

Strain	Genotype	Construction
GP1968	*trpC2* Δ*cspB::cat*	LFH → 168
GP1969	*trpC2* Δ*cspC::aad9*	LFH → 168
GP1970	*trpC2* Δ*cspB::cat* Δ*cspC::aad9*	chrom. DNA GP1968 → GP1969
GP1971	*trpC2* Δ*cspB::cat* Δ*cspD::aphA3*	chrom. DNA GP1968 → GP2614
GP1972	*trpC2* Δ*cspC::aad9* Δ*cspD::aphA3*	chrom. DNA GP1969 → GP2614
GP1981	*trpC2* Δ*cspB::cat* Δ*spoVG::tet*	chrom. DNA GP2109 → GP1968
GP1982	*trpC2 amyE::(*P_{degS}*-lacZ cat)*	pGP3129 → 168
GP1984	*trpC2 amyE::(*P_{cspC}*-lacZ cat)*	pGP3117 → 168
GP1986	*trpC2 amyE::(*P_{cspC}[G-65A]*-lacZ cat)*	pGP3119 → 168
GP1988	*trpC2 amyE::(*P_{cspC}[truncated]*-lacZ cat)*	pGP3120 → 168
GP1989	*trpC2* Δ*cspB::cat* Δ*cspD::aphA3* P_{cspC}-[G-65A]	Suppressor 1 of GP1971
GP1990	*trpC2* Δ*cspB::cat* Δ*cspD::aphA3* P_{veg}-[G-10T]	Suppressor 7 of GP1971
GP1995	*trpC2* Δ*cspB::cat* Δ*cspD::aphA3 yvcA-PmtlA-comKS-tet-hisI*	chrom. DNA GP1968 & chrom. DNA GP2614 → GP2619
GP2885	*trpC2* Δ*cspB::cat* Δ*cspC::aad9 spoVG::tet*	chrom. DNA GP2109 → GP1970
GP2886	*trpC2* Δ*cspB::cat* Δ*cspD::aphA3 spoVG::tet*	chrom. DNA GP1968 → GP2631

Strain	Genotype	Construction
GP2887	*trpC2* Δ*cspC::aad9* Δ*cspD::aphA3 spoVG::tet*	chrom. DNA GP2109 → GP1972
GP2888	*trpC2* Δ*veg::ermC*	LFH → 168
GP2889	*trpC2* Δ*cspD::aphA3 yvcA-*P_{mtlA}*-comKS-tet-hisI*	chrom. DNA GP2614 → GP2619
GP2890	*trpC2 amyE::(*P_{veg}*-*[G-10T]*-lacZ cat)*	pGP3131 → 168
GP2891	*trpC2 amyE::(*P_{veg}*-lacZ cat)*	pGP3132 → 168
GP2893	*trpC2* Δ*cspC::aad9* Δ*cspD::aphA3 xkdE::(*P_{xyl}*-cspC-ermC*)	pGP3127 → GP1972
GP2894	*trpC2 amyE::(*P_{degS}*-lacZ cat)* Δ*cspD::aphA4*	PCR (GP2614, MB21 & MB22) → GP1982
GP2895	*trpC2* Δ*cspB::cat* Δ*cspD::aphA3*	Suppressor 12 of GP1971
GP2896	*trpC2* Δ*veg::ermC* Δ*cspD::aphA3*	chrom. DNA GP2888 → GP2614
GP2897	*trpC2* Δ*veg::ermC* Δ*cspB::cat* Δ*cspD::aphA3*	PCR (GP1968, PF41 & PF44) → GP2896
GP2898	*trpC2 amyE::(*P_{veg}*-lacZ cat)*	pGP3133 → 168
GP2899	*trpC2 amyE::(*P_{veg}*-*[G-10T]*-lacZ cat)*	pGP3134 → 168
GP2900	*trpC2* Δ*cspB::cat* Δ*cspD::aphA3 degS*[P245S]	Suppressor 19 of GP1971
GP3251	*trpC2* Δ*cspB::tet*	LFH → 168
GP3252	*trpC2 amyE::(*P_{cspC}*-lacZ cat)* Δ*cspB::tet*	PCR (GP3251, PF41 & PF44) → GP1984
GP3253	*trpC2 amyE::(*P_{cspC}*-lacZ cat)* Δ*cspD::aphA3*	PCR (GP2614, MB21 & MB22) → GP1984
GP3254	*trpC2 amyE::(*P_{cspC}*-lacZ cat)* Δ*cspB::tet* Δ*cspD::aphA3*	PCR (GP3251, PF41 & PF44) → GP3253
GP3255	*trpC2 amyE::(*P_{cspC}[truncated]*-lacZ cat)* Δ*cspB::tet*	PCR (GP3251, PF41 & PF44) → GP1988
GP3256	*trpC2 amyE::(*P_{cspC}[truncated]*-lacZ cat)* Δ*cspD::aphA3*	PCR (GP2614, MB21 & MB22) → GP1988
GP3257	*trpC2 amyE::(*P_{cspC}[truncated]*-lacZ cat)* Δ*cspB::tet* Δ*cspD::aphA3*	PCR (GP3251, PF41 & PF44) → GP3256
GP3258	*trpC2 amyE::(*P_{veg}*-lacZ cat)* Δ*cspD::aphA3*	PCR (GP2614, MB21 & MB22) → GP2898
GP3259	*trpC2 amyE::(*P_{veg}*-lacZ cat)* Δ*cspB::tet* Δ*cspD::aphA3*	PCR (GP3251, PF41 & PF44) → GP3258
GP3260	*trpC2 amyE::(*P_{cspC}*-lacZ cat)* Δ*cspC::aad9*	PCR (GP1969, PF47 & PF50) → GP1984
GP3261	*trpC2 amyE::(*P_{cspC}*-lacZ cat)* Δ*cspB::tet* Δ*cspC::aad9*	PCR (GP1969, PF47 & PF50) → GP3252

Strain	Genotype	Construction
GP3262	*trpC2 amyE::(P_{cspC}-lacZ cat) ΔcspC::aad9 ΔcspD::aphA3*	PCR (GP1969, PF47 & PF50) → GP3253
GP3263	*trpC2 amyE::(P_{degS}-lacZ cat) ΔcspB::tet ΔcspD::aphA3*	PCR (GP3251, PF41 & PF44) → GP2894
GP3264	*trpC2 ΔcspC::P_{cspC}-[G-65A]-cspA$_{E.coli}$-aad9*	LFH → 168
GP3265	*trpC2 ΔcspC::P_{cspC}-[G-65A]-cspC$_{E.coli}$-aad9*	LFH → 168
GP3266	*trpC2 ΔcspC::P_{cspC}-cspD$_{E.coli}$-aad9*	LFH → 168
GP3267	*trpC2 ΔcspC::P_{cspC}-[G-65A]-infA$_{E.coli}$-aad9*	LFH → 168
GP3268	*trpC2 amyE::(P_{parE}-lacZ cat) ΔcspD::aphA3*	chrom. DNA GP2614 → GP2550
GP3269	*trpC2 amyE::(P_{degS}-lacZ cat) ΔcspB::tet*	PCR (GP3251, PF41 & PF44) → GP1982
GP3270	*trpC2 amyE::(P_{veg}-lacZ cat) ΔcspB::tet*	PCR (GP3251, PF41 & PF44) → GP2898
GP3271	*trpC2 amyE::(P_{parE}-lacZ cat) ΔcspB::tet*	PCR (GP3251, PF41 & PF44) → GP2550
GP3272	*trpC2 amyE::(P_{parE}-lacZ cat) ΔcspB::tet ΔcspD::aphA3*	PCR (GP3251, PF41 & PF44) → GP3268
GP3273	*trpC2 amyE::(P_{cspC}-lacZ cat) Δveg::ermC*	chrom. DNA GP2888 → GP1984
GP3274	*trpC2 cspC*[Ala58Pro]*-aad9 ΔcspD::aphA3*	LFH → GP2614
GP3275	*trpC2 cspC*[Ala58Pro]*-aad9 ΔcspB::tet ΔcspD::aphA3*	PCR (GP3251, PF41 & PF44) → GP3274
GP3276	*trpC2 ΔcspC::cspA$_{S. aureus}$-aad9 ΔcspD::aphA3*	LFH → GP2614
GP3277	*trpC2 ΔcspC::P_{cspC}-[G-65A]-cspC$_{E.coli}$-aad9 ΔcspD::aphA3*	PCR (GP2614, MB21 & MB22) → GP3265
GP3278	*trpC2 ΔcspC::P_{cspC}-[G-65A]-cspC$_{E.coli}$-aad9 ΔcspB::tet ΔcspD::aphA3*	PCR (GP3251, PF41 & PF44) → GP3277
GP3279	*trpC2 ΔcspC::P_{cspC}-cspA$_{E.coli}$-aad9*	LFH → 168
GP3280	*trpC2 amyE::cspB-cat*	LFH → 168
GP3281	*trpC2 ΔcspC::P_{cspC}-cspD$_{E.coli}$-aad9 ΔcspD::aphA3*	PCR (GP2614, MB21 & MB22) → GP3266
GP3282	*trpC2 ΔcspC::P_{cspC}-[G-65A]-infA$_{E.coli}$-aad9 ΔcspD::aphA3*	PCR (GP2614, MB21 & MB22) → GP3267
GP3283	*trpC2 amyE::(P_{cspB}-lacZ cat)*	pGP3136 → 168
GP3285	*trpC2 cspC::cspC-6xHis-cat*	LFH → GP1969
GP3286	*trpC2 amyE::(P_{cspD}-lacZ-cat)*	LFH → 168

Strain	Genotype	Construction
GP3287	*trpC2* Δ*cspC::*P_{cspC}-*cspA*$_{E.coli}$-*aad9* Δ*cspD::aphA3*	PCR (GP2614, MB21 & MB22) → GP2179
GP3288	*trpC2 purT-rpoB-rpoC-aad9*	LFH → GP3220
GP3289	*trpC2 dgk::rpoA-cat::yaaH* Δ*purT::rpoB-rpoC-aad9*	PCR (GP2903, SW17 & SW20) → GP3288
GP3290	*trpC2* Δ*amyE::*P_{pdhA}-Terminator$_{manR}$-*lacZ-cat*	pGP3144 → 168
GP3291	*trpC2* Δ*amyE::*P_{pdhA}-Terminator$_{manR}$-*lacZ-cat* Δ*cspB::tet* Δ*cspD::aphA3*	PCR (GP2614, MB21 & MB22) & PCR (GP3251, PF41 & PF44) → GP3290
GP3292	*trpC2* Δ*amyE::*P_{pdhA}-*lacZ-cat* Δ*cspB::tet* Δ*cspD::aphA3*	PCR (GP2614, MB21 & MB22) & PCR (GP3251, PF41 & PF44) → GP216
GP3293	*trpC2* Δ*amyE::*P_{pdhA}-Terminator$_{liaH}$-*lacZ-cat*	pGP3145 → 168
GP3294	*trpC2* Δ*amyE::*P_{pdhA}-Terminator$_{liaH}$-*lacZ-cat* Δ*cspB::tet* Δ*cspD::aphA3*	PCR (GP2614, MB21 & MB22) & PCR (GP3251, PF41 & PF44) → GP3293
GP3295	*trpC2 dgk::rpoA-cat::yaaH purT-rpoB-rpoC-aad9* Δ*rny::ermC*	chrom. DNA GP2524 → GP3289
GP3296	*trpC2 dgk::rpoA-cat::yaaH purT-rpoB-rpoC-aad9* Δ*cspD::aphA3* Δ*rny::ermC*	chrom. DNA GP2524 & chrom. DNA GP2614 → GP3289
GP3297	*trpC2 dgk::rpoA-cat::yaaH purT-rpoB-rpoC-aad9* Δ*rpoE::aphA3* Δ*rny::ermC*	chrom. DNA GP2524 & chrom. DNA GP3216 → GP3289
GP3298	*trpC2* Δ*amyE::*P_{pdhA}-Antiterminator$_{pyrR}$-*lacZ-cat*	pGP3146 → 168
GP3299	*trpC2* Δ*amyE::*P_{pdhA}-Antiterminator$_{pyrR}$-*lacZ-cat* Δ*cspB::tet* Δ*cspD::aphA3*	PCR (GP2614, MB21 & MB22) & PCR (GP3251, PF41 & PF44) → GP23298
GP3300	*trpC2 dgk::rpoA-cat::yaaH purT-rpoB-rpoC-aad9* Δ*amyE::*P_{pdhA}-*lacZ-aphA3*	pGP186 → GP3289
GP3301	*trpC2 dgk::rpoA-cat::yaaH purT-rpoB-rpoC-aad9* Δ*amyE::*P_{citG}-*lacZ-aphA3*	pGP387 → GP3289
GP3302	*trpC2 dgk::rpoA-cat::yaaH* Δ*purT::rpoB-rpoC-aad9* Δ*amyE::*P_{cggR}-*lacZ-aphA3*	pGP504 → GP3289
GP3303	*trpC2 dgk::rpoA-cat::yaaH purT-rpoB-rpoC-aad9* Δ*amyE::*P_{hag}-*lacZ-aphA3*	pGP755 → GP3289
GP3304	*trpC2* Δ*cspB::cat* Δ*cspD::aphA3* P_{cspC}-[G-65A]	Suppressor 6 of GP1971, evolved five passages
GP3305	*trpC2* Δ*cspB::cat* Δ*cspD::aphA3* P_{cspC}-[T-99C]	Suppressor 9 of GP1971, evolved five passages

Strain	Genotype	Construction
GP3306	*trpC2* Δ*cspB::cat* Δ*cspD::aphA3* P_{cspC}-[G-96A]	Suppressor 10 of GP1971, evolved five passages

Other bacterial strains used in this study

Strain	Genotype	Construction
B. subtilis		
168	*trpC2*	Laboratory collection
GP2614	*trpC2* Δ*cspD::aphA3*	Benda *et al.*, 2020
GP1966	*trpC2* Δ*ynfC*::P_{alf4}-*gfp ermC*	Reuß *et al.*, 2019
BKE04260	Δ*topB*::*ermC*	Koo *et al.*, 2017
GP469	Δ*csrA::spec*	Laboratory collection
MZ303	Δ*ptsH::cat*	Arnaud *et al.*, 1992
E. coli		
DH5α	*recA1 endA1 gyrA96 thi hsdR17rK- mK+relA1 supE44 Φ80ΔlacZΔM15 Δ(lacZYA-argF)U169*	Sambrook *et al.*, 1989
XL10-Gold	*endA1 glnV44 recA1 thi-1 gyrA96 relA1 lac Hte Δ(mcrA)183 Δ(mcrCB-hsdSMR-mrr)173 tet^R F'[proAB lacI^{q}ZΔM15 Tn10(Tet^R Amy Cm^R)]*	Stratagene
BL21 Rosetta (DE3)	F$^-$ *ompT hsdS$_B$*(r_B^- m_B^-) *gal dcm* (DE3) pRARE (Cam^R)	Novagen
S. aureus		
BB255	Equates NCTC8325 with mutated *rsbU5*	Chromosomal DNA in laboratory collection

7.3 Oligonucleotides

Oligonucleotides constructed in this study

Name	Sequence (5→3')	Purpose
PF33	TTTGGATCCCGCGTGTACTTGCTGCTTATC	Fwd, Primer for up fragment of pGP3114
PF34	GATAATTCAAAAGGGTTCCGTATATTGAAC	Rev, Primer for up fragment of pGP3114
PF35	GTTCAATATACGGAACCCTTTTGAATTATCGCA GGGTCTTGCTCACCTTC	Fwd, Primer for down fragment of pGP3114
PF36	TTTGAATTCACTGTTTCTGCTGATGTTAATGCT TC	Rev, Primer for down fragment of pGP3114
PF39	AATGGTGGAAAGCCGATCCG	Fwd, Seq-Primer for pGP3114
PF40	TAACAGGATGCTCTAGACCAACTG	Rev, Seq-Primer for pGP3114

Name	Sequence (5→3‘)	Purpose
PF41	ATGATCGGAATTCTGGGGCTG	Fwd, LFH-Primer for up-fragment for deletion of *cspB*
PF42	CCTATCACCTCAAATGGTTCGCTGGCATAAATTGATATGAAAAACTGCAGGTG	Rev, LFH-Primer for up-fragment for deletion of *cspB*
PF43	CCGAGCGCCTACGAGGAATTTGTATCGTGAAATTTCCTCCTAAAGCGATCATAAC	Fwd, LFH-Primer for down-fragment for deletion of *cspB*
PF44	ACAGCTTTTAATTTCAGGTGTCTCG	Rev, LFH-Primer for down-fragment for deletion of *cspB*
PF45	ACAAAATCATTAGAGGACCGTTTCTTAG	Fwd, Seq-Primer for deletion of *cspB*
PF46	ATGAGTCCGCCGCTCTTTAG	Rev Seq-Primer for deletion of *cspB*
PF47	GAAGGGCAGGTACGGAAGATAG	Fwd, LFH-Primer for up-fragment for deletion of *cspC*
PF48	CCTATCACCTCAAATGGTTCGCTGTTGTTGCCTCCTAGTGTGTAACC	Rev, LFH-Primer for up-fragment for deletion of *cspC*
PF49	CCGAGCGCCTACGAGGAATTTGTATCGTCTTCAATCGTTTATACAAACAGGCTC	Fwd, LFH-Primer for down-fragment for deletion of *cspC*
PF50	TACGACCAGTTACCGATATACTTGC	Rev, LFH-Primer for down-fragment for deletion of *cspC*
PF51	TGAACAGGAGATTTAATGCTTTCTGATG	Fwd, Seq-Primer for deletion of *cspC*
PF52	ACGGAGCAGGTATAATTGAAGCC	Rev Seq-Primer for deletion of *cspC*
PF53	CCGAGCGCCTACGAGGAATTTGTATCGGCATAAATTGATATGAAAAACTGCAGGTG	Rev, LFH-Primer for up-fragment for deletion of *cspB*
PF54	CCTATCACCTCAAATGGTTCGCTGTGAAATTTCCTCCTAAAGCGATCATAAC	Fwd, LFH-Primer for down-fragment for deletion of *cspB*
PF55	TTTGGATCCTCAGGACCAGGAAGAAGTTGC	Fwd, Primer for up fragment of pGP3115
PF56	GTTTATAATGAGTGAATGAATGCAGTGG	Rev Primer for up fragment of pGP3115
PF57	CCACTGCATTCATTCACTCATTATAAACAGGAATGGACGGAAGAATAGCTG	Fwd, Primer for down fragment of pGP3115
PF58	TTTCTCGAGATCATATCACCGGCCTGCAAG	Rev Primer for down fragment of pGP3115
PF59	CAAACAGCTGGTTGGGGTTC	Fwd, Seq-Primer for pGP3115
PF60	TGTGAATACAGTGTCGCCTGTG	Rev, Seq-Primer for pGP3115
PF61	TTTGGATCCTAGATCAGCTCTGCCGCTTTC	Fwd, Primer for up fragment of pGP3116
PF62	GCCATGCTTGATTTTGCTGAAC	Rev, Primer for up fragment of pGP3116
PF63	GTTCAGCAAAATCAAGCATGGCCTAAGCGGATATGTCAGCTTTGATTT	fwd, Primer for down fragment of pGP3116
PF64	TTTGAATTCGAGCATACGAAAGCGGAAACTG	rev, Primer for down fragment of pGP3116

Name	Sequence (5→3‘)	Purpose
PF65	TCTGTTTATCAGCAGCTGGAGG	fwd, Seq-Primer for pGP3116
PF66	TTTGGATCCGGGCGAATCCTCAGCTTTTTG	fwd, Primer for up fragment of pGP3117
PF67	CGCCTTATAGCTGATCAAGTTTATTCTC	rev, Primer for up fragment of pGP3117
PF68	GAGAATAAACTTGATCAGCTATAAGGCGGGAATCACACTGCTCACCATTG	fwd, Primer for down fragment of pGP3117
PF69	TTTCTCGAGGTGCGTCAGTTGATCTCCGA	rev, Primer for down fragment of pGP3117
PF70	ATCTGAGATTACAGGCTGGACG	fwd, Seq-Primer for pGP3117
PF71	CCAAGCGCCCAATAATCCATC	rev, Seq-Primer for pGP3117
PF72	TTTGGATCCATACCGCGATCCATCCGTAATG	fwd, Primer for up fragment of pGP3118
PF73	TTATAGGATGTGATCGGCTGGATATTC	rev, Primer for up fragment of pGP3118
PF74	GAATATCCAGCCGATCACATCCTATAACATGGTGTCATAAAATGTTCAAATGCC	fwd, Primer for down fragment of pGP3118
PF75	TTTCTCGAGTTACAAGGTTGCTTGCGTCAC	rev, Primer for down fragment of pGP3118
PF76	TGTTTCCAAATGGCTTTCTCGC	fwd, Seq-Primer for pGP3118
PF77	CCTACTAGATCAAGGCTAGGTGTAAG	rev, Seq-Primer for pGP3118
PF83	AATTCTACACAGCCCAGTCCAG	fwd, Check primer for chromosomal integration of pGP3122
PF87	TTTAAGCTTTCAGCGACTACGGAAGACAATG	fwd, Primer for amplification of *E. coli infA*
PF88	TTTGGATCCAGGAGGAAACAATCATGGCCAAAGAAGACAATATTGAAATG	rev, Primer for amplification of *E. coli infA*
PF89	TTTGGATCCAGGAGGCAACAAAAATGGAACAAG	fwd, Primer for amplification of *cspC* incl. RBS
PF90	TTTTCTAGATTAAGCTTTTTGAACGTTAGCAGCT	rev, Primer for amplification of *cspC*
PF91	TTTGAATTCTTATTTATCCAAACCGAGTTTTTTCAGC	rev, Primer for amplification of *topB*
PF92	AAAGGATCCGGCACAGGTTTTTTTATTATTTATCCAAAC	rev, Primer for amplification of *topB*
PF93	AAAGAATTCGGCACAGGTTTTTTTATTATTTATCCAAAC	rev, Primer for amplification of *topB*
PF94	TGCCTTTATTACCGGAACCTATGG	Seq. Primer for *manP* on pGP1022
PF95	GCTCAAATTTTCGCCTCTTTAACAG	Seq. Primer for *manP* on pGP1022
PF96	ACGAACGAAAATCGCCATTCG	Seq. Primer for *manP* on pGP1022
PF97	TTTGAATTCAGGGGGCTTTGCGATTGAG	fwd, Primer for amplification of *cspC* promoter
PF98	TTTGGATCCTCTAAAGATTTGAATCCGTCACTTTGG	rev, Primer for amplification of *cspC* promoter

Name	Sequence (5→3‘)	Purpose
PF99	CCTATCACCTCAAATGGTTCGCTGATCCTTTAC ACCGAACAAAAATAATTCTTC	rev, Primer for truncated *S179*
PF100	CAGCGAACCATTTGAGGTGATAGGCACTAGG AGGCAACAAAAATGGAA	fwd, Primer for truncated *S179*
PF101	TTTTCTAGACAATTTATGCTTACGCTTCTTTAGT AACG	fwd, Primer for amplification of *cspB*
PF102	TTTGGATCCATGTTAGAAGGTAAAGTAAAATG GTTCAACT	rev, Primer for amplification of *cspB*
PF103	TTTGGATCCTGATCGCTTTAGGAGGAAATTTC ATG	rev, Primer for amplification of *cspB* incl. Shine-Dalgarno
PF104	TTTTCTAGACGCTTCTTTAGTAACGTTAGCAGC	fwd, Primer for amplification of *cspB* w/o Stop-Codon
PF105	TTTGGATCC**AGGAGGA**AGAGAGAATGGCTAA GGGGC	fwd, Primer for amplification of *E. coli* BL21 *hfq*
PF106	TTTAAGCTTTTATTCGGTTTCTTCGCTGTCCT	rev, Primer for amplification of *E. coli* BL21 *hfq*
PF107	TTTGGATCC**AGGAGGA**ATACACTATGTCCGGT AAAATGACTG	fwd, Primer for amplification of *E. coli* BL21 *cspA*
PF108	TTTAAGCTTAGCAGAGATTACAGGCTGGTTAC	rev, Primer for amplification of *E. coli* BL21 *cspA*
PF109	TTTGGATCC**AGGAGGA**AATTTTGATGTCTAAG ATTAAAGGTAACGTTAAG	fwd, Primer for amplification of *E. coli* BL21 *cspE*
PF110	TTTAAGCTTTTACAGAGCGATTACGTTTGCAG	rev, Primer for amplification of *E. coli* BL21 *cspE*
PF111	TTTGGATCC**AGGAGGA**AAATTTCATGGAAAA TCAACCTAAGTTGAA	fwd, Primer for amplification of *E. coli* BL21 *proQ*
PF112	TTTAAGCTTTCCGTTTCAGAACACCAGGTG	rev, Primer for amplification of *E. coli* BL21 proQ
PF113	TTTGAGCTCCATGTTAGAAGGTAAAGTAAAAT GGTTCAAC	fwd, Primer for amplification of *cspB*
PF114	TTTGGATCCCAATTTATGCTTACGCTTCTTTAG TAACG	rev, Primer for amplification of *cspB*
PF115	TTTGGATCCCGCTTCTTTAGTAACGTTAGCAGC	rev, Primer for amplification of *cspB* w/o Stop-Codon
PF116	TCAAGAGTCAATATTCATGCGCTTG	fwd, Primer for sequencing of *veg* promoter region
PF117	TTTGAATTCTTGACAAAAATGGGCTCGTGTT	fwd, Primer for amplification of *veg* Promoter for pGP3131/pGP3132
PF118	TTTGGATCCCCTAAATTCCCATCAAGCGATCTT TT	rev, Primer for amplification of *veg* Promoter for pGP3131/pGP3133

Name	Sequence (5→3‘)	Purpose
PF119	CTGGTGGCAGTGAAAAAGGATG	fwd, LFH-Primer for up-fragment for deletion of *veg*
PF120	CCGAGCGCCTACGAGGAATTTGTATCGTTGCATCCACCTCACTACATTTATTG	Rev, LFH-Primer for up-fragment for deletion of *veg*
PF121	CCTATCACCTCAAATGGTTCGCTGTTGTTTACTGCTTTTTGTTTTGCCC	Fwd, LFH-Primer for down-fragment for deletion of *veg*
PF122	GAAACGTCAGAGCCAATTTCCG	Rev, LFH-Primer for down-fragment for deletion of *veg*
PF123	GTTTCGAATTATAGGAATAGAGCAAACAAG	Fwd, Seq-Primer for deletion of *veg*
PF124	AGCAGTTGAAACACCGATTGTC	Rev, Seq-Primer for deletion of *veg*
PF125	AAATCTAGAAATGGAACAAGGTACAGTTAAATGGTTT	Fwd, Primer for amplification of *cspC*
PF126	AAAGGATCCCTATTAAGCTTTTTGAACGTTAGCAGCT	Rev, Primer for amplification of *cspC*
PF127	AAAGAATTCAGAGAAAGGGCTTGGAGGTATTG	fwd, *veg* Promoter, for insert in pGP3133/pGP3134
PF128	TGCCAATGATGAACTATGAAGACATC	fwd, Seq-Primer for *yxbD, yxbC*
PF129	GGATAATATGAGTGCTGTAACCGAATC	rev, Seq-Primer for *yxbD, yxbC*
PF130	TTTGAATTCCAATTTATGCTTACGCTTCTTTAGTAACG	fwd, *cspB*
PF131	TTTGGATCCATGGAACAAGGTACAGTTAAATGGTTTA	fwd, *cspC,* pGP3128
PF132	TTTGAATTCCTCCTGCTAAGCATAAAAGACTGC	fwd, *degS* Promoter
PF133	TTTGGATCCATCTTCATCAAAATAGAATCCAGCACTTT	rev, *degS* Promoter
PF134	[Biotin]AAAGAAGAATTATTTTTGTTCGGTGTAAAGGATAGTATGAAGATTGACTTTTCGTCTTGATGATACTTTGGGCAAGGATAGTATATACTGTGTGGTTACACACTAGGAGGCAACAAAA	cspC 5'-UTR DNA Oligo for Affinity chromatography
PF135	TTTCTGCAGCGCTTCTTTAGTAACGTTAGCAGC	rev, *cspB,* pGP3126
PF136	TTTCTGCAGAGCTTTTTGAACGTTAGCAGCTT	rev, *cspC,* pGP3130
PF137	TTTGGATCCATGCAAAACGGTAAAGTAAAATGGTTC	fwd, *cspD,* pGP3135
PF138	TTTCTGCAGGAGTTTTACAACATTAGAAGCTTGAGGT	rev, *cspD*, pGP3135
PF139	CCTATCACCTCAAATGGTTCGCTGTCTTCAATCGTTTATACAAACAGGCTC	fwd, Down fragment Δ*cspC*

Name	Sequence (5→3‘)	Purpose
PF140	TTTTGTTGCCTCCTAGTGTGTAAC	rev, Up fragment *ΔcspC*
PF141	GTTACACACTAGGAGGCAACAAAAATGTCCG GTAAAATGACTGGTATCG	fwd, *cspA*, *E. coli* K-12
PF142	CCGAGCGCCTACGAGGAATTTGTATCGAGAG ATTACAGGCTGGTTACGTTAC	rev, *cspA, E. coli* K-12
PF143	GTTACACACTAGGAGGCAACAAAAATGGCAA AGATTAAAGGTCAGGTTAAG	fwd, *cspC, E. coli* K-12
PF144	CCGAGCGCCTACGAGGAATTTGTATCGTTACT GATGGCAAAGTGGACAGGA	rev, *cspC, E. coli* K-12
PF145	GTTACACACTAGGAGGCAACAAAAATGGAAA AGGGTACTGTTAAGTGGT	fwd, *cspD, E. coli* K-12
PF146	CCGAGCGCCTACGAGGAATTTGTATCGAGACA GAAGAGCTATGCGACTG	rev, *cspD, E. coli* K-12
PF147	GTTACACACTAGGAGGCAACAAAAATGGCCA AAGAAGACAATATTGAAATG	fwd, *infA, E. coli* K-12
PF148	CCGAGCGCCTACGAGGAATTTGTATCGTCAGC GACTACGGAAGACAATG	rev, *infA, E. coli* K-12
PF149	GTTACACACTAGGAGGCAACAAAAATGACTG AATCTTTTGCTCAACTCTTT	fwd, *rpsA, E. coli* K-12
PF150	CCGAGCGCCTACGAGGAATTTGTATCGAATTA CTCGCCTTTAGCTGCTTTG	rev, *rpsA E. coli* K-12
PF151	TTTGAATTCTCATACGCTCTCTTAGTTGATAAA CGT	fwd, P_{cspB}, pGP3136
PF152	TTTGGATCCAACATGAAATTTCCTCCTAAAGCG ATC	rev, P_{cspB}, pGP3136
PF153	TTTGAATTCTCAGCCATCAATAAAAGCGGTTA C	fwd, P_{cspD}, pGP3137
PF154	TTTGGATCCTGCATATTGCTTAATTCCTCCTAG TACT	rev, P_{cspD}, pGP3137
PF155	AAAGGATCCAGGTGGATGCAATGGCGAA	fwd, *veg*, pGP3138
PF156	AAACTGCAGTTAAAATGCCACTGAGCTTGCG	rev, *veg,* pGP3138
PF157	CCTTTTTTCAAATTGCGGATGGCTCCATCCTCC ACTTCCTCCCGCTTCTTTAGTAACGTTAGCAGC	rev, *cspB*
PF158	TGGAGCCATCCGCAATTTGAAAAAAGGTAATA ACCAGCGTGGACCGGCGAGGCTAGTTACCC	rev, *cat*
PF159	CCTTTTTTCAAATTGCGGATGGCTCCATCCTCC ACTTCCTCCAGCTTTTTGAACGTTAGCAGCTT	rev, *cspC*

Name	Sequence (5→3‘)	Purpose
PF160	CCTTTTTTCAAATTGCGGATGGCTCCATCCTCC ACTTCCTCCGAGTTTTACAACATTAGAAGCTTG AGGT	rev, *cspD*
PF161	CCTATCACCTCAAATGGTTCGCTGACTCAATAC ATGATGATGAGATGACAAATA	fwd, LFH primer, GP3276
PF162	ATGTTTGCAAAACGATTCAAAACCTC	fwd, *amyE,* GP3280
PF163	GCCTAAACGGATATCATCATCGC	rev, *amyE*, GP3280
PF164	GCGATGATGATATCCGTTTAGGCGATCACATA TCGAGAAAACAGATGAATTTC	fwd, *cspB*, GP3280
PF165	CCGAGCGCCTACGAGGAATTTGTATCGTTCAT GAAGCGGGATATTGCAAAC	rev, *cspB*, GP3280
PF166	CCTATCACCTCAAATGGTTCGCTGTGGGCGGT GATAGCTTCTCG	fwd, *amyE*, GP3280
PF167	CATCACCATCACCATCACTAATAACCAGCGTG GACCGGCGAGGCTAGTTACCC	rev, *cat*
PF168	GTGATGGTGATGGTGATGTCCTCCACTTCCTC CCGCTTCTTTAGTAACGTTAGCAGC	rev, *cspB*, GP3284
PF169	GTGATGGTGATGGTGATGTCCTCCACTTCCTC CAGCTTTTTGAACGTTAGCAGCTT	rev, *cspC*, GP3285
PF170	GTGATGGTGATGGTGATGTCCTCCACTTCCTC CGAGTTTTACAACATTAGAAGCTTGAGGT	rev, *cspD*, GP3286
PF171	CAAATTGCAAAGGTGTATATCTCGGT	fwd, readthrough transcript *rbfA-truB*
PF172	CTGATACTTCCGGATCGAGCG	rev, readthrough transcript *rbfA-truB*
PF173	CGTGAACTTAGAGCGTGTTAATGG	fwd, readthrough transcript *mlpA-ymxH*
PF174	ACTGTGGGAATGAGGAGTGC	rev, readthrough transcript *mlpA-ymxH*
PF175	CAGAATTTGTGTCTTTAGATCTGCCAT	rev, readthrough transcript *treR-hypO*
PF176	CTGTCTCAATATCTCGCACACAAAC	fwd, readthrough transcript *yqfL-yqxD*
PF177	GGAGAAATTCTTGACATCTTACCCATAATAG	rev, readthrough transcript *yqfL-yqxD*
PF178	5'-[Phos]ACGTTAGCAGCTTGAGGTCCACGAG	5'phosphorylated CCR primer for CspC Ala58Pro mutation
PF179	CCGAGCGCCTACGAGGAATTTGTATCGCCTTG TAGCATCTCCCTACTCG	For Up fragment of LFH with CspC Ala58Pro
PF180	GTTACACACTAGGAGGCAACAAAAATGAAAC AAGGTACAGTTAAATGGTTTAAC	fwd, *cspA*, *S. aureus NCTC8325*
PF181	CCGAGCGCCTACGAGGAATTTGTATCGCACCT TACTTCTTGGTAAGGTGTTAG	rev, *cspA*, *S. aureus NCTC8325*
PF182	AGGAGGCAACAAAAATGGAACAAG	fwd, *cspC*, Northern probe

Name	Sequence (5→3‘)	Purpose
PF183	CTAATACGACTCACTATAGGGAGATTAAGCTT TTTGAACGTTAGCAGCTT	rev, *cspC*, Northern probe
PF184	CAAACCTTTAAGCAAAATCATGTCGC	fwd, *rbsA,* Northern probe
PF185	CTAATACGACTCACTATAGGGAGAGTAGAAA GTGGCGGGAACAGA	rev, *rbsA,* Northern probe
PF186	GAAGCATTATCGCATTGATGGCA	fwd, *mtlA,* Northern probe
PF187	CTAATACGACTCACTATAGGGAGACAATCAGC TCGTCGTATTTCGG	rev, *mtlA,* Northern probe
PF188	CAGTGAAGGCCTATGGGAAGAC	fwd, *cydA,* Northern probe
PF189	CTAATACGACTCACTATAGGGAGACAGTGCAC CAAGAATCATGTACATC	rev, *cydA,* Northern probe
PF190	GTTTAAACAAGCCATTTTGAATCGTGA	fwd, *manP,* readthrough trancript *manP-manA*
PF191	CAATCGCATGAACAGTACCGC	rev, *manA,* readthrough trancript *manP-manA*
PF192	GAGGTTCGTACTGCCAGATCAC	fwd, *liaG,* readthrough trancript *liaG-liaH*
PF193	GCTGAAGTGGCTGGCAAAC	rev, *liaH,* readthrough trancript *liaG-liaH*
PF194	AGACTCTTCCAGCAGACACAAG	fwd, *ywsB,* readthrough trancript *ywsB-ywsA*
PF195	GATCTTGTGCTGACTTATGGCTG	rev, *ywsA,* readthrough trancript *ywsB-ywsA*
PF196	GAACGCATTGAACAGATTGAGGG	fwd, *pyrR,* readthrough trancript *pyrR-pyrP*
PF197	CAGCCATCCTGTTCCAAGCT	rev, *pyrP,* readthrough trancript *pyrR-pyrP*
PF198	CTGAGCAAGGTTGTCGGACA	fwd, *pyrP,* readthrough trancript *pyrP-pyrB*
PF199	AGACGTCCACACCGATTGATTC	rev, *pyrB,* readthrough trancript *pyrP-pyrB*
PF200	GAGAAAGGCTATGTTGATAAGGACTATG	fwd, *manR,* readthrough trancript *manR-manP*
PF201	AGCTGACGAAAGAAACCAATGT	fwd, readthrough transcript *manR-manP*, qPCR primer
PF202	CGAAATCAGCTCATTAAAATCGC	rev, readthrough transcript *manR-manP*, qPCR primer
PF203	ACCGGCAGTGATCAACAGTT	fwd, readthrough transcript *liaH-liaG*, qPCR primer
PF204	GCGGCAAATGAATAAGCGGA	rev, readthrough transcript *liaH-liaG*, qPCR primer
PF205	GGTCTTTGTATGCCTCTTTGCG	fwd, readthrough transcript *pyrR-pyrP*, qPCR primer
PF206	CCCAAGAGAAAGGTGTCGGG	rev, readthrough transcript *pyrR-pyrP*, qPCR primer
PF207	CAGAGAGGCTTGGAAGGGTT	fwd, readthrough transcript *pyrP-pyrB*, qPCR primer

Name	Sequence (5→3‘)	Purpose
PF208	GCTAAGTTCACTCATCGTCGT	rev, readthrough transcript *pyrP-pyrB*, qPCR primer
PF209	GTAAAACGACGGCCAGTGAATT	fwd, P_{deg} Promoter from pBQ200
PF210	TTTGGATCCCCCATTTTTGTTGCCTCCTATAACAAAAAAAGCAAGGAATAATCCCTGCTTTTAATAATCGGTGAACGAGTCCTAGGTATTTGAT	rev, P_{deg} Promoter from pBQ200
PF211	GGTGAACGAGTCCTAGGTATTTGAT	rev, P_{deg} Promoter from pBQ200
PF212	ATCAAATACCTAGGACTCGTTCACCGCGGCAAATGAATAAGCGGA	fwd, *liaHG* intercistronic region
PF213	TTTGGATCCCCCATTTTTGTTGCCTCCTTCGGTTTCATCCTTCTCATTCATTCT	rev, *liaHG* intercistronic region
PF214	ATCAAATACCTAGGACTCGTTCACCACCTTTTTAAGGGCAATCCAGAGA	fwd, *pyrRP* intercistronic antiterminator
PF215	TTTGGATCCCCCATTTTTGTTGCCTCCTTTTACGCAAAGAGGCATACAAAGAC	rev, *pyrRP* intercistronic antiterminator
PF216	ATCAAATACCTAGGACTCGTTCACCAAACCTTTTAATGAAAGTCCAGAGAGG	fwd, *pyrPB* intercistronic region
PF217	TTTGGATCCCCCATTTTTGTTGCCTCCTGTTCTTTCCCCTCTCTTTTCAACTTAAG	rev, *pyrPB* intercistronic region
PF218	GTGAAAGCGAATTATAAAATTCAGCCG	fwd, Up fragment Δ*pyrR*
PF219	CCTATCACCTCAAATGGTTCGCTGCAGCTTTTTGATTCAATGTGTGACAC	rev, Up fragment Δ*pyrR*
PF220	CCGAGCGCCTACGAGGAATTTGTATCGGCCATTTATGAAAACGAATAATAGATCACC	fwd, Down fragment Δ*pyrR*
PF221	TGTCCGACAACCTTGCTCAG	rev, Down fragment Δ*pyrR*
PF222	GCTTCAGAAGAACAAAAAAGTGAGC	fwd, Seq-Primer for Δ*pyrR*
PF223	CACGCCAATGTTTTCTCCGTAAG	rev, Seq-Primer for Δ*pyrR*
PF224	TTTCCGGTCTCATGGTATGTTAGAAGGTAAAGTAAAATGGTTCAAC	fwd, *cspB,* pGP3140
PF225	AAACTCGAGTTATGCTTACGCTTCTTTAGTAACGTTAG	rev, *cspB,* pGP3140
PF226	TTCGTCTTGATGATACTTTGGGC	fwd, *cspC,* qPCR primer
PF227	CGTCTCCATTTTCGCGTTCG	rev, *cspC,* qPCR primer
PF228	CAGATGGTGTGATCGCGAGT	fwd, *rbsR,* qPCR primer
PF229	AAAGTGGCGGGAACAGAAGT	rev, *rbsR*, qPCR primer
PF230	TTCTGGCGACTACAACGGAA	fwd, *gapA*, qPCR primer

Name	Sequence (5→3‘)	Purpose
PF231	CTGCAAGGTCAACAACGCG	rev, *gapA,* qPCR primer
PF232	TTTGGATCCCCCATTTTTGTTGCCTCCTGGTGAACGAGTCCTAGGTATTTGAT	rev, P_{degQ}
PF233	CTAATACGACTCACTATAGGGAGATCAAATACCTAGGACTCGTTCACC	fwd, P_{degQ}, for *in vitro* transcription
PF234	GCCTCAGGAAGATCGCACTC	rev, *lacZ*
PF235	TTTGGATCCCCCATTTTTGTTGCCTCCTGCAAAAAACCCCTCAAGACCCGTTTAGAGGCCCCAAGGGGTTATGCTAGTTATTGCTCAGCGGGGTGAACGAGTCCTAGGTATTTGAT	rev, P_{degQ}, for pGP3142
PF236	CTAATACGACTCACTATAGGGAGAGAACTAATGGGTGCTTTAGTTGAAGA	fwd, *cat*, for *in vitro* transcription
PF237	TTTGGATCCCCCATTTTTGTTGCCTCCTCAAATAAAAAGGCCTGCGATTACCAGCAGGCCTGTTATTAGCGATCCGGTGAACGAGTCCTAGGTATTTGAT	rev, $P_{degQ,}$ tR2-4 terminator
PF238	AAAGGTACCAGCTGACGAAAGAAACCAATGTC	fwd, *manR* terminator
PF239	AAAGGTACCACCGAAATCAGCTCATTAAAATCGC	rev, *manR* terminator
PF240	TTTGGTACCTCAGACCAGACAAAAGCGGC	fwd, *liaHG* intercistronic region
PF241	TTTGGTACCTCGGTTTCATCCTTCTCATTCATTCT	rev, *liaHG* intercistronic region
PF242	TTTGGTACCACCTTTTTAAGGGCAATCCAGAGA	fwd, *pyrRP* Antiterminator
PF243	TTTGGTACCTTTACGCAAAGAGGCATACAAAGAC	rev, *pyrRP* Antiterminator
PF244	TTTGGTACCCAAATAAAAAGGCCTGCGATTACCAGCAGGCCTGTTATTAGCGATCCGGTACCCTAAAGTATCAGCAGTAAGT	fwd, *pdhA* 5'UTR, tR2-4 terminator from Nudler *et al.*, 1995
PF245	CAAATAAAAAGGCCTGCGATTACCA	rev, tR2-4 terminator, check-primer
PF246	AGGGTATGTTTCTCTTTGATGTCTTTTTG	fwd, up fragment LFH P_{cspD}-*lacZ*
PF247	CGGCAATAGTTACCCTTATTATCAAGATAAG	rev, up fragment LFH P_{cspD}-*lacZ*
PF248	CTTATCTTGATAATAAGGGTAACTATTGCCGTCAGCCATCAATAAAAGCGGTTAC	fwd, mid fragment LFH P_{cspD}-*lacZ*
PF249	GTCACGACGTTGTAAAACGACGGGATCCCCGTTGAACCATTTTACTTTACCGTTTTGC	rev, mid fragment LFH P_{cspD}-*lacZ*

Name	Sequence (5→3‘)	Purpose
PF250	GGGGATCCCGTCGTTTTACAA	fwd, down fragment LFH P_{cspD}-*lacZ*
PF251	AACAAAATTCTCCAGTCTTCACATCG	rev, down fragment LFH P_{cspD}-*lacZ*

Restriction sites are <u>underlined</u>.

Shine-Dalgarno sequences are **bold**.

Other oligonucleotides used in this study

Name	Sequence (5→3‘)	Purpose	Reference
cat-fwd, (kan)	CAGCGAACCATTTGAGGTGATAGGC GGCAATAGTTACCCTTATTATCAAG	fwd, amplification of *cat*-resistance cassette	Laboratory collection
cat-rev (kan)	CGATACAAATTCCTCGTAGGCGCTCG GCCAGCGTGGACCGGCGAGGCTAGT TACCC	rev, amplification of *cat*-resistance cassette	Laboratory collection
ML84	CTAATGGGTGCTTTAGTTGAAGA	fwd, sequencing of *cat*-cassette	Laboratory collection
ML85	CTCTATTCAGGAATTGTCAGATAG	rev, sequencing of *cat*-cassette	Laboratory collection
ML229	AAATCTAGAGATGTTAGAAGGTAAA GTAAAATGGTTCAACTC	fwd, *cspB*	Laboratory collection
ML230	TTTGGTACCCGCGCTTCTTTAGTAAC GTTAGCAGC	rev, *cspB*	Laboratory collection
ML231	AAATCTAGAGATGGAACAAGGTACA GTTAAATGGTTTAATGC	fwd, *cspC*	Laboratory collection
ML232	TTTGGTACCCGAGCTTTTTGAACGTT AGCAGCTTGAG	rev, *cspC*	Laboratory collection
kan-fwd,	CAGCGAACCATTTGAGGTGATAGG	fwd, amplification of *aphA3*-resistance cassette	Laboratory collection
kan-rev	CGATACAAATTCCTCGTAGGCGCTCG G	rev, amplification of *aphA3*-resistance cassette	Laboratory collection
kan-check-fwd,	CATCCGCAACTGTCCATACTCTG	fwd, sequencing of *aphA3*-cassette	Laboratory collection
kan-check-rev	CTGCCTCCTCATCCTCTTCATCC	rev, sequencing of *aphA3*-cassette	Laboratory collection
spec-fwd, (kan)	CAGCGAACCATTTGAGGTGATAGGG ACTGGCTCGCTAATAACGTAACGTG ACTGGCAAGAG	fwd, amplification of *spec*-resistance cassette	Laboratory collection

Name	Sequence (5→3‘)	Purpose	Reference
spec-rev (kan)	CGATACAAATTCCTCGTAGGCGCTCG GCGTAGCGAGGGCAAGGGTTTATTG TTTTCTAAAATCTG	rev, amplification of *spec*-resistance cassette	Laboratory collection
spec-check-fwd,	GTTATCTTGGAGAGAATATTGAATG GAC	fwd, sequencing of *spec*-cassette	Laboratory collection
spec-check-rev	CGTATGTATTCAAATATATCCTCCTCA C	rev, sequencing of *spec*-cassette	Laboratory collection
mls-fwd, (kan)	CAGCGAACCATTTGAGGTGATAGGG ATCCTTTAACTCTGGCAACCCTC	fwd, amplification of *ermC*-resistance cassette	Laboratory collection
mls-rev (kan)	CGATACAAATTCCTCGTAGGCGCTCG GGCCGACTGCGCAAAAGACATAATC G	rev, amplification of *ermC*-resistance cassette	Laboratory collection
mls-check-fwd,	CCTTAAAACATGCAGGAATTGACG	fwd, sequencing of *ermC*-cassette	Laboratory collection
mls-check-rev	GTTTTGGTCGTAGAGCACACGG	rev, sequencing of *ermC*-cassette	Laboratory collection
tc-check-fwd,	CGGCTACATTGGTGGGATACTTGTT G	fwd, sequencing of *tet*-cassette	Laboratory collection
tc-check-rev	CATCGGTCATAAAATCCGTAATGC	rev, sequencing of *tet*-cassette	Laboratory collection
tc-fwd,2 (kan)	CAGCGAACCATTTGAGGTGATAGGG CTTATCAACGTAGTAAGCGTGG	fwd, amplification of *tet*-resistance cassette	Laboratory collection
tc-rev (kan)	CGATACAAATTCCTCGTAGGCGCTCG GGAACTCTCTCCCAAAGTTGATCCC	rev, amplification of *tet*-resistance cassette	Laboratory collection
KG42	GAAACGGCAAAACGTTCTGG	fwd, *rpsJ* for qRT-PCR	Laboratory collection
KG43	GTGTTGGGTTCACAATGTCG	rev, *rpsJ* for qRT-PCR	Laboratory collection
KG44	GCGTCGTATTGACCCAAGC	fwd, *rpsE* for qRT-PCR	Laboratory collection
KG45	TACCAGTACCGAATCCTACG	rev, *rpsE* for qRT-PCR	Laboratory collection
MB21	GGCGAACTTGTCGATGAACATCAG	fwd, Seq-primer for *cspD*	Laboratory collection
MB22	GGCAGCTGGCCTTGTTATGATC	rev, Seq-primer for *cspD*	Laboratory collection
MB48	AAAGTCGACGAGTTTTACAACATTAG AAGCTTGAGGTC	rev, *cspD*	Laboratory collection
MB49	AAAGGATCCCAAAACGGTAAAGTAA AATGGTTCAACAAC	fwd, *cspD*	Laboratory collection
MB79	CCTATCACCTCAAATGGTTCGCTGGT TTACTTTAGTCACAAGCCACGC	fwd, sequencing of *degS*	Laboratory collection
MB82	GCAGGTGTATGAAGTGATTGAGC	rev, sequencing of *degS*	Laboratory collection

Name	Sequence (5→3‘)	Purpose	Reference
MD33	GAAACGGTTTGTGCTGGATGA	rev, check of integration at *xkdE* site	Laboratory collection
JK158	ATAGAGTGATTGTGATAATTTTAAATGTAAGCG	fwd, check for integration at *amyE* site	Laboratory collection
AL41	CAATGGGGAAGAGAACCGCT	rev, check for integration at *amyE* site	Laboratory collection
JG155	CGGCTTGACAATCAAAAAGGACCATACTG	rev, amplification of readthrough transcript *sinR-…*	Laboratory collection
CD179	TGGCCAGCGTATTAAACAATACCGT	fwd, amplification of readthrough transcript *sinR-…*	Laboratory collection
DR43	GAAAGAAATTTGTGAAAACTCCATATATGAAT	fwd, amplification of readthrough transcript *treR-yfkO*	Laboratory collection
DR506	GGAAATTGATTAAAATCTTGCAGCAAACA	fwd, amplification of readthrough transcript *glcT-ptsG*	Laboratory collection
DR507	GGATCCCTAACACACCGACGATAATACCG	rev, amplification of readthrough transcript *glcT-ptsG*	Laboratory collection
HE260	GTCAGAGTTGCAATGATTCCTGACGGATTGG	rev, amplification of readthrough transcript *dnaG-sigA*	Laboratory collection
HE261	CCTATCACCTCAAATGGTTCGCTGCCAGACTCTGTTAATTGCTCTTTTACTTGGTCG	amplification of readthrough transcript *dnaG-sigA*	Laboratory collection

Restriction sites are underlined.

Shine-Dalgarno sequences are **bold**.

7.4 Plasmids

Plasmids constructed in this study

Name	Vector	Construction
pGP3117	pAC5/*BamHI+EcoRI*	PCR prod. *cspC* PF97/PF98, templ. 168 /*BamHI+EcoRI*
pGP3119	pAC5/*BamHI+EcoRI*	PCR prod. *cspC* PF97/PF98, templ. GP1989/*BamHI+EcoRI*

Name	Vector	Construction
pGP3120	pAC5/*BamHI+EcoRI*	LFH prod. *cspC* PF97/PF99 & PF100/PF98 templ. 168/*BamHI+EcoRI*
pGP3121	pHT01/*XbaI+BamHI*	PCR prod. PF79/PF80, templ. *E. coli* BL21 /*XbaI+BamHI*
pGP3123	pBQ200/*BamHI+HindIII*	PCR prod. *infA (E. coli)* PF88/PF87, templ. *E. coli* BL21/*BamHI+HindIII*
pGP3124	pBQ200/*BamHI+XbaI*	PCR prod. *cspC* PF89/PF90, templ. 168/*BamHI+XbaI*
pGP3125	pGP380/*BamHI+XbaI*	PCR prod. *cspB* PF101/PF102, templ. 168/*BamHI+XbaI*
pGP3126	pAC5/*EcoRI+BamHI*	PCR prod. P_{degQ}-$Term_{manR}$PF209/PF210, templ. pBQ200/*EcoRI+BamHI*
pGP3127	pGP886/*BamHI+XbaI*	PCR prod. *cspC* PF125/PF126, templ. 168/*BamHI+XbaI*
pGP3128	pHT01/*BamHI+XbaI*	PCR prod. *cspC* PF131/PF90, templ. 168/*BamHI+XbaI*
pGP3129	pAC5/*EcoRI+BamHI*	PCR prod. *degS* Promoter PF132/PF133, templ. 168/*EcoRI+BamHI*
pGP3130	pAC5/*EcoRI+BamHI*	LFH prod. P_{degQ}-*liaHG* intercistronic region PF209/PF213/*EcoRI+BamHI*
pGP3131	pAC5/*EcoRI+BamHI*	PCR prod. *veg* Promoter mutated SD PF117/PF118, templ. GP1990/*BamHI+XbaI*
pGP3132	pAC5/*EcoRI+BamHI*	PCR prod. *veg* Promoter WT PF117/PF118, templ. 168/*BamHI+XbaI*
pGP3133	pAC5/*EcoRI+BamHI*	PCR prod. *veg* Promoter WT PF127/PF118, templ. 168/*BamHI+XbaI*
pGP3134	pAC5/*EcoRI+BamHI*	PCR prod. *veg* Promoter mutated SD PF127/PF118, templ. GP1990/*BamHI+XbaI*
pGP3135	pAC5/*EcoRI+BamHI*	LFH prod. P_{degQ}-*pyrRP* intercistronic region PF209/PF215/*EcoRI+BamHI*
pGP3136	pAC5/*EcoRI+BamHI*	PCR prod. P_{cspB} PF151/PF152, templ. 168/*EcoRI+BamHI*
pGP3138	pBQ200/*BamHI+PstI*	PCR prod. *veg* PF155/PF156, templ. 168/*BamHI+PstI*
pGP3139	pAC5/*EcoRI+BamHI*	LFH prod. P_{degQ}-*pyrPB* intercistronic region PF209/PF217/*EcoRI+BamHI*
pGP3140	pETSUMOadapt/*BsaI+XhoI*	PCR prod. *cspB* templ. 168/*BsaI+XhoI*
pGP3141	pAC5/*EcoRI+BamHI*	P_{degQ} PF209/PF232/*EcoRI+BamHI*
pGP3142	pAC5/*EcoRI+BamHI*	PCR prod. P_{degQ}-TermT7 PF209/PF235, templ. pBQ200/*EcoRI+BamHI*
pGP3143	pAC5/*EcoRI+BamHI*	PCR prod. P_{degQ}-TermtR2-4 PF209/PF237, templ. pBQ200/*EcoRI+BamHI*
pGP3144	pGP721/*KpnI*	PCR prod. $Term_{manR}$ PF238/PF239, templ. 168/*KpnI*

Name	Vector	Construction
pGP3145	pGP721/*KpnI*	PCR prod. $Term_{liaH}$ PF240/PF241, templ. 168/*KpnI*
pGP3146	pGP721/*KpnI*	PCR prod. $Antiterm_{pyrR}$ PF242/PF243, templ. 168/*KpnI*

Other plasmids used in this study

Name	Description	Source/Reference
pAC5	translational *lacZ* fusions that can be integrated at the *amyE* site in *B. subtilis*	Weinrauch *et al.*, 1991
pBQ200	Constitutive overexpression of proteins in *B. subtilis*	Martin-Verstraete *et al.*, 1994
pHT01	Overexpression pf genes under the control of an IPTG-inducible promoter in *B. subtilis*	MoBiTec, Göttingen
pDG780	Vector for kanamycin resistance cassette	Guérout-Fleury *et al.*, 1995
pDG647	Vector for erythromycin resistance cassette	Guérout-Fleury *et al.*, 1995
pDG1514	Vector for tetracycline resistance cassette	Guérout-Fleury *et al.*, 1995
pDG1726	Vector for spectinomycin resistance cassette	Guérout-Fleury *et al.*, 1995
pGEM-cat	Vector for chloramphenicol resistance cassette	Torsten Mascher, laboratory collection
pGP380	Constitutive overexpression of C-terminally *Strep*-tagged proteins in *B. subtilis*	Herzberg *et al.*, 2007
pGP381	Expression of Strep-CsrA by pGP381	Laboratory collection
pGP382	Constitutive overexpression of N-terminally *Strep*-tagged proteins in *B. subtilis*	Herzberg *et al.*, 2007
pGP721	translational *pdhA-lacZ* fusion in pAC5	Laboratory collection
pGP886	Expression of genes under the control of a xylose-inducible promoter in *B. subtilis*, integrates in *xkdE*	Gerwig *et al.*, 2014

Name	Description	Source/Reference
pGP961	Constitutive overexpression of C-terminally *Strep*-tagged PtsH in *B. subtilis*	Fabian M. Commichau, laboratory collection
pGP2164	Expression of CspD-Strep by pGP382	Laboratory collection
pGP2165	Expression of Strep-CspD by pGP380	Laboratory collection

7.5 Chemicals, utilities, equipment, antibodies, enzymes, software, and webpages

Chemicals

Chemical	Supplier
Acrylamide	Carl Roth, Karlsruhe
Agar	Carl Roth, Karlsruhe
Ammonium iron (III) sulfate	Sigma-Aldrich, Taufkirchen
Ammonium peroxydisulfate	Carl Roth, Karlsruhe
Antibiotics	Sigma-Aldrich, Taufkirchen
β-Mercaptoethanol	Sigma-Aldrich, Taufkirchen
Bacto agar	Becton, Dickinson and Company, Heidelberg
Bromophenol blue	Serva, Heidelberg
CDP*	Roche Diagnostics, Mannheim
Coomassie Brilliant Blue R-250	Carl Roth, Karlsruhe
D(+)-Glucose	Merck, Darmstadt
dNTPs	Roche Diagnostics, Mannheim
Skimmed milk powder	Carl Roth, Karlsruhe
TEMED	Carl Roth, Karlsruhe
Tween 20	Sigma, München
X-Gal	Peqlab, Erlangen
Yeast Extract	Oxoid, Heidelberg

Further chemicals were purchased from Carl Roth, Merck, Peqlab, or Sigma-Aldrich.

Enzymes

Enzyme	Supplier
Ampligase	Biozym, Hessisch Oldendorf
DNase I	Roche Diagnostics, Mannheim
DreamTaq DNA Polymerase	ThermoFisher, Waltham

Enzyme	Supplier
FastAP	ThermoFisher, Waltham
Lysozyme	Merck, Darmstadt
Restriction endonucleases	ThermoFisher, Waltham
RNase A	Roche Diagnostics, Mannheim
RNase Inhibitor 40 U	Roche Diagnostics, Mannheim
S7 Fusion High-Fidelity DNA Polymerase	Biozym, Hessisch Oldendorf
T4-DNA ligase	Roche Diagnostics, Mannheim
T7 RNA polymerase 80 U	Roche Diagnostics, Mannheim

Commercial systems

Enzyme	Supplier
HDGreen™ Plus DNA Stain	Intas, Göttingen
iScript One-Step RT-PCR kit with SYBR green	Bio-Rad, München
NucleoSpin Plasmid-Kit	Macherey-Nagel, Düren
PageRuler™ Plus Prestained Protein Ladder	ThermoFisher, Waltham
peqGOLD Bacterial DNA Kit	PEQLAB, Erlangen
QIAquick PCR purification kit	Qiagen, Düsseldorf
RevertAid First Strand cDNA Synthesis Kit	ThermoFisher, Waltham
RNeasy Plus Mini Kit	Qiagen, Düsseldorf

Equipment

Device	Supplier
Autoclave	Zirbus technology, Bad Grund
Biofuge fresco	Heraeus Christ, Osterode
Blotting device VacuGeneTMXI	Amersham, Freiburg
ChemoCam imager	Intas, Göttingen
Corning 384 well low volume black round bottom polystyrene NB microplates	GE, Frankfurt a. M.
Cuvettes (microliter, plastic)	Greiner, Nürtingen
DAWN HELEOS II MALS detector	Wyatt Technology, Haverhill, UK
Electronic scale Sartorius universal	Sartorius, Göttingen
Fluorescence microscope Axioskop 40 FL + camera AxioCam MRm	Carl Zeiss, Göttingen
Fiberlite F9 / F40 rotors	ThermoFisher, Bonn

Device	Supplier
GelDoc™ XR+	Bio-Rad, München
Gel electrophoresis apparatus	PeqLab, Erlangen
Gel electrophoresis device	Waasetec, Göttingen
Heating block Dri Block DB3	Waasetec, Göttingen
Heraeus Pico 21	ThermoFisher, Bonn
Horizontal shaker	GFL, Burgwedel
Hydro tech vacuum pump	Bio-Rad, München
Ice machine	Ziegra, Isernhagen
Incubator Innova R44	New Brunswick, Neu-Isenburg,
Incubator shaker Innova 2300	New Brunswick, Neu-Isenburg
LabCycler SensorQuest, Göttingen	LabCycler SensorQuest, Göttingen
Magnetic stirrer	JAK Werk, Staufen
Microplate reader SynergyMx Mini-Protean	BioTek, Bad Friedrichshall
Mikroprozessor pH-Meter 766 Calimatic	Knick, Berlin
Mini-Protean III System	Bio-Rad, München
Nanodrop ND-1000	ThermoFisher, Bonn
Open air shaker Innova 2300	New Brunswick, Neu-Isenburg
Polyvinylidendifluoride membrane (PVDF)	Bio-Rad, München
PHERAstar FS plate reader	Thermo Fisher, Bonn
iCycler iQ™ Real-Time PCR Detection System	Bio-Rad, München
Refrigerated centrifuge PrimoR	Heraeus Christ, Osterode
Scale Sartorius universal	Sartorius, Göttingen
SDS-PAGE glass plates	Bio-Rad, München
Special accuracy weighing machine	Sartorius, Göttingen
Spectral photometer Ultraspec 2000	Amersham, Freiburg
Standard power pack	Bio-Rad, München
Steam autoclave	Zirbus, Bad Grund
Stereo Lumar V12 stereo microscope	Carl Zeiss, Göttingen
Sterile bench Hera Safe	ThermoFisher, Bonn
Thermocycler	Biometra, Göttingen
TLA 110 rotor	Beckmann Coulter, Krefeld
TS Sorvall WX utraseries centrifuge / RC 6+	Beckmann Coulter, Krefeld
Ultracentrifuge, Sorvall Ultra Pro 80	ThermoFisher, Bonn
UV Transilluminator 2000	Bio-Rad Laboratories GmbH, München

Device	Supplier
Vortex	Bender and Hobein, Bruchsal
Water desalination plant	Millipore, Schwalbach

Software

Software	Provider/Reference	Application
AxioVision	Zeiss	Image acquisition and processing
ChemoStar Imager	Intas	Image acquisition and processing
FIJI	Schindelin *et al.*, 2012	Image processing
Gen5TM Data analysis software	BioTek®	Reader control and data analysis
Geneious	Biomatters	DNA and sequence analysis
ImageLabTM Software	BioRad	Image acquisition, processing of images, densitometry
Mendeley Desktop	PDFTron™ Systems Inc.	PDF and references Manager
Microsoft Office 365	Microsoft Inc.	Data processing, writing, image processing
Zen	Zeiss	Image processing

Web applications

URL	Provider	Application
http://biotools.nubic.northwestern.edu/OligoCalc.html	Kibbe, 2007	Primer design
http://rssf.i2bc.paris-saclay.fr/toolbox/arnold/	University Paris-Saclay	Prediction of intrinsic terminators
http://www.subtiwiki.uni-goettingen.de/	Zhu & Stülke, 2018	*B. subtilis* database
http://www.listiwiki.uni-goettingen.de/	University of Göttingen	*L. monocytogenes* database
https://ecocyc.org/	SRI International,	*E. coli* database
http://www.ncbi.nlm.nih.gov/	National Institutes of Health, Bethesda	Literature research
http://genolist.pasteur.fr/SubtiList/	Institute Pasteur, Paris	*B. subtilis* sequence analysis
http://bioinfo.ut.ee/primer3/	Whitehead Institute	qRT-PCR primer design